

**LOCALIZATION AND LOCAL MATURATION OF PRECURSOR
MICRORNAS IN AXONS OF SENSORY NEURONS**

by

Monichan Phay

A dissertation submitted to the Faculty of the University of Delaware in partial fulfillment of the requirements for the degree of Doctor of Philosophy in Biological Sciences

Summer 2018

© 2018 Monichan Phay
All Rights Reserved

**LOCALIZATION AND LOCAL MATURATION OF PRECURSOR
MICRORNAS IN AXONS OF SENSORY NEURONS**

by

Monichan Phay

Approved: _____

E. Fidelma Boyd, Ph.D.
Interim Chair of the Department of Biological Sciences

Approved: _____

George H. Watson, Ph.D.
Dean of the College of Arts and Sciences

Approved: _____

Douglas J. Doren, Ph.D.
Interim Vice Provost for Graduate and Professional Education

I certify that I have read this dissertation and that in my opinion it meets the academic and professional standard required by the University as a dissertation for the degree of Doctor of Philosophy.

Signed:

Deni S. Galileo, Ph.D.
Co-professor in charge of dissertation

I certify that I have read this dissertation and that in my opinion it meets the academic and professional standard required by the University as a dissertation for the degree of Doctor of Philosophy.

Signed:

Soonmoon Yoo, Ph.D.
Co-professor in charge of dissertation

I certify that I have read this dissertation and that in my opinion it meets the academic and professional standard required by the University as a dissertation for the degree of Doctor of Philosophy.

Signed:

Jia Song, Ph.D.
Member of dissertation committee

I certify that I have read this dissertation and that in my opinion it meets the academic and professional standard required by the University as a dissertation for the degree of Doctor of Philosophy.

Signed:

Robert W. Mason, Ph.D.
Member of dissertation committee

I certify that I have read this dissertation and that in my opinion it meets the academic and professional standard required by the University as a dissertation for the degree of Doctor of Philosophy.

Signed:

Blake Meyers, Ph.D.
Member of dissertation committee

ACKNOWLEDGMENTS

One of the most valuable lessons I've learned during my time as a graduate student at the University of Delaware and at Nemours A.I duPont is that we all need support and to be supportive of one another to foster an effective research environment. I would like to take this opportunity to express my deepest appreciation to the people who have supported me over the past five years.

First, I want to thank my mum and papa, Ii Lee Li and Dara Phay for the sacrifices they have made to give me the opportunity to pursue all my hopes and dreams. Mum, thank you for teaching me the value of education and instilling me with persevering attitude and an open mindset. Your words of encouragement got me through many difficult times. To my little sister, Monirath, thank you for lending me an ear and listening to me complaining about life and always cheering me on 110% in all my endeavors. I couldn't have done it without your unconditional love and supports.

I am immensely grateful to my exemplary mentor, Dr. Soonmoon Yoo. He has taught me how to think critically, logically, and objectively. I remember being scared during one of the early survival surgeries I had to perform, and Dr. Yoo notice my anxiety and said, "You have to be brave." That was the defining moment that fundamentally changed the way I approach challenges. I'm no longer intimidated by challenges in science but rather welcome them. So thank you for instilling confident in me and for your patients, encouragement, and faith in my abilities throughout the years.

I thank my committee members, Dr. Deni Galileo, Dr. Jia Song, Dr. Blake Meyers, and Dr. Robert Mason for their time, patients, expertise, critiques, and insightful comments and invaluable suggestions on my research project. This work would not have been possible without their supports.

I want to express my gratitude to everyone (former and current labmates) in the Yoo lab. They have made lab life didactic, mirthful, and enjoyable. I have to especially thank Dr. Hak Hee Kim for her guidance on many laboratory techniques and procedures when I entered the lab. I've learned a great deal of little tricks that helped improve my techniques. I'm grateful to have Shiva Shrestha as a labmate, who spent many hours listening to my frustrations and lame science jokes. He has definitely made our cube farm and bench row extra fun. I want to give a shout out Thanmayi Raganath (former lab manager). I will never forget that time you helped me doing 40 different mini preps in one go (that was savage). Thank you for always lifting up my spirit when the going gets tough in lab. Your grad school horror stories were terrifying but truly made me appreciate the Yoo lab and the MBG program even more.

I would like to thank my grad school friends for their feedback and comments on my dissertation, late night study sessions, stimulating scientific discussions, and supporting me through my intellectual development and personal growth. I especially thank Mike Colgan for his invaluable advice, continuous support (in and out of grad school bubble), and teaching me how to be selfless and mindful. I wouldn't be the person I am today without him. I thank, Katherine Robbins, Miho Maeda, Effie Halakos, Sambee Kanda, Cinsley Gentillon, Aparna Swarup, Nicole Flynn, Hannah Puttre, the SNERPs, and other graduate students for their supports and

encouragements. You have been a great source of support and I will forever treasure our friendship.

Lastly, I thank the faculty and staff in the department of biological sciences, the wonderful scientists and staff at Nemours A.I duPont Hospital for Children and the staff at Delaware Biotechnology Institute. I wouldn't be at the University of Delaware if it weren't for Dr. Melinda Duncan. Thank you for recognizing my potential and supported me over the years. I thank Dr. Erica Selva for her compassion and counsel during a particularly stressful time last summer. I thank Betty Cowgill for helping me stay on track and coordinating between UD and Nemours. I would be lost without you Betty! Lisa Glazewski, Stephanie Tantzer, Ellen Hitchens, Megan Simon, Kathy Sewell, Suzanne Purfield, Jen Holbrook, and Deb Stabley, thank you so much for helping me with my research and making me apart of your Nemours family.

TABLE OF CONTENTS

LIST OF TABLES	xi
LIST OF FIGURES	xii
LIST OF ABBREVIATIONS	xiv
ABSTRACT	xvii

Chapter

1 INTRODUCTION	1
Subcellular Localization of mRNAs	1
MRNA Localization in Neuronal Processes.....	3
Significance of Local Protein Synthesis in Neurons	6
MicroRNAs are Small Non-coding Regulatory RNAs	14
MicroRNA Localizes to Neuronal Dendrites and Axons.....	18
Focus of Current Study.....	21
REFERENCES	22
2 DYNAMIC CHANGE OF AXON-SPECIFIC MICRORNAS IN REGNERATING SCIATIC NERVE	32
Introduction	32
Material and Methods.....	38
Survival surgery and tissue processing.....	38
RNA extraction and small RNA enrichment.....	38
Illumina sequencing of small RNA	39
Small-RNA sequencing analysis	40
Statistical analysis	42
RT-qPCR validation of differentially regulated miRNA	43
MicroRNA target prediction.....	44
Functional annotation of predicted miRNA targets.....	44
Results	45
RNA extraction from sciatic nerves yields highly enriched axoplasmic RNAs.....	45

Small-RNA sequencing revealed two population of small non-coding RNAs	47
Regenerating sciatic nerve exhibits temporal changes in the levels of axoplasmic miRNAs	50
Absolute RT-qPCR analysis confirms accurate representation in the alteration of axoplasmic miRNAs levels observed by small-RNA sequencing.....	56
Putative mRNA targets of significantly altered axoplasmic miRNAs shows a strong association with multiple processes involved in neurological functions	58
Discussion.....	61
REFERENCES	67
3 AXONAL LOCALIZATION AND LOCAL MATURATION OF SPECIFIC SUBSETS OF PRECURSOR MICRORNAS AND THEIR BIOLOGICAL ROLE IN REGENERATING AXONS.....	72
Introduction	73
Materials and Methods	83
Dissociated DRG culture and transfection	83
Fluorescence <i>in situ</i> hybridization and immunofluorescence	84
Animal surgery and procedures.....	87
Axoplasmic RNA extraction from rat sciatic nerve	88
Axonal RNA isolation from compartmentalized primary DRG neuronal culture	89
Quantification of RNA by quantitative real time polymerase chain reaction (RT-qPCR).....	91
Fluorescence recovery after photobleaching (FRAP)	95
Plasmid constructs	97
Dual luciferase reporter assay	98
Analysis of axonal growth	99
Results	100
Pre-miR-433 is selectively localized to distal axons of DRG neurons	100
The terminal loop region of pre-miR-433 structure is sufficient to drive the localization of eGFP reporter mRNA into axons of DRG neurons	104
Specific endogenous miRNA precursors localized into distal axons are processed to give rise to corresponding mature miRNAs	124

Overexpression of miR-433-3p attenuates axon growth <i>in vitro</i>	129
Mature miR-433-3p regulates the translation of RanBP1 mRNA containing an extended 3'UTR	132
Discussion.....	141
REFERENCES.....	147
4 CONCLUSION AND PERSPECTIVE.....	154
REFERENCES.....	162
Appendix	
A IACUC APPROVAL.....	164
B PERMISSION LETTER.....	166

LIST OF TABLES

Table 2.1	Adapters are removed from a majority of Illumina sequencing reads.....	48
-----------	--	----

LIST OF FIGURES

Figure 2.1	Axoplasm samples extracted from sciatic nerve are free of cell body and glia cell contamination.....	46
Figure 2.2	Enriched axoplasmic RNA contains two distinct classes of small non-coding RNAs, miRNA and piRNA.....	50
Figure 2.3	Changes in axoplasmic miRNA profiles in response to nerve injury.....	53
Figure 2.4	Changes in axoplasmic miRNA repertoires in response to nerve injury.....	55
Figure 2.5	Validation of small-RNA sequencing data by absolute real time qPCR.....	57
Figure 2.6	Strategy to identify axonally localized mRNA target(s) of differentially regulated axoplasmic miRNAs.....	59
Figure 2.7	Ingenuity pathway analysis of mRNA targets of 7 up-regulated and 8 down-regulated axoplasmic miRNAs.....	60
Figure 3.1	Pre-miR-433 is selectively localized to distal axons of sensory neurons.....	103
Figure 3.2	Pre-miR-433 can drive the localization of <i>eGFP</i> reporter mRNA into distal axon of DRG neurons.....	111
Figure 3.3	<i>eGFP-pre-miR-433</i> mRNA is localized do distal axons and intra-axonally translatable.....	113
Figure 3.4	<i>eGFP-pre-miR-138-1</i> mRNA does not localize to axons of DRG neurons.....	115
Figure 3.5	Prediction of precursor miRNA structure based on thermodynamics.....	117

Figure 3.6	The terminal loop region of pre-miR-433 structure strongly governs the localization of <i>eGFP</i> reporter mRNA into axons.....	119
Figure 3.7	Stem region of pre-miR-433 structure alone is not sufficient to localize eGFP reporter mRNA into axons.....	121
Figure 3.8	Reporter <i>eGFP</i> mRNA is driven into distal axons by the terminal loop regions of pre-miR-433 structure and is locally translated.....	123
Figure 3.9	Axoplasmic levels of pre-miR433 and mature miR-433-3p <i>in vivo</i> is increased after nerve injury.....	126
Figure 3.10	Specific axonal miRNA precursors are processed into their corresponding mature miRNAs independently from the neuronal cell body.....	128
Figure 3.11	Transient transfection of miR-433-3p mimic attenuates axon growth in DRG neurons.....	132
Figure 3.12	miR-433-3p targets an mRNA encoding Ran binding protein 1.....	136
Figure 3.13	miR-433-3p negatively regulates RanBP1 expression in distal axons.....	138
Figure 3.14	miR-433-3p mediates silencing of RanBP1 expression by inducing transcript degradation.....	140

LIST OF ABBREVIATIONS

AGO	argonaute
AMPR	α -amino-3-hydroxy-5-methyl-4-isoxazolepropionic acid receptor
Ara C	cytosine arabinoside
Arc	activity-regulated cytoskeleton-associated protein
ASH1	asymmetric synthesis of HO
ATP5G1	ATP synthase
BDNF	brain derive neurotrophic factor
CaMKII	Ca ²⁺ /calmodulin-dependent kinase II alpha
CNS	central nervous system
COXIV	cytochrome c-oxidase subunit IV
DGCR8	DiGeorge syndrome critical region 8
DHX36	DEAH-box helicase
DIG	digoxigenin
DRG	dorsal root ganglia
eGFP	enhanced green fluorescent protein
ErbB3	receptor tyrosine-protein kinase family 3
FISH	fluorescence in situ hybridization
FRAP	fluorescence recovery after photobleaching

GAP43	growth associated protein 43
H1F0	histone 1 family member 0
KSRP	KH-type splicing regulatory protein
LIMKI	LIM kinase 1
LNA	locked nucleic acid
LTD	long-term depression
LTP	long-term potentiation
MAG	myelin associated protein
MAP2	microtubule associated protein 2
MBP	myelin basic protein
miRISC	micro RNA induced silencing complex
miRNA	micro RNA
mRNA	messenger RNA
NLS	nuclear localization signal
nt	nucleotide
OMgp	oligodendrocytes-myelin glycoprotein
p250GAP	Rho GTPase activating protien p25
PET	polyethylene tetrathalate
piRNA	piwi-interacting RNA
PNS	peripheral nervous system
pre-miRNA	precursor microRNA
pri-miRNA	primary microRNA

RanBP1	ran binding protein 1
RanGAP	ran GTPase activating protein
RBP	RNA binding protein
RISC	RNA induced silencing complex
rRNA	ribosomal RNA
RT-PCR	reverse transcription polymerase chain reaction
RT-qPCR	reverse transcription quantitative polymerase chain reaction
STAT3	signal transducer and activator of transcription 3
TRBP	trans activating response RNA binding protein
UTR	untranslated region
ZBP1	zipcode binding protein 1

ABSTRACT

Subcellular localization of messenger RNAs (mRNAs) is a conserved mechanism that enables highly polarized cells such as adult mammalian neurons to exert spatial and temporal control over protein synthesis. In neurons, hundreds, if not thousands, of mRNAs are transported into distal axons and undergo local translation. Intra-axonal protein synthesis has been implicated in axon growth and pathway finding during development and rapid injury response and regeneration in adult neurons. Although it is now clear that localized axonal protein synthesis plays an important role in regenerating axons, there has been little understanding of how these localized mRNA translation is temporally regulated.

MicroRNA (miRNA) is a major class of small non-coding RNAs that acts as a regulator of gene expression at the post-transcriptional level. Over the past decade, miRNA-mediated regulation of gene expression has been gaining functional importance in neurons. Recent studies have shown that specific miRNAs are highly enriched in distal axons. These axonally enriched miRNAs could serve as molecular switches for temporal regulation of local protein synthesis. To understand how axon-specific miRNAs respond to nerve injury, I conducted deep sequencing studies using purified axoplasmic RNA from the proximal nerve stump of injured rat sciatic nerve. My sequencing studies identified 141 different miRNAs in rat sciatic nerve axoplasm.

Sixty-three of these miRNAs showed significant differential changes in their levels at five time points following nerve injury compared to uninjured sham operated controls. Bioinformatics analysis of predicted axonal mRNA targets of the differentially altered miRNAs revealed that their potential targets were involved in numerous neurological functions in ER response, cytoskeleton dynamics, vesicle formation, neuro-degeneration and-regeneration. These results suggest a vital role of axoplasmic miRNA in the regenerative response for the first time.

Although the role of miRNA-mediated regulation of intra-axonal protein synthesis is beginning to emerge, the mechanism underlying the translocation of specific miRNAs into distal axons remains unknown. Our lab and others showed that both miRNA precursors (pre-miRNAs) and protein components of their processing machinery such as Dicer and KH-type splicing regulatory protein (KSRP) were localized to axons. Based on these findings, I hypothesized that a subset of pre-miRNAs were selectively localized to distal axons, where they were subsequently processed to give rise to biologically active mature miRNAs that function to regulate specific intra-axonal mRNA translation. My results showed that the terminal loop region of axonally localizing pre-miR-433 structure contained a *cis*-element(s) that strongly governed the localization of RNA to distal axons. Using a compartmentalized culture system, I further demonstrated that selective pre-miRNAs (including pre-miR-433) were processed into the corresponding mature miRNAs in the axonal compartment independent of the cell body. To determine the biological function of mature miR-433-3p, I performed gain of function studies through transient

transfection of miR-433-3 mimic in cultured DRG neurons. My results showed that miR-433-3p negatively regulated the expression of Ran binding protein 1 in the growth cone leading to a significant decrease in axonal length.

Altogether, the studies presented in this dissertation provide new insight into the mechanism of differential expression of miRNAs via active transport of the pre-miRNAs, which consequently are processed to corresponding miRNAs and their neurological roles in axon regeneration following injury.

Chapter 1

INTRODUCTION

Subcellular Localization of mRNAs

Subcellular localization of messenger RNAs (mRNAs) is a post-transcriptional regulation mechanism that enables cells to exert spatial control of protein function by determining the location and time where protein is produced. This mechanism is evolutionarily conserved and is used by organisms from prokaryotes to eukaryotes to compartmentalize different activities to specific domains. Although mRNA localization is generally thought to occur exclusively in eukaryotes, recent studies have shown that several mRNAs in bacteria are capable of migrating to specific domains of the cell (Montero Llopis et al., 2010; Nevo-Dinur et al., 2011; Buskila et al., 2014). For example, *Escherichia coli* (*E. coli*) *bgl* operon encodes three functionally different proteins that are necessary for the metabolism of aryl- β -glucosides. Monocistronic transcripts of these genes have been shown to localize to the subsequent locations of its respective gene products where they carry out special functions; *BglF* mRNA encoding membrane bound sugar permease is directed to the inner membrane, *BglG* mRNA encoding a transcription factor is directed to the cytosol, and *BglB* mRNA encoding soluble phosphor- β -glucosidase is directed to the pole (Nevo-Dinur et al, 2011). The existence of RNA localization mechanism in

prokaryotes highlights the importance and the fundamental requirement for organisms to restrict specific activities to distinct subcellular sites through spatial and temporal regulation of protein synthesis.

In eukaryotes, targeting mRNAs to specific subcellular sites becomes extremely important in arrays of biological processes that occur in diverse organisms, from single cells to vertebrates. In yeast, mRNA localization is required for the determination of mating type (Paquin and Chartrand 2008). During the budding process, *asymmetric synthesis of HO (ASH1)* mRNA is targeted to the bud tip during late anaphase for exclusive expression of ASH1 protein in the nucleus of the daughter cell, where it serves as a transcriptional repressor that inhibit mating type switching (Long et al., 1997; Takizawa et al., 1997). It is through this mechanism that yeast ensures mother and daughter cells have distinct mating type. In higher eukaryotes, spatial restriction of protein synthesis through mRNA localization provides a means for cells to respond to environmental cues. For example, migrating fibroblasts localize *β-actin* mRNAs to the lamellipodia to establish and maintain polarized movement by producing high concentration of β-actin protein at the leading edge (Condeelis and Singer, 2005). In *Drosophila*, regulation of spatially restricted gene expression through mRNA localization is necessary for the establishment of molecular asymmetries that coordinate early patterning and axis formation during development (Holt and Bullock, 2009). For example, 71 % of more than 3,000 mRNAs analyzed in *Drosophila* embryo using *in situ* hybridization localized to distinct subcellular domains (Lecuyer et al., 2007; Rangan et al., 2009) and mislocalization of these

mRNAs resulted in detrimental defects. Studies by the Lehman group showed that disruption of polar distribution of *oskar* mRNAs, whose proteins participate in the formation of germ plasm during oogenesis, as well as *nanos* and *bicoid* mRNAs whose proteins generate opposing gradient during embryonic development, led to the formation of a second abdomen in place of head and thorax (Ephrussi et al., 1991; Gavis et al., 1992). Taken together, mRNA localization enables compartmentalization of protein synthesis that is essential in diverse biological processes.

MRNA Localization in Neuronal Processes

In a highly polarized cell like neurons, the physical distance separating the distal processes including axons/dendrites from the cell body could be extreme, reaching more than 1,000-fold the diameter of the neuronal cell body. Under this extreme scenario where the length of some axons can exceed over one meter in human peripheral nerves, regulation of gene expression through selective targeting of mRNAs offers multiple advantages. First, localization of mRNAs coupled with regulated local translation allows neurons to decentralize the control over gene expression to individual subcellular compartments. This permits axons and dendrites to autonomously regulate protein synthesis and rapidly respond to their microenvironment and extracellular stimuli. Second, it is energetically more efficient to transport mRNA templates where they can be translated multiple times to generate many copies of proteins as needed than to transport individual proteins. Lastly, since mRNAs are translationally repressed during transport, inappropriate protein activities

are suppressed until they reach their final destination. For example, myelin basic protein (MBP) is a membrane fusion protein that is involved in the compaction such as myelination around axons. The activity of MBP would adversely compromise cell functions if it was expressed or accumulated at inappropriate subcellular locations.

Transport and localization of mRNAs into neuronal dendritic and axonal compartments is precisely regulated. It appears that transcripts that are targeted into dendrites and axons encode functionally specialized proteins rather than those of housekeeping proteins. For example, mRNAs encoding proteins with specialized synaptic function that are localized into dendrites such as calcium/calmodulin-dependent kinase II alpha (CaMKII α), activity-regulated cytoskeleton-associated protein (Arc), α -amino-3-hydroxy-5-methyl-4-isoxazolepropionic acid receptor (AMAPR), and *N*-methyl-D-aspartate receptor (NMDAR) play key roles in modulating dendrite spine morphology and mediating synaptic plasticity (Steward et al., 1998; Bramham and Wells, 2007; Andreassi and Ricco, 2009; Wang et al., 2010). Likewise, transcripts of proteins that are highly abundant in the axonal compartment such as Tau, β -actin, and Growth Associated Protein 43 (GAP43) play essential roles in axon outgrowth, pathfinding, and structural maintenance (Leung et al., 2006; Yao et al., 2006; Willis et al., 2007; Welshhans and Bassell, 2011). The precise targeting of mRNAs to distinct subcellular locations within neurons suggests that neurons use highly selective and regulated mechanisms to confer differential distribution of a subset of transcripts.

Transport and localization of mRNAs to neuronal processes is a complex process that requires both *cis*-elements that physically reside within the localizing transcript and *trans*-acting RNA binding proteins (RBPs). Localization *cis*-elements are molecular “zipcodes” mostly found in the 3’ untranslated regions (3’UTRs) of mRNAs that direct specific transcripts to their final subcellular locations. For example, the 3’UTR of *CaMKII α* mRNA contains multiple localization elements needed for its transport into dendrites. Deletion of the localization *cis*-element within the 3’UTR impaired selective localization of the *CaMKII α* mRNAs (Miller et al., 2002), indicating that the *cis*-element present in the 3’UTR of localizing transcripts is necessary for their subcellular localization. Additionally, recognition of localization *cis*-element by *trans*-acting RBPs is necessary for the transport of mRNAs to neuronal processes. For example, localization of *β -actin* mRNA into axonal growth cones requires a 54 nucleotide (nt) zipcode or localization *cis*-element in the 3’UTR that is targeted by a *trans*-acting RBP called zipcode binding protein 1 (ZBP1) (Bassell et al., 1998; Kislauskis et al., 1993). Disruption of ZBP1 binding to the 54 nt localization *cis*-element by antisense oligonucleotides has been shown to hinder the localization of *β -actin* mRNAs into growth cones of developing axons (Zhang et al., 2001). Furthermore, an *in vivo* study using adult dorsal root ganglia (DRG) neurons cultured from haploinsufficient *ZBP1^{+/-}* mice showed a significant reduction in axonal *β -actin* mRNAs compared to *ZBP^{+/+}* neurons (Donnelly et al., 2011). Together these studies

point to the necessity of both localization *cis*-element and *trans*-acting RBPs in directing mRNA transport.

Significance of Local Protein Synthesis in Neurons

Local protein synthesis in dendrites

Neurons are morphologically subdivided into dendritic, somal (cell body), and axonal compartments. Traditionally, the soma had been thought to be the source for all protein synthesis until Steward and Levy visually confirmed the presence of polyribosomes at the base of dendritic spines using electron microscopy in the early 1980s, hinting at the possibility that dendrites have the capacity for local protein synthesis (Steward et al., 1982). Following this observation, subsequent work has focused on the functional role of local protein synthesis in the post-synaptic compartment. The Schuman lab was the first to show that local protein synthesis in post-synaptic spines was required for neurotrophin-induced synaptic plasticity in rat hippocampal neurons (Kang and Schuman, 1996). Since then, local protein synthesis in neuronal dendrites has been implicated in structural and functional physiology of the synapse (Frey et al., 1988; Jiang and Shuman, 2002; Sutton and Shuman, 2005).

A number of studies using physiological models of synaptic plasticity showed that translation of dendritically localized mRNAs play a role in the regulation of synaptic function. For example, mRNAs encoding activity-regulated cytoskeleton-associated protein (Arc) have been shown to be selectively transported to active post-

synaptic compartments where it undergoes rapid translation in response to specific patterns of synaptic activity (Lyford et al., 1995; Steward et al., 1998; Guzowski et al., 1999). In addition, a series of *in vitro* and *in vivo* studies have demonstrated that locally synthesized Arc protein is involved in the internalization of AMPA receptor in active post-synaptic spines (Chowdhury et al., 2006; Rial Verde et al., 2006; Shepherd et al., 2006) and, thereby, reduces the synaptic strength leading to long-term depression (LTD). CaMKII α is a kinase that phosphorylates key proteins (AMPA subunit, GluR1, and AMPAR auxiliary proteins) that are important in enhancing excitatory synaptic transmission (Hayashi et al., 2000). *In vivo* studies on dendritic localization of mRNA encoding CaMKII α revealed that its local translation is essential in mediating long-term potentiation (LTP) and memory consolidation (Ouyang et al., 1999; Miller et al., 2002; Lisman et al., 2002). Taken together, these studies emphasize the importance of dendritically synthesized proteins in synaptic function.

Local protein synthesis in axons – developing axons

In contrast to the excitement in neurobiology generated by the possibility of dendritic protein synthesis, local protein synthesis in pre-synaptic terminals was quite controversial. This was primarily due to the lack of direct evidence demonstrating the presence of translational machinery in mammalian axons (Lasek et al., 1973). As image resolution and detection sensitivity greatly improved in electron microscopy and immunochemistry techniques, numerous studies have since confirmed the

presence of ribosomal RNAs (rRNAs), mRNAs, and active translational machinery in both developing and mature axons (Giuditta et al., 1991; Deitch and Banker, 1993; Zheng et al., 2001; Merianda et al., 2009).

Functional studies in developing neurons have shown that local axonal protein synthesis contributes to growth cone turning and axon pathfinding (Campbell and Holt, 2001; 2003). During development, neurons must extend axons over long distances to innervate specific targets. To find their targets, axons rely on a dynamic structure at the axonal-tips called a growth cone. Growth cones are highly motile and exhibit chemotropic responses to molecular cues that are expressed in the surrounding environment. These chemotropic guidance cues provide navigational directions for the growing axons by acting as attractants or repellants depending on receptors that are present on the surface of the growth cone (Colamario and Tessier-Lavigne, 1995; Kobayashi et al., 1997). Initial studies in rodent models showed that severed axons from the cell bodies not only were able to consistently find their target but also exhibited appropriate responses to chemotropic guidance cues, netrin-1 (attractive response) and semaphorin3A (repulsive response) (Shaw and Bray, 1977; Campbell and Holt, 2001). Interestingly, these responses were abolished in the presence of translational inhibitors suggesting that local protein synthesis was required for chemotropic-induced growth cone responses (Campbell and Holt 2001; Wu et al., 2005). This observation led researchers to further identify newly synthesized axonal proteins and their roles in regulating growth cone responses.

Subsequent studies revealed that directional growth cone steering is mediated by chemotropic cues induced by local synthesis of cytoskeletal proteins and their regulators (Leung et al., 2006; Yao et al., 2006). For example, gradients of netrin-1 have been shown to induce asymmetrical translation of β -actin mRNAs in the growth cone. Locally synthesized β -actin contributes to asymmetrical formation of filopodial and lamellopodial protrusion and eventually caused the axon to turn towards the attractive gradient (Shestakova et al., 2001; Condeelis and Singer, 2005). This attractive response of growth cone was blocked when axonal synthesis of β -actin proteins was inhibited by antisense oligonucleotides to the zipcode sequences within 3'UTR (Leung et al., 2006) or antisense morpholino oligonucleotide against the AUG start site of β -actin mRNA (Yao et al., 2006). Conversely, a gradient application of a chemo-repellent, slit2, induced local synthesis of an actin depolymerizing protein called cofilin-1 within the growth cone (Piper et al., 2006). This asymmetrical increase of cofilin-1 induced by local protein synthesis led to growth cone collapse and ultimately caused the growing axon to turn away from the repellent molecule. Collectively, these studies show that local protein synthesis contributes to growth cone remodeling.

Local protein synthesis in axons – Mature axons

The capacity for axons to synthesize proteins decreases dramatically as they mature (Piper and Holt, 2004; Verma et al., 2005). This is correlated with a significant reduction of axonal rRNA and mRNA observed in cultured hippocampal

and cortical neurons as they differentiate and form synapses (Bassel et al., 1994; Kleiman et al., 1990). However, several reports indicated that rRNA and mRNA were still present in the axonal compartment of a number of mature neurons including the goldfish mauther neurons, mammalian hypothalamic neurons, olfactory neurons, and dorsal root ganglion (DRG) neurons (Weiner et al., 1996; Trembleau et al., 1996; Ressler et al., 1994; Vassar et al., 1994; Koenig and Martin, 1996; Koenig et al., 2000). Even though mounting evidence showed that mature axons were capable of local mRNA translation, it was not until recently that studies in regenerating mammalian axons shed light on the biological relevance of intra-axonal protein synthesis in adult neurons. Studies in the Twiss lab showed that axons of sensory neurons preconditioned with nerve injury can robustly synthesize protein and regrow to some extent *in vitro* even in the absence of the neuronal cell body (Zheng et al., 2001). Furthermore, blocking protein synthesis in these regenerating axons led to growth cone collapse and rapid axon retraction when the communication with the cell bodies was compromised by axon transection or by inhibiting axonal transport (Zheng et al., 2001). Altogether, these findings indicate that intra-axonal protein synthesis plays a functional role in facilitating axon regeneration in adult sensory neurons (Zheng et al., 2001; Verma et al., 2005).

Local protein synthesis in axons – Injured axons

Intra-axonal translation not only contributes to the structural integrity of the regenerating distal axon but also provides a means for injured axons to communicate

and coordinate gene expression between the cell body. Pioneering works in axon regeneration suggest that macromolecule retrograde signals play a role in the regenerating process. This was primarily based on observational changes in neuronal morphology induced by the axoplasm of injured nerve (Hanz and Fainzilber, 2006). In *Aplysia*, microinjection of the axoplasm isolated from injured nerves into the cell body of naïve (uninjured) neurons elicited both, growth and survival responses (Zhang and Ambron, 2000). In rodents, DRG neurons preconditioned with sciatic nerve lesion several days prior to culture displayed elongating axonal growth in contrast to branching axonal morphology typically seen in naïve DRG culture (Smith and Skene, 1997). The work in the Fainzilber lab demonstrated that injury to the peripheral nerve triggered rapid intra-axonal mRNA translation of retrograde transporting protein component, Importin- β 1 (Hanz et al., 2003).

Importin- β 1 is a member of importin/karyopherin family that acts as a carrier to facilitate the transport of cargo proteins bearing nuclear localization signal (NLS) from the cytoplasm into the nucleus (Perry and Fainzilber, 2009). Initially, importins were thought to be restricted around the nuclear pore periphery. However, the work in the Fainzilber lab showed that both importin- α and importin- β were present in axons of cultured sensory neurons. Interestingly, even though importin- α proteins were found to be present in the axoplasm of both naïve and injured peripheral nerve, importin- β proteins were undetectable in the axoplasm under normal condition until axons are injured (Hanz et al., 2003). Upon nerve injury, local synthesis of importin- β led to the formation of importin α/β complex containing injury signal protein cargos

that retrogradely transported into the cell body by dynein motor and subsequently activate gene transcriptions that are necessary for neuronal survival and axon regeneration.

Studies in the Fainzilber lab also showed that regulation of importins mediated retrograde transport relied on localized mRNA translation of a Ran GTPase effector, Ran binding protein 1 (RanBP1) (Yudin et al., 2008). To prevent unintended injury signaling, the formation of importin α/β complex is tightly regulated by axonal RanGTPase system. Under normal axonal condition, the interaction between importin- α and importin- β subunits and their binding to the protein cargo is prevented by bound-RanGTP. Following nerve injury, intra-axonal synthesis of RanBP1 stimulates the dissociation of RanGTP from importins and allows the formation of retrograde injury signaling complex. To prevent re-association of RanGTP and importins, RanGTPase activating protein (RanGAP) is recruited to the injury site and rapidly hydrolyses RanGTP to RanGDP (Yudin et al., 2008). Together, this mechanism ensures that newly synthesized signaling proteins at the injury site are efficiently incorporated into the retrograde transport complex.

Studies in multiple labs have since uncovered a variety of axonally synthesized retrograde injury signaling proteins induced by nerve lesions. The involvement of importins in retrograde transport suggests that cargo proteins of retrograde injury signaling complex are likely to be transcription factors, since members of importin superfamily are known to interact with proteins bearing nuclear localization signal (NLS). Consistent with this speculation, Ben-Yaakvo et al. (2012) showed that

mRNA encoding the transcription factor, signal transducer and activator of transcription 3 (STAT3), is rapidly translated at the injury site in response to axon injury in both *in vitro* and *in vivo* rodent models. Newly synthesized STAT3 is activated by phosphorylation (pSTAT3) and subsequently undergoes importin mediated retrograde transport via NLS domain to the nucleus. In the cell body, pSTAT3 activates gene expression that promotes neuronal survival following peripheral nerve injury.

Besides transcription factors, intra-axonal synthesis of a scaffolding protein also contributed to retrograde injury signaling in injured axon. For example, Perlson et al. (2005) has shown that a soluble fragment of intermediate filament, vimentin, is generated in the axoplasm of injured nerves by local translation and subsequently undergoes calpain mediated cleavage. Since vimentin can directly interact with both activated (phosphorylated) Erk1/2 (Erk1/2 is phosphorylated at the site of axonal injury) and importin β , locally generated vimentin at the site of axon injury serves as a scaffolding protein linking non-NLS bearing protein cargos to importin mediated retrograde trafficking (Perlson et al., 2005).

Collectively, the works discussed above indicate that selective localization and subsequent local translation of axonal mRNAs play important functional roles in both developing and mature axons as well as regenerating axons after injury. In many cases, intra-axonal mRNA translation must be precisely activated at specific subcellular locations at an appropriate moment of time. Although previous studies had shed some light on spatial regulation of axonal mRNAs, the mechanism underlying the

temporal control of mRNA translation in axon remained poorly understood. Recently, a novel class of non-coding RNAs that play a role in regulating gene expression at the post-transcriptional level called microRNAs (miRNAs) were found in the axonal compartment of sensory neurons (Natera-Naranjo et al., 2010). These findings suggest the involvement of miRNA in axonal function and hint at the possibility that miRNA-mediated translational silencing pathway may play a role in spatiotemporal regulation of intra-axonal protein synthesis.

MicroRNAs are Small Non-coding Regulatory RNAs

MicroRNAs are a class of 18 – 25 nucleotides single stranded small non-coding RNAs that regulate gene expression at the post-transcriptional level by binding, most often, to the 3'UTR of target mRNAs to induce translational repression or transcript degradation (Bartel, 2004; Kim, 2005). These small regulatory RNAs are ubiquitously encoded in the genomes of both plants and animals with notably high sequence conservation across species. For example, a genome-wide computation approach based on primary sequence and secondary structure alignment showed that miR-854 family is expressed in plant, nematode, rodent, and human (Arteaga-Vazquez et al., 2006). It is also noteworthy that even across diverse species, miR-854 regulates common mRNA targets (Hill et al., 2014; Pogue et al., 2014). This evolutionarily conserve mechanism indicates the importance of miRNA-mediated regulation of eukaryotic transcriptome.

MicroRNAs are encoded in various locations within the genome. Depending on the genomic context of where miRNAs are found, they are either classified as “intergenic” miRNAs or “intronic” miRNAs. MicroRNAs that reside in the intergenic regions are transcribed as an independent entity, while miRNAs that are located in the intron regions of protein-coding gene are co-transcribed and co-expressed with their host gene (Lee et al., 2004).

In mammalian cells, most miRNA genes are transcribed by RNA polymerase II, and in some cases RNA polymerase III, to generate a long primary miRNA (pri-miRNA) (Cai et al., 2004; Lee et al., 2004). This pri-miRNA transcript can vary in size ranging from hundreds to thousands of nucleotides in length and occasionally contains sequences for multiple different miRNAs (Monteys et al., 2010; Lee et al., 2002; Roush et al., 2008). Following transcription, miRNA maturation starts in the nucleus with the cleavage of pri-miRNAs by a microprocessor complex containing an RNase III enzyme, Drosha, and a double stranded RNA binding protein DiGeorge syndrome critical region 8 (DGCR8) into a 70 – 120 nt long hairpin structure known as precursor miRNAs (pre-miRNAs) (Kim, 2005; Ha and Kim, 2014). Alternatively, for intronic miRNAs, pre-miRNAs are generated as a product of premature mRNA splicing event and are independent of Drosha/DGCR8 processing (Sibley et al., 2012). Once pre-miRNA is generated in the nucleus, it is exported into the cytoplasm by exportin-5 and further processed by another endonuclease of RNase III family, Dicer and its co-factor, TAR RNA binding protein (TRBP) to create a ~ 22 nt miRNA duplex. The miRNA duplex consists of a guide strand/predominant strand (miR) and

passenger strand/less abundant strand (miR*). Guide strand is typically thermodynamically less stable at the 5' terminus and is selected to function as mature miRNA, while the passenger strand is degraded (Khvorova et al., 2003; Schwarz et al., 2003; Kim, 2005). However, occasionally both strands of the miRNA duplex can function as mature miRNAs (Chiang et al., 2010; Saugstad et al., 2010). In the cytoplasm, mature miRNA directly associates with Argonaute (AGO) protein within the RNA induced silencing complex (RISC) and guide this complex to target mRNAs to mediate translational regulation.

In animal cells, miRNAs identify their target transcripts based on the complementarity of sequences that are typically located in the 3'UTR of the target mRNAs. The ability of miRNAs to elicit translational repression depends on Watson-Crick pairing of first 2 – 8 nt at the 5' proximal region of the miRNA called the “seed region” to their target mRNAs (Filipowicz et al., 2008; Bartel et al., 2009). Consistent with the requirement for the seed region in miRNA target recognition, the 5' proximal region has been shown to be the most conserved portion of metazoan miRNAs (Lim et al., 2005). Although pairing of the 3' region of miRNA to the target mRNAs is not required for translational regulation, 3 – 4 continuous perfect pairing centered on nucleotides 13 – 17 of miRNA can stabilize miRNA:mRNA interaction and compensate for a single nucleotide bulge or mismatch in the seed region (Yekta et al., 2004; Grimson et al., 2007). Furthermore, the presence of multiple miRNA binding sites in the target mRNA has been shown to significantly increase silencing efficiency (Doench and Sharp, 2004; Bartel, 2004).

Upon recognition of target mRNAs, miRNA exerts control over gene expression by two post-transcriptional mechanisms, mRNA degradation and/or translational repression. mRNA degradation pathway occurs when there is a high degree of miRNA:mRNA complementarity. In this case, perfect base pair complementarity allows AGO-catalyzed cleavage of the target transcript and facilitates mRNA decay through other degradation mechanisms such as deadenylation, decapping, and exonucleolysis. MicoRNA can also silence gene expression through translational repression. Although the mechanism of miRNA-mediated translational repression is still unclear, recent studies showed that this process could take place either during translation initiation phase or during post-translational initiation. Generally, translation initiation requires the interaction of eIF4E with the 5' cap of mRNA. Several studies show that miRNA-RISC complex (miRISC) bound to the 3'UTR of mRNA competes with eIF4E for the binding of the 5' caps leading to translational inhibition by preventing the recruitment of ribosomes (Chen and Gao, 2017). Even if translation has already taken place, miRISC can still repress translation by blocking translational progression and causes ribosomes to drop off from the mRNA.

Since only pairing of the seed region in miRNA:mRNA is required for translational repression, a single miRNA could target hundreds of different mRNAs. Conversely, individual mRNA may contain multiple binding sites for different miRNAs (Bartel, 2004). This suggests that miRNAs are not only capable of simultaneously regulating multiple gene expression but also cooperatively fine-tune

the expression of a single mRNA. A recent study estimated that approximately 60% of mammalian transcriptome are regulated by miRNAs (Friedman et al., 2009). Thus, it is not surprising that miRNAs are involved in various cellular processes.

MicroRNA Localizes to Neuronal Dendrites and Axons

Recent studies show that miRNAs are differentially distributed in neuronal processes. Using laser capture micro-dissection technique, Kye et al. (2007) profiled miRNA population in isolated somatic and dendritic compartments. *In situ* hybridization and Real Time quantitative PCR (RT-qPCR) analysis revealed that a small population of miRNAs is in fact enriched in dendrites compared to the soma (Kye et al., 2007). Since then, a number of miRNAs have been implicated in post-synaptic functions and physiology. For example, brain specific miR-134 has been shown to localize to the synpato-dendritic compartment where it negatively regulates spine development by inhibiting the expression of LIM Kinase 1 (LIMK1). Since LIMK1 controls actin filament dynamics and promotes spine outgrowth, miR-134 restricts the growth of dendritic spine in the absence of synaptic activity by limiting local synthesis of LIMK1 proteins (Schratt et al., 2006). In another example, dendritically localized miR-132 has been shown to enhance dendritic morphogenesis and regulate synaptic plasticity by repressing the expression of Rho GTPase activating protein p250 (p250GAP), a protein that regulates spine formation by controlling the activities of Rac1 and RhoA (Impey et al., 2010). Subsequent studies showed that levels of dendritic miRNAs were altered following long-term potentiation and thus

confirmed the involvement of miRNA pathway in synaptic function and plasticity (Ye et al., 2016).

In contrast to dendritic miRNAs, very little is known about the functional role of axonal miRNAs. It was only recently that critical components of miRNA-mediated silencing machinery were shown to be localized to axon and growth cones of DRG neurons and rodent sciatic nerve (Hengst et al., 2006; Murashov et al., 2007). These axonal microRNA induced silencing complex (miRSIC) associated proteins were shown to be functional and capable of silencing specific mRNA (Hengst et al., 2006; Murashov et al., 2007). This provides a compelling evidence to suggest that axons are capable of miRNA-mediated regulation of local protein synthesis.

Interestingly, studies on isolated axonal RNA from compartmentalized culture system detected over a 100 different mature miRNAs in the axonal compartment of sensory neurons (Netera-Naranjo et al., 2010; Sasaki et al., 2014). Microarray and RT-qPCR analysis showed that some of these miRNAs were highly enriched in axons compared to the soma. Among those axonally abundant miRNAs are miR-16 and miR-338. Mir-16 has been shown to regulate axonal protein synthesis activity by modulating local expression of eukaryotic translational initiation factor, eIF2B2 and eIF4G2, by binding to the 3'UTR of their mRNAs (Kar et al., 2013). On the other hand, miR-338 has been shown to modulate axon metabolism and function by negatively regulating the expression of mitochondria proteins, cytochrome c-oxidase subunit IV (COX IV) and ATP synthase (ATP5G1) (Achrafi et al., 2008). Furthermore, *in vitro* studies in sympathetic neurons showed that an increase in the

axonal level of either miR-16 or miR-338 resulted in attenuation of axon outgrowth (Aschrafi et al., 2008; Kar et al., 2013). It is important to note that both miR-16 mediated regulation of axonal protein synthesis activity and miR-338 mediated regulation of axonal metabolism are the result of an additive effect of miR-16 on eIF2B2 and eIF4G3 expressions, and miR-338 on COXIV and ATP5G1 expressions, respectively. Taken together, axonally enriched miRNAs are likely to play a role as a molecular switch that fine-tunes the expression of axonal proteins and modulates axonal functions. Although miRNA localization in axons is notable and its role in regulating intra-axonal protein synthesis is beginning to emerge, the mechanisms underlying differential enrichment of these specific miRNAs within subcellular regions of neurons remain unknown.

Several models have been proposed for the selective targeting and localization of miRNAs into axons. These hypotheses include co-transport of miRNA with its associated target mRNA in the transport granule and the delivery of pre-miRNAs followed by subsequent local processing of the precursors into functional mature miRNAs (Kosik, 2006). Studies in our laboratory and others have shown that distal axons of rat sensory neurons contain components of miRNA biogenesis machineries such as Dicer and KH-type splicing regulatory protein (KSRP) that bind and promote the maturation of microRNA precursors (Kim et al., 2015, Henst et al., 2006; Murashov et al., 2007; Wu et al., 2011; 2012). Using RT-qPCR analysis in combination with fluorescence *in situ* hybridization (FISH), we further showed that a subset of precursor miRNAs were selectively targeted into axons of adult DRG

neurons (Kim et al., 2015). The levels of these axonal pre-miRNAs were shown to dramatically alter in response to sciatic nerve crush injury, suggesting that nerve injury could perhaps trigger changes in the population of axonal miRNAs. Collectively, these findings provide compelling evidence to support the hypothesis that pre-miRNAs are selectively targeted into axons, where they are locally processed to give rise to functional mature miRNAs that would in turn regulate intra-axonal protein synthesis.

Focus of Current Study

The studies in this dissertation primarily focus on understanding the mechanism underlying axon localization of miRNAs and the role of miRNAs in regenerating nerve. In the following chapter, I will address axon specific miRNA profiles in regenerating nerves. In chapter 3, I will address miRNA transporting mechanism and the functional role of axonally localized miRNA in axon regeneration following injury.

REFERENCES

- Andreassi C, Riccio A (2009) To localize or not to localize: mRNA fate is in 3'UTR ends. *Trends Cell Biol* 19:465-474.
- Arteaga-Vazquez M, Caballero-Perez J, Vielle-Calzada JP (2006) A family of microRNAs present in plants and animals. *Plant Cell* 18:3355-3369.
- Aschrafi A, Schwechter AD, Mameza MG, Natera-Naranjo O, Gioio AE, Kaplan BB (2008) MicroRNA-338 regulates local cytochrome C oxidase IV mRNA levels and oxidative phosphorylation in the axons of sympathetic neurons. *J Neurosci* 28:12581-12590.
- Bartel DP (2004) MicroRNAs: genomics, biogenesis, mechanism, and function. *Cell* 116:281-297.
- Bartel DP (2009) MicroRNA Target Recognition and Regulatory Functions. *Cell* 136:215-233.
- Bassel (1994) Association of poly(A) mRNA with microtubules in cultured neurons. *Neuron* 12:571-582.
- Bassell GJ, Zhang H, Byrd AL, Femino AM, Singer RH, Taneja KL, Lifshitz LM, Herman IM, Kosik KS (1998) Sorting of beta-actin mRNA and protein to neurites and growth cones in culture. *J Neurosci* 18:251-265.
- Ben-Yaakov K, Dagan SY, Segal-Ruder Y, Shalem O, Vuppalanchi D, Willis DE, Yudin D, Rishal I, Rother F, Bader M, Blesch A, Pilpel Y, Twiss JL, Fainzilber M (2012) Axonal transcription factors signal retrogradely in lesioned peripheral nerve. *EMBO J* 31:1350-1363.
- Bramham CR, Wells DG (2007) Dendritic mRNA: transport, translation and function. *Nat Rev Neurosci* 8:776-789.
- Buskila Aa A, Kannaiah S, Amster-Choder O (2014) RNA localization in bacteria. In: *RNA Biol*, pp 1051-1060.
- Cai X, Hagedorn CH, Cullen BR (2004) Human microRNAs are processed from capped, polyadenylated transcripts that can also function as mRNAs. *RNA* 10:1957-1966.
- Campbell DS, Holt CE (2001) Chemotropic responses of retinal growth cones mediated by

rapid local protein synthesis and degradation. *Neuron* 32:1013-1026.

Campbell DS, Holt CE (2003) Apoptotic pathway and MAPKs differentially regulate chemotropic responses of retinal growth cones. *Neuron* 37:939-952.

Chiang HR, Schoenfeld LW, Ruby JG, Auyeung VC, Spies N, Baek D, Johnston WK, Russ C, Luo S, Babiarz JE, Belloch R, Schroth GP, Nusbaum C, Bartel DP (2010) Mammalian microRNAs: experimental evaluation of novel and previously annotated genes. *Genes Dev* 24:992-1009.

Chowdhury S, Shepherd JD, Okuno H, Lyford G, Petralia RS, Plath N, Kuhl D, Huganir RL, Worley PF (2006) Arc/Arg3.1 interacts with the endocytic machinery to regulate AMPA receptor trafficking. *Neuron* 52:445-459.

Colamarino SA, Tessier-Lavigne M (1995) The axonal chemoattractant netrin-1 is also a chemorepellent for trochlear motor axons. *Cell* 81:621-629.

Condeelis J, Singer RH (2005) How and why does beta-actin mRNA target? *Biol Cell* 97:97-110.

Deitch JS, Banker GA (1993) An electron microscopic analysis of hippocampal neurons developing in culture: early stages in the emergence of polarity. *J Neurosci* 13:4301-4315.

Doench JG, Sharp PA (2004) Specificity of microRNA target selection in translational repression. *Genes Dev* 18:504-511.

Donnelly CJ, Willis DE, Xu M, Tep C, Jiang C, Yoo S, Schanen NC, Kirn-Safran CB, van Minnen J, English A, Yoon SO, Bassell GJ, Twiss JL (2011) Limited availability of ZBP1 restricts axonal mRNA localization and nerve regeneration capacity. *EMBO J*, pp 4665-4677.

Elvira G, Wasiak S, Blandford V, Tong XK, Serrano A, Fan X, del Rayo Sanchez-Carbente M, Servant F, Bell AW, Boismenu D, Lacaille JC, McPherson PS, DesGroseillers L, Sossin WS (2006) Characterization of an RNA granule from developing brain. *Mol Cell Proteomics* 5:635-651.

Ephrussi A, Dickinson LK, Lehmann R (1991) Oskar organizes the germ plasm and directs localization of the posterior determinant nanos. *Cell* 66:37-50.

Filipowicz W, Bhattacharyya SN, Sonenberg N (2008) Mechanisms of post-transcriptional regulation by microRNAs: are the answers in sight? *Nat Rev Genet* 9:102-114.

- Frey U, Krug M, Reymann KG, Matthies H (1988) Anisomycin, an inhibitor of protein synthesis, blocks late phases of LTP phenomena in the hippocampal CA1 region in vitro. *Brain Res* 452:57-65.
- Friedman RC, Farh KK, Burge CB, Bartel DP (2009) Most mammalian mRNAs are conserved targets of microRNAs. *Genome Res* 19:92-105.
- Gavis ER, Lehmann R (1992) Localization of nanos RNA controls embryonic polarity. *Cell* 71:301-313.
- Giuditta A, Menichini E, Perrone Capano C, Langella M, Martin R, Castigli E, Kaplan BB (1991) Active polysomes in the axoplasm of the squid giant axon. *J Neurosci Res* 28:18-28.
- Grimson A, Farh KK, Johnston WK, Garrett-Engele P, Lim LP, Bartel DP (2007) MicroRNA targeting specificity in mammals: determinants beyond seed pairing. *Mol Cell* 27:91-105.
- Guzowski JF, McNaughton BL, Barnes CA, Worley PF (1999) Environment-specific expression of the immediate-early gene *Arc* in hippocampal neuronal ensembles. *Nat Neurosci* 2:1120-1124.
- Ha M, Kim VN (2014) Regulation of microRNA biogenesis. *Nature Reviews Molecular Cell Biology* 15:509.
- Hanz S, Fainzilber M (2006) Retrograde signaling in injured nerve--the axon reaction revisited. *J Neurochem* 99:13-19.
- Hanz S, Perlson E, Willis D, Zheng JQ, Massarwa R, Huerta JJ, Koltzenburg M, Kohler M, van-Minnen J, Twiss JL, Fainzilber M (2003) Axoplasmic importins enable retrograde injury signaling in lesioned nerve. *Neuron* 40:1095-1104.
- Hengst U, Cox LJ, Macosko EZ, Jaffrey SR (2006) Functional and selective RNA interference in developing axons and growth cones. *J Neurosci* 26:5727-5732.
- Hill JM, Zhao Y, Bhattacharjee S, Lukiw WJ (2014) miRNAs and viroids utilize common strategies in genetic signal transfer. *Front Mol Neurosci* 7:10.
- Holt CE, Bullock SL (2009) Subcellular mRNA localization in animal cells and why it matters. *Science* 326:1212-1216.

- Impey S, Davare M, Lesiak A, Fortin D, Ando H, Varlamova O, Obrietan K, Soderling TR, Goodman RH, Wayman GA (2010) An activity-induced microRNA controls dendritic spine formation by regulating Rac1-PAK signaling. *Mol Cell Neurosci* 43:146-156.
- Jiang C, Schuman EM (2002) Regulation and function of local protein synthesis in neuronal dendrites. *Trends Biochem Sci* 27:506-513.
- Kanai Y, Dohmae N, Hirokawa N (2004) Kinesin transports RNA: isolation and characterization of an RNA-transporting granule. *Neuron* 43:513-525.
- Kang H, Schuman EM (1996) A requirement for local protein synthesis in neurotrophin-induced hippocampal synaptic plasticity. *Science* 273:1402-1406.
- Kar AN, MacGibeny MA, Gervasi NM, Gioio AE, Kaplan BB (2013) Intra-axonal synthesis of eukaryotic translation initiation factors regulates local protein synthesis and axon growth in rat sympathetic neurons. *J Neurosci* 33:7165-7174.
- Khvorova A, Reynolds A, Jayasena SD (2003) Functional siRNAs and miRNAs exhibit strand bias. *Cell* 115:209-216.
- Kiebler MA, Bassell GJ (2006) Neuronal RNA granules: movers and makers. *Neuron* 51:685-690.
- Kim HH, Kim P, Phay M, Yoo S (2018) Identification of precursor microRNAs within distal axons of sensory neuron. *Journal of Neurochemistry* 134:193-199.
- Kim VN (2005) MicroRNA biogenesis: coordinated cropping and dicing. *Nat Rev Mol Cell Biol* 6:376-385.
- Kislauskis EH, Li Z, Singer RH, Taneja KL (1993) Isoform-specific 3'-untranslated sequences sort alpha-cardiac and beta-cytoplasmic actin messenger RNAs to different cytoplasmic compartments. *J Cell Biol* 123:165-172.
- Kleiman R, Banker G, Steward O (1990) Differential subcellular localization of particular mRNAs in hippocampal neurons in culture. *Neuron* 5:821-830.
- Kobayashi NR, Fan DP, Giehl KM, Bedard AM, Wiegand SJ, Tetzlaff W (1997) BDNF and NT-4/5 prevent atrophy of rat rubrospinal neurons after cervical axotomy, stimulate GAP-43 and α -tubulin mRNA expression, and promote axonal regeneration. *J Neurosci* 17:9583-9595.
- Koenig E, Martin R (1996) Cortical plaque-like structures identify ribosome-containing domains in the Mauthner cell axon. *J Neurosci* 16:1400-1411.

- Koenig E, Martin R, Titmus M, Sotelo-Silveira JR (2000) Cryptic peripheral ribosomal domains distributed intermittently along mammalian myelinated axons. *J Neurosci* 20:8390-8400.
- Kosik KS (2006) The neuronal microRNA system. *Nat Rev Neurosci* 7:911-920.
- Kye MJ, Gonçalves Ido CG (2014) The role of miRNA in motor neuron disease. *Front Cell Neurosci* 8.
- Kye MJ, Liu T, Levy SF, Xu NL, Groves BB, Bonneau R, Lao K, Kosik KS (2007) Somatodendritic microRNAs identified by laser capture and multiplex RT-PCR. *RNA* 13:1224-1234.
- Lasek RJ, Dabrowski C, Nordlander R (1973) Analysis of axoplasmic RNA from invertebrate giant axons. *Nat New Biol* 244:162-165.
- Lecuyer E, Yoshida H, Parthasarathy N, Alm C, Babak T, Cerovina T, Hughes TR, Tomancak P, Krause HM (2007) Global analysis of mRNA localization reveals a prominent role in organizing cellular architecture and function. *Cell* 131:174-187.
- Lee Y, Jeon K, Lee JT, Kim S, Kim VN (2002) MicroRNA maturation: stepwise processing and subcellular localization. *EMBO J* 21:4663-4670.
- Lee Y, Kim M, Han J, Yeom KH, Lee S, Baek SH, Kim VN (2004) MicroRNA genes are transcribed by RNA polymerase II. *EMBO J* 23:4051-4060.
- Leung KM, van Horck FP, Lin AC, Allison R, Standart N, Holt CE (2006) Asymmetrical beta-actin mRNA translation in growth cones mediates attractive turning to netrin-1. *Nat Neurosci* 9:1247-1256.
- Lim LP, Lau NC, Garrett-Engele P, Grimson A, Schelter JM, Castle J, Bartel DP, Linsley PS, Johnson JM (2005) Microarray analysis shows that some microRNAs downregulate large numbers of target mRNAs. *Nature* 433:769-773.
- Lisman J, Schulman H, Cline H (2002) The molecular basis of CaMKII function in synaptic and behavioural memory. *Nat Rev Neurosci* 3:175-190.
- Long RM, Singer RH, Meng X, Gonzalez I, Nasmyth K, Jansen RP (1997) Mating type switching in yeast controlled by asymmetric localization of ASH1 mRNA. *Science* 277:383-387.
- Lyford GL, Yamagata K, Kaufmann WE, Barnes CA, Sanders LK, Copeland NG, Gilbert DJ,

- Jenkins NA, Lanahan AA, Worley PF (1995) Arc, a growth factor and activity-regulated gene, encodes a novel cytoskeleton-associated protein that is enriched in neuronal dendrites. *Neuron* 14:433-445.
- McCoy CC (2012) Identification of miRNA-targeted cellular pathways in flavivirus-infected cells. In: Oregon Health & Science University.
- Merianda TT, Lin AC, Lam JS, Vuppalanchi D, Willis DE, Karin N, Holt CE, Twiss JL (2009) A functional equivalent of endoplasmic reticulum and Golgi in axons for secretion of locally synthesized proteins. *Mol Cell Neurosci* 40:128-142.
- Miller S, Yasuda M, Coats JK, Jones Y, Martone ME, Mayford M (2002) Disruption of dendritic translation of CaMKIIalpha impairs stabilization of synaptic plasticity and memory consolidation. *Neuron* 36:507-519.
- Montero Llopis P, Jackson AF, Sliusarenko O, Surovtsev I, Heinritz J, Emonet T, Jacobs-Wagner C (2010) Spatial organization of the flow of genetic information in bacteria. *Nature* 466:77-81.
- Monteys AM, Spengler RM, Wan J, Tecedor L, Lennox KA, Xing Y, Davidson BL (2010) Structure and activity of putative intronic miRNA promoters. *RNA* 16:495-505.
- Murashov AK, Chintalgattu V, Islamov RR, Lever TE, Pak ES, Sierpinski PL, Katwa LC, Van Scott MR (2007) RNAi pathway is functional in peripheral nerve axons. *FASEB J* 21:656-670.
- Natera-Naranjo O, Aschrafi A, Gioio AE, Kaplan BB (2010) Identification and quantitative analyses of microRNAs located in the distal axons of sympathetic neurons. In: *RNA*, pp 1516-1529.
- Nevo-Dinur K, Nussbaum-Shochat A, Ben-Yehuda S, Amster-Choder O (2011) Translation-independent localization of mRNA in *E. coli*. *Science* 331:1081-1084.
- Ouyang Y, Rosenstein A, Kreiman G, Schuman EM, Kennedy MB (1999) Tetanic stimulation leads to increased accumulation of Ca(2+)/calmodulin-dependent protein kinase II via dendritic protein synthesis in hippocampal neurons. *J Neurosci* 19:7823-7833.
- Paquin N, Chartrand P (2008) Local regulation of mRNA translation: new insights from the bud. *Trends Cell Biol* 18:105-111.
- Perlson E, Hanz S, Ben-Yaakov K, Segal-Ruder Y, Seger R, Fainzilber M (2005) Vimentin-dependent spatial translocation of an activated MAP kinase in injured nerve. *Neuron* 45:715-726.

- Perry RB, Fainzilber M (2009) Nuclear transport factors in neuronal function. *Semin Cell Dev Biol* 20:600-606.
- Piper M, Holt C (2004) RNA translation in axons. *Annu Rev Cell Dev Biol* 20:505-523.
- Piper M, Anderson R, Dwivedy A, Weinl C, van Horck F, Leung KM, Cogill E, Holt C (2006) Signaling mechanisms underlying Slit2-induced collapse of *Xenopus* retinal growth cones. *Neuron* 49:215-228.
- Pogue AI, Hill JM, Lukiw WJ (2014) MicroRNA (miRNA): Sequence and stability, viroid-like properties, and disease association in the CNS. *Brain Res* 0:73-79.
- Ramalingam P, Palanichamy JK, Singh A, Das P, Bhagat M, Kassab MA, Sinha S, Chattopadhyay P (2014) Biogenesis of intronic miRNAs located in clusters by independent transcription and alternative splicing. *RNA*, pp 76-87.
- Rangan P, DeGennaro M, Jaime-Bustamante K, Coux RX, Martinho RG, Lehmann R (2009) Temporal and spatial control of germ-plasm RNAs. *Curr Biol* 19:72-77.
- Ressler KJ, Sullivan SL, Buck LB (1994) Information coding in the olfactory system: evidence for a stereotyped and highly organized epitope map in the olfactory bulb. *Cell* 79:1245-1255.
- Rial Verde EM, Lee-Osbourne J, Worley PF, Malinow R, Cline HT (2006) Increased expression of the immediate-early gene *arc/arg3.1* reduces AMPA receptor-mediated synaptic transmission. *Neuron* 52:461-474.
- Roush S, Slack FJ (2008) The *let-7* family of microRNAs. *Trends Cell Biol* 18:505-516.
- Sasaki Y, Gross C, Xing L, Goshima Y, Bassell GJ (2014) Identification of axon-enriched microRNAs localized to growth cones of cortical neurons. *Dev Neurobiol* 74:397-406.
- Saugstad JA (2010) MicroRNAs as effectors of brain function with roles in ischemia and injury, neuroprotection, and neurodegeneration. *J Cereb Blood Flow Metab* 30:1564-1576.
- Schratt GM, Tuebing F, Nigh EA, Kane CG, Sabatini ME, Kiebler M, Greenberg ME (2006) A brain-specific microRNA regulates dendritic spine development. *Nature* 439:283-289.
- Schwarz DS, Hutvagner G, Du T, Xu Z, Aronin N, Zamore PD (2003) Asymmetry in the assembly of the RNAi enzyme complex. *Cell* 115:199-208.

- Shaw G, Bray D (1977) Movement and extension of isolated growth cones. *Exp Cell Res* 104:55-62.
- Shepherd JD, Rumbaugh G, Wu J, Chowdhury S, Plath N, Kuhl D, Huganir RL, Worley PF (2006) Arc/Arg3.1 mediates homeostatic synaptic scaling of AMPA receptors. *Neuron* 52:475-484.
- Shestakova EA, Singer RH, Condeelis J (2001) The physiological significance of beta -actin mRNA localization in determining cell polarity and directional motility. *Proc Natl Acad Sci U S A* 98:7045-7050.
- Sibley CR, Seow Y, Saayman S, Dijkstra KK, El Andaloussi S, Weinberg MS, Wood MJ (2012) The biogenesis and characterization of mammalian microRNAs of mirtron origin. *Nucleic Acids Res* 40:438-448.
- Smith DS, Skene JH (1997) A transcription-dependent switch controls competence of adult neurons for distinct modes of axon growth. *J Neurosci* 17:646-658.
- Stefani G, Slack FJ (2008) Small non-coding RNAs in animal development. *Nat Rev Mol Cell Biol* 9:219-230.
- Steward O, Levy WB (1982) Preferential localization of polyribosomes under the base of dendritic spines in granule cells of the dentate gyrus. *J Neurosci* 2:284-291.
- Steward O, Wallace CS, Lyford GL, Worley PF (1998) Synaptic activation causes the mRNA for the IEG Arc to localize selectively near activated postsynaptic sites on dendrites. *Neuron* 21:741-751.
- Sutton MA, Schuman EM (2005) Local translational control in dendrites and its role in long-term synaptic plasticity. *J Neurobiol* 64:116-131.
- Takizawa PA, Sil A, Swedlow JR, Herskowitz I, Vale RD (1997) Actin-dependent localization of an RNA encoding a cell-fate determinant in yeast. *Nature* 389:90-93.
- Trembleau A, Morales M, Bloom FE (1996) Differential compartmentalization of vasopressin messenger RNA and neuropeptide within the rat hypothalamo-neurohypophysial axonal tracts: light and electron microscopic evidence. *Neuroscience* 70:113-125.
- Vassar R, Chao SK, Sitcheran R, Nunez JM, Vosshall LB, Axel R (1994) Topographic organization of sensory projections to the olfactory bulb. *Cell* 79:981-991.
- Verma P, Chierzi S, Codd AM, Campbell DS, Meyer RL, Holt CE, Fawcett JW (2005)

- Axonal protein synthesis and degradation are necessary for efficient growth cone regeneration. *J Neurosci* 25:331-342.
- Wang DO, Martin KC, Zukin RS (2010) Spatially restricting gene expression by local translation at synapses. *Trends Neurosci* 33:173-182.
- Wang J, Liew OW, Richards AM, Chen YT (2016) Overview of MicroRNAs in Cardiac Hypertrophy, Fibrosis, and Apoptosis. *Int J Mol Sci*.
- Weiner OD, Zorn AM, Krieg PA, Bittner GD (1996) Medium weight neurofilament mRNA in goldfish Mauthner axoplasm. *Neurosci Lett* 213:83-86.
- Welshhans K, Bassell GJ (2011) Netrin-1-induced local beta-actin synthesis and growth cone guidance requires zipcode binding protein 1. *J Neurosci* 31:9800-9813.
- Willis DE, van Niekerk EA, Sasaki Y, Mesngon M, Merianda TT, Williams GG, Kendall M, Smith DS, Bassell GJ, Twiss JL (2007) Extracellular stimuli specifically regulate localized levels of individual neuronal mRNAs. *J Cell Biol* 178:965-980.
- Wu D, Raafat M, Pak E, Hammond S, Murashov AK (2011) MicroRNA machinery responds to peripheral nerve lesion in an injury-regulated pattern. *Neuroscience* 190:386-397.
- Wu D, Raafat A, Pak E, Clemens S, Murashov AK (2012) Dicer-microRNA pathway is critical for peripheral nerve regeneration and functional recovery in vivo and regenerative axonogenesis in vitro. *Exp Neurol* 233:555-565.
- Wu KY, Hengst U, Cox LJ, Macosko EZ, Jeromin A, Urquhart ER, Jaffrey SR (2005) Local translation of RhoA regulates growth cone collapse. *Nature* 436:1020-1024.
- Yao J, Sasaki Y, Wen Z, Bassell GJ, Zheng JQ (2006) An essential role for beta-actin mRNA localization and translation in Ca²⁺-dependent growth cone guidance. *Nat Neurosci* 9:1265-1273.
- Ye Y, Xu H, Su X, He X (2016) Role of MicroRNA in Governing Synaptic Plasticity. *Neural Plast* 2016:4959523.
- Yekta S, Shih IH, Bartel DP (2004) MicroRNA-directed cleavage of HOXB8 mRNA. *Science* 304:594-596.
- Yudin D, Hanz S, Yoo S, Iavnilovitch E, Willis D, Gradus T, Vuppalachchi D, Segal-Ruder Y, Ben-Yaakov K, Hieda M, Yoneda Y, Twiss JL, Fainzilber M (2008) Localized regulation of axonal RanGTPase controls retrograde injury signaling in peripheral nerve. *Neuron* 59:241-252.

Zhang HL, Eom T, Oleynikov Y, Shenoy SM, Liebelt DA, Dichtenberg JB, Singer RH, Bassell GJ (2001) Neurotrophin-induced transport of a beta-actin mRNP complex increases beta-actin levels and stimulates growth cone motility. *Neuron* 31:261-275.

Zhang XP, Ambron RT (2000) Positive injury signals induce growth and prolong survival in *Aplysia* neurons. *J Neurobiol* 45:84-94.

Chapter 2

DYNAMIC CHANGE OF AXON-SPECIFIC MICRORNAS IN REGENERATING SCIATIC NERVE

The work in this chapter was published in the journal *PLoS One*.

Dynamic Change and Target Prediction of Axon-Specific MicroRNAs in Regenerating Sciatic Nerve.

Phay M, Kim HH, and Yoo S.

PLoS One. 2015 Sep 2;10(9):e0137461. doi: 10.1371/journal.pone.0137461

Introduction

Neurons are the basic building unit of the nervous system. These cells are highly specialized and are responsible for transmitting information over long distances in both electrical and chemical forms. Unlike most other somatic cells, mature neurons are post-mitotic, unable to divide past developmental time point (Frade and Ovejero-Benito, 2015). Thus injuries to the nervous system that result in the disconnection of axons to the neuronal cell bodies in adult animals often lead to permanent impairment of neurological functions. Even though adult neurons are replication incompetent, they have the ability to regenerate following injury.

Over the past century, numerous studies have been carried out to understand the regenerative potential of the nervous system. The mammalian nervous system is

divided into the central nervous system (CNS), which includes the brain and spinal cord, and the peripheral nervous system (PNS), which consists of the nerves and ganglia (cranial nerves and spinal nerves) that relay information between the CNS and the rest of the body (periphery). Mature neurons of the CNS and PNS respond differently to injury (He and Jin, 2016). Axons of adult CNS neurons do not spontaneously regenerate after injury, while PNS neurons show robust axon regeneration. Previous studies have identified and characterized extrinsic factors (axon growth inhibitory and growth promoting factors that are secreted from surrounding cells) and intrinsic growth capacity of injured neurons that determines the extent of axon regeneration (Abe and Cavali, 2009; Ma and Willis, 2015; McKerracher and Rosen, 2015).

In both CNS and PNS, axonal injury triggers Wallerian degeneration, a process of axon degeneration and myelin sheath degradation/fragmentation distal to the injury site (Stoll et al., 2002; Vargas and Barres, 2007). For adequate regenerative responses to occur after axonal injury, clearance of myelin debris is particularly important as it removes growth-inhibitory molecules associated with myelin. In the CNS, a slow elimination of myelin fragments contributes to growth-inhibitory environment that hinders axon regeneration (Vargas and Barres, 2007). For example, glial cells that myelinate CNS axon called oligodendrocytes produce molecules that inhibit regrowth of the severed axon. These growth-inhibitory molecules include myelin-associated protein (MAG) (Mukhopadhyay et al., 1994; McKerracher et al., 1994), Nogo (GrandPre et al., 2000; Prinjha et al., 2000) oligodendrocytes-myelin

glycoprotein (OMgp) (Ji et al., 2008; Cafferty et al., 2010), and chondroitin sulfate proteoglycans (Lemon et al., 1999; Moon et al., 2002). In addition to growth inhibitory molecules, the glial scar formed from astrocytes (CNS neuron supporting cells) after injury in the CNS physically obstructs axon regrow (Filbin, 2003). In contrast to the CNS, the environment within the PNS permits axon regeneration. Following peripheral nerve injury, an increase in the permeability of the blood-nerve barrier recruits macrophages to the injury site to aid in myelin clearance (via phagocytosis) (Stoll and Muller, 1999). In addition, injury-activated Schwann cells (glia cells that myelinate PNS axon) stimulated by loss of axon contact also facilitate the elimination of myelin debris. The rapid clearance of myelin debris in the PNS contributes to growth permissive environment for axon regeneration (Jessen and Mirsky, 2016). For example, within 12 – 48 hours of peripheral nerve injury, Schwann cell significantly decreases the synthesis of myelin lipid and proteins (Ngeow, 2010), and dedifferentiates from adult myelinating phenotype to non-myelinating growth supporting phenotype to support axon regeneration by producing growth promoting neurotrophic factors (Assouline et al., 1987; Jessen and Mirsky, 2016; Bhatheja and Field et al., 2006). Further supporting the PNS permissive environment for axon regeneration, several studies have shown that CNS axons provided with peripheral nerve graft can regenerate their injured axons (David and Aguayo, 1981; Richardson et al., 1980). Taken together, the PNS provides an overall permissive environment for axon regeneration compared to that of the CNS.

On the other hand, less knowledge is known about the intrinsic mechanisms that activate regenerative growth in neurons following axonal injury. As a neuron matures, the intrinsic neuronal growth activity is significantly decreased to allow for proper establishment of synaptic connections (Abe and Cavali, 2008). Surprisingly, adult PNS neurons, but not CNS neurons, have the ability to reactivate intrinsic growth capacity after injury that enables them to robustly regenerate axons. Over the past decades, numerous studies have linked the regenerative ability of injured PNS neurons to the intrinsic growth capacity that allows intra-axonal protein synthesis. Locally synthesized proteins at the injury site not only contribute to growth cone formation but also provide a means for injured axons to communicate with the cell bodies and initiate proper regenerative responses (Zheng et al., 2001; Hanz and Fainzilber, 2006). Using rodent models in axon regeneration research (or, in mRNA localization studies), sciatic nerve lesion has been shown to induce rapid translation of a variety of axonal mRNAs including components of retrograde trafficking proteins (importin- β 1, RanBP1, and vimentin) and transcription factor STAT3 (Hanz et al., 2003; Perlson et al., 2005; Yudin et al., 2008; Ben-Yaakov et al., 2012). At the injury site, local production of importin- β 1, RanBP1, and vimentin proteins aid in the incorporation of locally generated injury signals including STAT3 into retrograde complex formation. These complexes are then trafficked to the cell body where they activate gene transcriptions that are necessary for neuronal survival and axon regeneration. Although it is now clear that intra-axonal protein synthesis is required

for successful axon regeneration, to date, it is unclear how injury induced intra-axonal protein synthesis is regulated when it is no longer needed.

Recently, a subset of small non-coding regulatory RNAs, microRNAs (miRNAs), have been gaining functional importance in neurobiology. These RNAs are approximately 22 nucleotides in length and are mostly known to negatively regulate gene expression at the post-transcriptional level by binding to the 3'UTR of their target mRNAs to either induce translational repression or promote mRNA degradation. Over the past years, several groups have demonstrated the ability of sensory axons to confer miRNA-mediated translation repression (Hengst et al., 2006; Murashov et al., 2007; Aschrafi et al., 2008). Microarray study by Natera-Naranjo et al. (2010) has uncovered a surprising complexity of miRNA population in axons of sympathetic neurons. Bioinformatics analysis revealed that putative mRNA targets of these axonally enriched miRNAs encode a variety of proteins that play an essential role in axonal functions. These findings suggest that axonal miRNAs could play a role in regulating intra-axonal mRNA translation and modulate axonal functions.

Previous studies showed that injury significantly altered the composition of axonal RNA constituents (Willis et al., 2007; 2010; Taylor et al., 2009). The shift in mRNA profile enables axons to generate proteins where they are needed to support different mode of axon activities such as growth and regeneration (Taylor et al., 2009). Consistent with this observation, several laboratories have reported temporal changes in miRNAs expression following spinal cord and sciatic nerve injury (Zhou et al., 2011; Liu et al., 2009; Nakanishi et al., 2010; Yu et al., 2011). Although these studies

linked the involvement of miRNAs to nervous system injury and repair, it failed to address whether axon-specific miRNAs are directly involved in the regenerative responses following axon injury.

This chapter focuses on temporal changes in the axoplasmic miRNAs of rat sciatic nerve in response to crush injury. Since axon-specific miRNAs are the main focus of this study, contamination from glial cells and surrounding tissues was a major concern. To minimize contaminations, I used an optimized mechanical squeeze method to isolate axoplasmic RNA from the proximal nerve stump and carried out RNA purity analysis before subjecting the sample to small RNA (< 200 nt) fractionation. Using deep sequencing, I established the axoplasmic miRNA profiles for uninjured nerve ($t=0$), and injured sciatic nerve at days 1, 4, 7, and 14 following crush injury. Here, I identified 141 different axoplasmic miRNAs and showed that the levels of these miRNAs are significantly altered following sciatic nerve crush injury. Using bioinformatics analysis, I further showed that the putative mRNA targets of differentially regulated axoplasmic miRNAs encode proteins that play key roles in numerous neurological functions involving ER stress response, cytoskeletal dynamics, vesicle formations, neuro-degenerative and –regenerative processes.

Materials and Methods

Survival surgery and tissue processing

All animal procedures were conducted under protocols approved by the Institutional Animal Care and Use Committee (IACUC) of Alfred I. duPont Hospital for Children. *Sprague Dawley* (SD) male rats weighing approximately 150-250g were used in sciatic nerve crush injury. Before surgery, anesthesia was induced using intraperitoneal injection of Ketamine and Xylazine cocktail. Loss of consciousness was confirmed by cornea reflex and response to hind leg pinch. Surgical sites were prepared by removing hair from both hindquarters followed by application of 70% ethyl alcohol and Betadine disinfection solution. Right and left sciatic nerves were exposed at mid-lateral thigh level by gluteal muscle-splitting incision. Crush injury was induced to the left sciatic nerve twice for 15 seconds using fine forceps. For sham operated (uninjured) control, contralateral sciatic nerve was exposed and left intact. Incision sites were closed with 4-0 Ethion sutures followed by an application of 70% ethyl alcohol. The animals were then placed on heating pad to recover until awake and then returned to cages. On days 1, 4, 7, and 14 following crush injury, animals were euthanized by asphyxiation with CO₂, and sciatic nerves were collected and processed for RNA extraction as described by Kim et al. (2016).

RNA extraction and small RNA enrichment

To minimize non-axonal contamination from surrounding tissues, total axoplasmic RNAs were extracted from sciatic nerve using mechanical squeeze method as previously described (Rishal et al., 2010; Kim et al., 2016). In brief, sciatic nerves

were washed twice in cold phosphate buffer saline (PBS), cleared of connective tissues, and cut into 0.5 cm fragments. Total RNAs were then extracted from these fragments via manual mechanical squeezing method directly into Trizol (Invitrogen). The Trizol containing axoplasmic RNA was processed for total RNA isolation according to manufacture protocol. After RNA quantification was determined by fluorometric Quant-IT RiboGreen RNA assay (Invitrogen), 100 ng of total RNA was reversed transcribed to cDNA with *iScript RT Kit* (BioRad) followed by RNA purity assessment using extended RT-PCR (40 cycles) amplification for the following transcripts; axon enriched β -actin, cell body restricted [*microtubule-associated protein 2 (MAP2)* and *H1 histone family member 0 (H1F0)*], and non-neuronal cell [*glial fibrillary acidic protein (GFAP)*, and *receptor tyrosine-protein kinase family 3 (ErbB3)*]. After the assessment of axoplasmic RNA extraction, the remaining total RNA was further fractionate to < 200 nucleotides in length by using *RNeasy Mini spin column* followed by *RNeasy MiniElute Cleanup Kit* (Qiagen).

Illunima sequencing of small RNA

A total of 15 samples containing three biological replicates of highly enriched axoplasmic small RNAs (100 ng/each replicate) extracted from uninjured nerves and injured nerves collected at different time points (1, 4, 7, and 14 days) following crush injury were submitted to the University of Delaware DNA Sequencing and Genotyping Center (UDSGC) for library construction (Illumina TruSeq Small RNA library Prep Kit) and small-RNA sequencing (Illumina HiSeq 2500). In short, adapters were ligated to the 5' and 3' termini of small RNAs followed by reverse

transcription to generate single stranded cDNAs. These cDNAs were subsequently PCR amplified using common primers and illumina index primers for multiplexing in a single flow cell on Illumina HiSeq 2500.

Small-RNA sequencing analysis

CLC Genomic Workbench (Qiagen) software package (7.0.3) was used for all sequence analysis. Overall sequencing quality for each biological replicate was assessed using a per-sequence, per-base, and over-representation analysis.

Subsequently, 3' and 5' adapters (Illumina multiplex PCR primer 2.01) were trimmed off using Next Gen Sequencing (NSG) trim, and sequencing reads were counted and filtered by length distribution to partition miRNAs from other small non-coding RNAs. Trimmed sequences ranging from 16 – 25 nts were annotated to rat miRBase (Version 21) and sequences ranging from 23 – 36 nts were annotated to piRNA Bank rat database (2014). Un-annotated sequences were saved and mapped to the genome of *Rattus Norvegicus*. Only sequencing containing ≥ 50 reads were used for further differential expression analysis

NGS Trimming Parameter

- 1) Trim quality score limit = 0.05
- 2) Trim ambiguous nucleotides, maximum number of ambiguities = 2
- 3) Search adapter on both strand (Illumina multiplex PCR primer 2.01)

miRBase (Version 21) Annotation Parameter

- 1) Specie miRNA data base used: Rat, Mouse, and Human
- 2) Mature length variant (isomiRs)
 - a. Additional upstream bases = 2
 - b. Additional downstream bases = 2
 - c. Missing upstream bases = 2
 - d. Missing down stream bases = 2
- 3) Alignment setting
 - a. Maximum mismatch = 2

piRNABank Annotation (2014 version) Parameter

- 1) Specie rat piRNA database used: *Rattus Norvegicus*
- 2) Maximum mismatch = 2
- 3) Performed strand specific alignment

Read mapping to Rattus Norvegicus Genome Parameter

- 1) Annotate to genes and intergenic regions
- 2) Read alignment
 - a. Mismatch = 2
 - b. Insertion cost = 3
 - c. Deletion cost = 3
 - d. Length fraction = 0.95
 - e. Similarity fraction = 0.95
- 3) Strand specificity = Both Strands
- 4) Maximum hit for read = 10

5) Expression values = Total counts

Statistical analysis

Normalization and differential expression of miRNAs were performed in RStudio using edgeR package (default parameter). In edgeR, normalization of read counts is implemented by trimmed means of M value (TMM) method. Since read counts for moderately or lowly expressed genes can be strongly influenced by small changes in the expression levels of highly expressed gene, TMM uses scaling factor to adjust this for each library. In this method, scaling factors are calculated by removing lowly and highly expressed genes and assumed that a majority of genes are not differentially expressed between any two samples. To determine miRNAs that are differentially altered across time points following crush injury, edgeR utilized an *exact test* (et, command), a method similar to Fisher's exact test to calculate for *p*-values and false discovery rate (FDR) values. FDR values < 0.05 were considered statistically significant.

Cluster analysis (Euclidean distances metric and average linkage method) was used to assess the relationship between the levels of axoplasmic miRNAs that were differentially altered in response to nerve injury. To establish axon-specific miRNA profiles in regenerating sciatic nerve, datasets for each injury time point were first directly compared with uninjured (sham) control to calculate for the mean fold change values. These values were subsequently used for hierarchical clustering analysis that group temporal changes of axoplasmic RNAs based on similarity in their responses to nerve injury. To determine the relationship between miRNA profiles across

regenerating time points [uninjured, 1-, 4-, 7-, 14-day post injury (DPI)], the average read counts for each miRNA were mean centered in \log_2 -space, and then two-ways hierarchical clustering analysis was implemented on differentially regulated axoplasmic miRNAs and time array. All the clustering analyses were visualized in form of a heat map on \log_2 scale.

RT-qPCR validation of differentially regulated miRNA

The results from Illumina sequencing of small RNAs were validated using real time quantitative polymerase chain reaction (RT-qPCR). While traditional relative RT-qPCR measures the abundance of transcripts of interest relative to a reference gene, absolute RT-qPCR quantifies the total copy number of the transcript of interest within a given sample using standard curve and mathematical extrapolation. Thus, absolute quantitation method was used to directly compare RT-qPCR results to small-RNA sequencing data. First, small RNA (<200 nt) fraction was converted to poly A tailed cDNA using *NCodeTM VILOTM miRNA cDNA Synthesis Kit* (Invitrogen). The resulting cDNA was then used as a template for absolute RT-qPCR analyses with *NCodeTM EXPRESS SYBR GreenERTM miRNA qRT-PCR Kit* (Invitrogen) on ABI Prism 7900HT. To verify primer specificity, RT-qPCR products were subjected to melting curve and 4% agarose gel analyses (NuSieve 3: 1; Lonza) to ensure that a single PCR product is generate during the amplification process. Amplification specificity is reflected as a single peak in melting curve analysis and a single band with a molecular weight at approximately 80 base pair (bp) on 4% agarose gel.

miRNA target prediction

The following strategy was used to identify potential miRNAs' targets. First, putative mRNA targets of differentially expressed miRNAs were predicted using two web-based algorithms, TargetScan and miRanda. To further improve prediction sensitivity, common mRNA targets were identified from the gene lists generated by these algorithms. Since axoplasmic miRNAs were hypothesized to regulate axonally localized mRNAs, I further narrowed down potential targets by overlapping commonly predicted mRNA targets to the list of transcripts that had previously been identified in axons of adult DRG neurons (Gumy et al., 2011).

Functional annotation of predicted miRNA targets

First, Gene Ontology (GO) enrichment analysis was used to determine the biological functions of the predicted mRNA targets of axoplasmic miRNAs that were significantly altered following nerve injury. Then Ingenuity Pathway Analysis (IPA) (Qiagen) was used to identify cellular functions that are most relevant for the predicted axonal mRNA targets. The significance of these cellular processes was measured by the number of predicted molecules mapped to the pathways and a *p* value that determines the probability of the association between the predicted molecules and the pathways.

Results

RNA extraction from sciatic nerves yields highly enriched axoplasmic RNAs

To understand the responses of axon-specific miRNAs to nerve injury, axoplasmic RNA isolates extracted from sciatic nerves must be free of contaminations from neuronal cell body and non-neuronal cells, as these contaminations could significantly impact down-stream analyses. Due to the anatomical structure of the sciatic nerve, Schwann cell contamination is a widespread problem in the axoplasmic RNA preparation from sciatic nerve tissue samples. To address this issue, purity of RNA samples was assessed by extended cycles of RT-PCR (40 cycles) using specific primer sets for mRNAs that are present in the neuronal cell body (*MAP2* & *HIF0*) and glial cell (*GFAP* & *ErbB3*). As a control, I first examined the purity of RNA sample isolated from DRG tissues and whole sciatic nerve. As shown in Fig. 2.1, whole sciatic nerve RNA preparation was positive for *GFAP*, *ErbB3*, and *HIF0* amplicons, which indicated significant levels of glia/non-neuronal contamination. Since nerves contain bundles of axons and their supporting cells but do not contain the neuronal cell body, the absence of *MAP2* amplicon was anticipated in RNA preparation from whole sciatic nerve. Axoplasmic RNA preparations extracted from proximal nerve stumps using mechanical squeeze method showed undetectable levels of *MAP2*, *GFAP*, *ErbB3*, and *HIF0* amplicons that suggest a significantly low level of non-neuronal cellular contamination (Fig 2.1). Since *β -actin* mRNAs are present in the axonal compartment, the positive amplification for *β -actin* in axoplasmic preparations and the

absence of *MAP2*, *GFAP*, *ErbB3*, and *HIF0* amplicons suggest that RNA samples are highly enriched with axoplasmic RNAs (Fig 2.1).

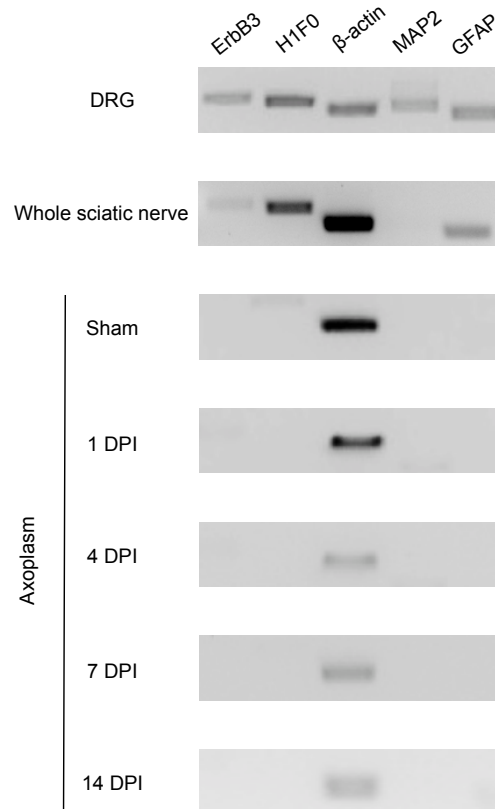


Figure 2.1 Axoplasm samples extracted from sciatic nerves are free of neuronal cell body and glial cell contamination. Axoplasmic RNA isolates extracted from rat sciatic nerves at 1-, 4-, 7-, 14-days post injury (DPI) and sham operated uninjured control nerves were tested for contamination from neuronal cell body and non-neuronal cells including glial cells using extended RT-PCR (40 cycles). RNA isolated from DRGs and whole sciatic nerve tissues were used as positive controls for contaminations. A primers set for *β -actin* mRNA was used as positive control for PCR amplification in axoplasm isolates. Primers specific for *microtubule associated protein 2 (MAP2)* mRNA were used to test for neuronal cell body contamination and primers specific for *Erb-B2 receptor tyrosine kinase 3 (ErbB3)*, *glial fibrillary acidic protein (GFAP)*, and *H1 histone family member 0 (HIF0)* mRNAs were used to test for glial cells and other non-neuronal cell contaminations. Analysis of RT-PCR products by 1% agarose gel electrophoresis with ethidium bromide staining showed that axoplasmic RNA isolates extracted from indicated sciatic nerve samples were free of contaminations from the neuronal cell body and glial cells.

Small-RNA sequencing revealed two populations of small non-coding RNAs

Prior to downstream analyses, raw sequence from each data set was subjected to standard CLC Genomic Workbench assessment of sequencing quality. This analysis was carried out to detect possible errors or issues during sequencing processes that could impact further analyses. Based on quality analysis, reads of low quality were discarded and the remaining sequences underwent adapter trimming and subsequent read count. As results, a dataset of 10.9 ± 1.5 (uninjured), 12.4 ± 1.0 (1 DPI), 11 ± 0.8 (4 DPI), 11.4 ± 1.1 (7 DPI), and 10.1 ± 1.5 (14 DPI) million reads, ranging from 17 – 38 nt was obtained for each time point (Table 2.1).

Since miRNAs are approximately 18 - 22 nucleotides in length, I first looked at sequence length distribution to determine the representation of read sequences that falls within the mammalian miRNA population. Surprisingly, this analysis revealed two distinct populations of small RNAs in our datasets (Fig 2.2A). The first small RNA population ranged from 18 – 24 nts with an enrichment of read sequences measured at 22 nts in length, suggesting that this group of reads belongs to mammalian miRNAs. The second group of reads ranging from 28 – 36 nts in length contained an enrichment of read sequences measured at 31 and 32 nts, which was consistent with another class of 26 – 32 nts small non-coding RNAs, piwi-interacting RNAs (piRNAs) (Zev et al., 2015).

Based on the analysis of sequence length distribution, trimmed reads ranging from 16 – 25 nts were annotated to miRBase, 23 – 36 nts were annotated to rat piRNA Bank database, and the remaining unannotated reads were mapped to the rat genome.

Annotation of sequence reads revealed that $43.6\% \pm 8.1$ (uninjured), $46.7\% \pm 4.4$ (1 DPI), $57.6\% \pm 2.5$ (4 DPI), $40.0\% \pm 2.4$ (7 DPI), and $32.1\% \pm 2.1$ (14 DPI) of sequencing reads were mapped to a total of 141 different miRNAs (Fig 2.2C and appendix). On the other hand, $26.6\% \pm 2.7$ (uninjured), $20.4\% \pm 1.8$ (1 DPI), $15.0\% \pm 1.4$ (4 DPI), $28.6\% \pm 1.3$ (7 DPI), and $33.4\% \pm 2.1$ (14 DPI) of reads were mapped to a total of 31 different piRNAs (Fig 2.2C).

Name	Number of reads	Average length	Number of reads after trim	Percent trim	Average length after trim
Sham A	9,502,794	51.0	9,339,585	98.28%	28.5
Sham B	11,494,793	51.0	11,280,422	98.14%	27.5
Sham C	12,524,122	51.0	12,306,489	98.26%	26.7
1 DPI A	13,986,573	51.0	13,713,636	98.05%	26.8
1 DPI B	12,106,954	51.0	11,889,082	98.04%	28.0
1 DPI C	12,174,654	51.0	11,853,502	97.36%	27.2
4 DPI A	10,956,800	51.0	10,578,821	96.55%	25.4
4 DPI B	12,379,416	51.0	12,004,546	96.97%	26.0
4 DPI C	10,794,098	51.0	10,485,392	97.14%	25.8
7 DPI A	12,411,611	51.0	12,070,784	97.25%	26.9
7 DPI B	10,439,342	51.0	10,186,163	97.57%	27.7
7 DPI C	12,486,189	51.0	12,118,024	97.05%	27.3
14 DPI A	10,340,851	51.0	10,141,280	98.07%	28.0
14 DPI B	12,017,300	51.0	11,725,708	97.57%	27.6
14 DPI C	8,744,503	51.0	8,527,906	97.52%	27.9

Table 2.1 Adapters are removed from a majority of Illumina sequencing reads. Since adapter contamination could lead to errors in next generation sequencing (NGS) alignment and mapping processes, it is necessary that both 3' and 5' adapters are removed from raw sequences reads before moving onto downstream analysis. After trimming, sequencing adapters are removed from over 95% of sequencing reads.

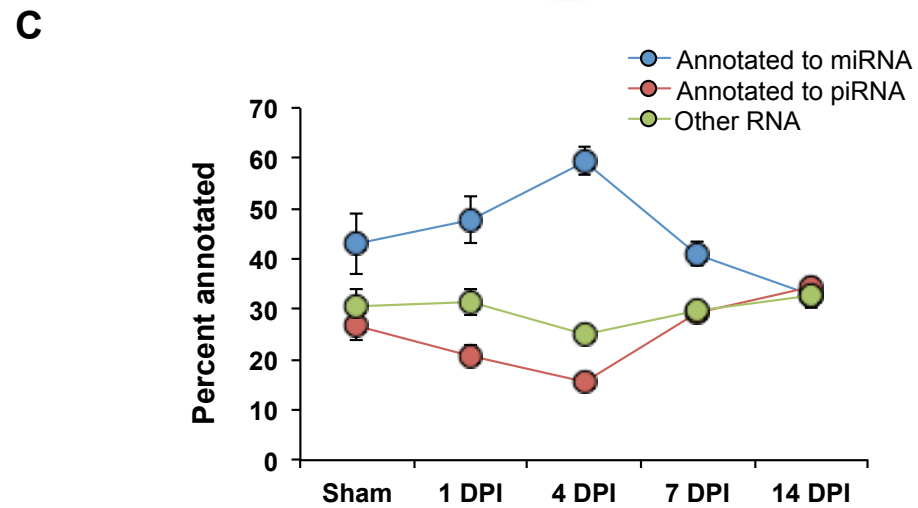
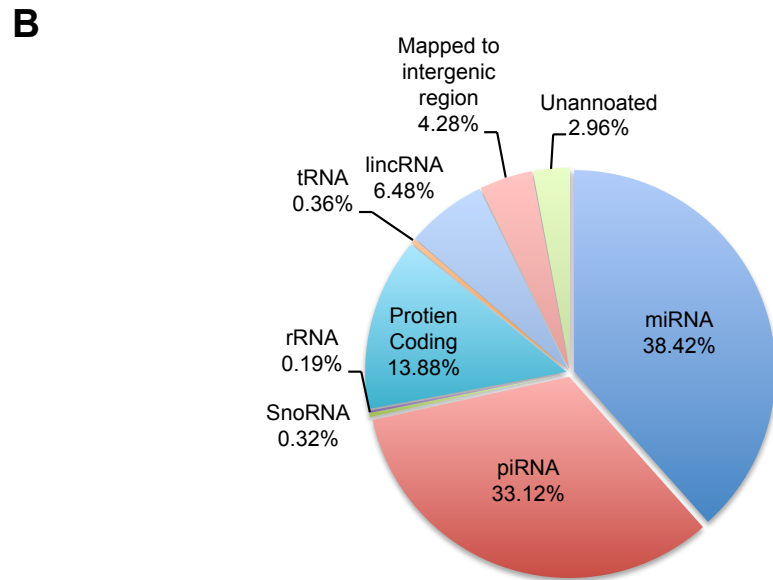
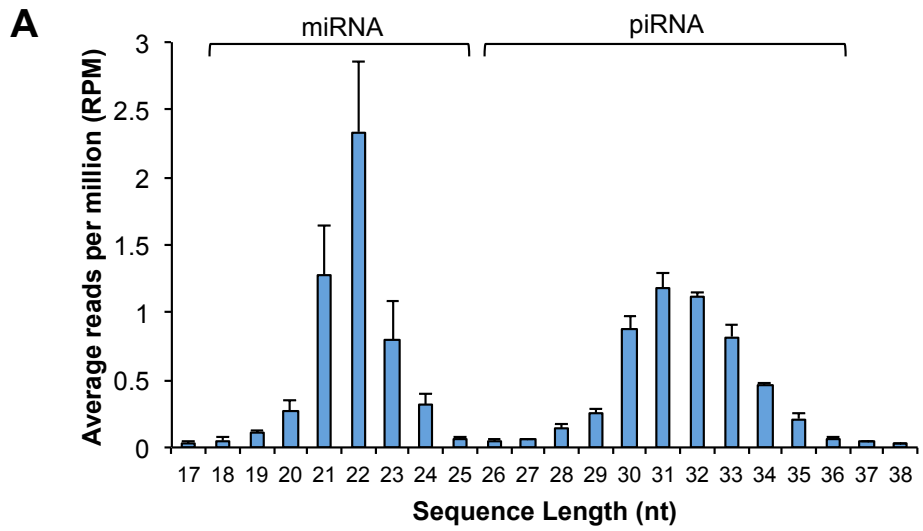


Figure 2.2 Enriched axoplasmic RNA contains two distinct classes of small non-coding RNAs, miRNAs and piRNAs. Size and frequency distribution (A) of sequencing read from sham axoplasm showed that two population of small RNAs; 1) 20 – 24 nt, showing an enrichment of 22 nt in length that corresponds to the size of miRNAs and 2) 29 – 34 nt, showing an enrichment of 31 nt in length, corresponding to piRNAs. Sequence alignment (B) showed that 38% of sequencing reads from sham axoplasm were mapped to miRBase, 33% were mapped to piRNA bank, and the remaining sequences were mapped to other small RNAs and fragments of protein coding region. Panel C showed percentage of sequences mapped to miRNA and piRNA in axoplasmic RNA isolates extracted from injured sciatic nerve collected at 1-, 4-, 7-, and 14-days post injury (DPI).

Regenerating sciatic nerve exhibits temporal changes in the levels of axoplasmic miRNAs

To identify axoplasmic miRNAs that respond to nerve injury, I first directly compared the levels of miRNAs in uninjured nerve to those of regenerating sciatic nerve at each different time points (1-, 4-, 7-, and 14-days) following crush injury. Pairwise comparison was conducted in edgeR and p -values < 0.05 and FDR < 0.05 were considered to be statistically significant. The analysis showed that 63 out of the total 141 different miRNAs identified in the axoplasm responded differentially to sciatic nerve injury across all time points. For instance, nerve injury caused changes in the levels of 17 miRNAs (8 up-regulated & 9 down-regulated) at 1 DPI, 38 miRNAs (18 up-regulated & 20 down-regulated) at 4 DPI, 12 miRNAs (5 up-regulated & 7 down-regulated) at 7 DPI, and 31 miRNAs (16 up-regulated & 15 down-regulated) at 14 DPI (Fig 2.3A). These results highlight differences in axoplasmic miRNA repertoire that are deployed in response to different stages of nerve regeneration. To group miRNAs that exhibit similar responses to nerve injury, I

used a mean fold change (FC) value (the average level of a given miRNA at a specific time point divided by the average level of the same miRNA in uninjured controls) calculated in previous pairwise comparison analysis and conducted hierarchical clustering. As shown in Fig 2.3, FC in the levels axoplasmic miRNAs is visualized in form of a heat map with cluster dendrogram. This analysis grouped axoplasmic miRNAs into three distinct clusters. miRNA cluster 1 at the top left of the heat map showed a significant increase along the regenerating time series. In contrast, the second cluster of miRNAs in the top middle of the heat map showed an initial increase at 1 DPI and a subsequent decrease in later time point following injury. Lastly, the third cluster at the top right contained a group of miRNAs that exhibit a gradual decrease along the time series after nerve injury. These results suggest a complexity in the regulatory role of axoplasmic miRNAs in response to different stages of nerve regeneration.

To assess the relationship between the axoplasmic miRNA profiles of uninjured nerve to those of regenerating sciatic nerve, I implemented a two-way clustering analysis based on the average counts of individual miRNAs and the time points following crush injury (Fig 2.4). The analysis showed that miRNA profile of uninjured control is closely related to the profiles of injured nerve at 1 DPI and 7 DPI. In contrast, miRNA profiles of injured nerve at 4 DPI and 14 DPI were classified as individual clusters. These results indicate that changes in the levels of axoplasmic miRNAs do not correlate with the time course of the regenerative response.

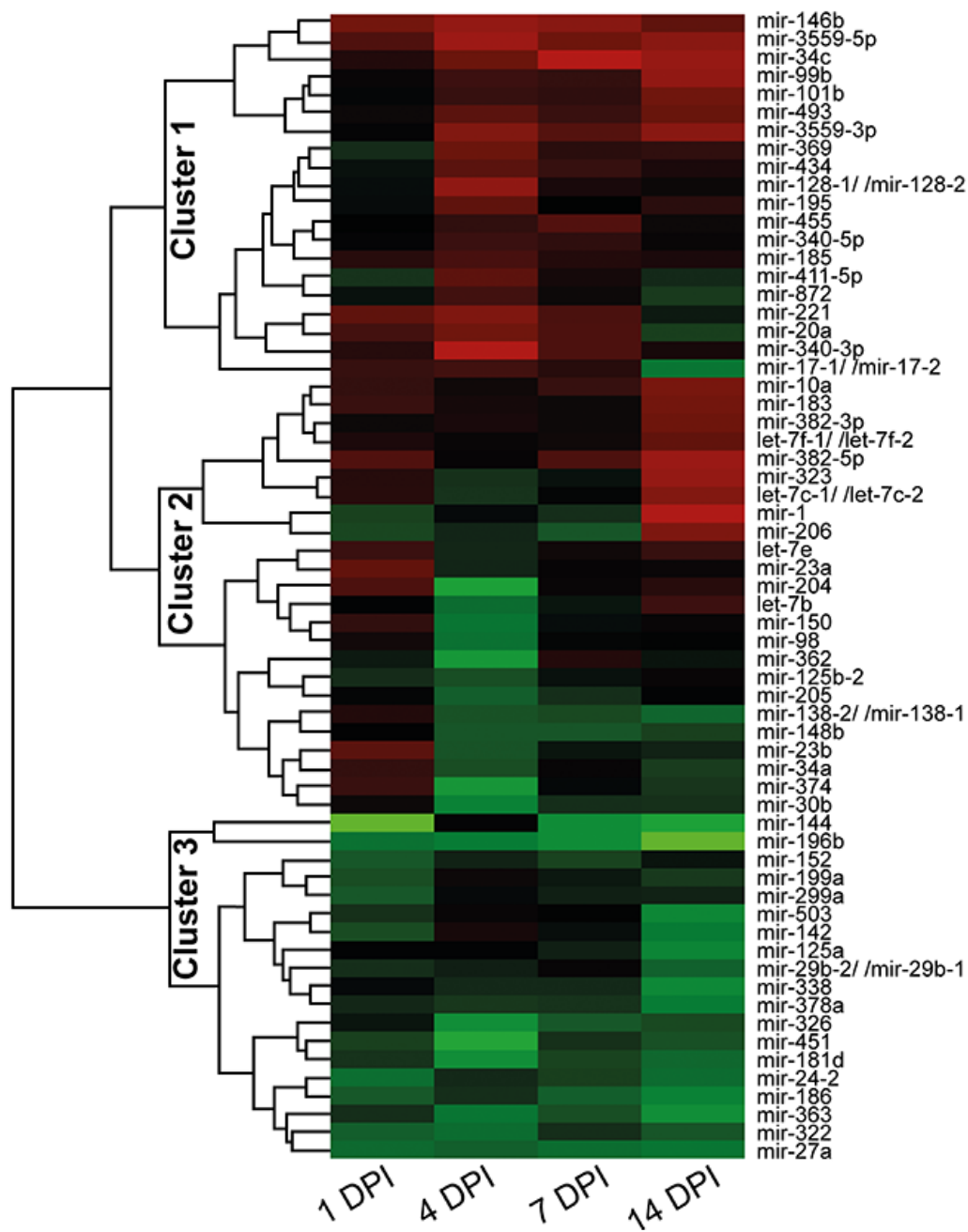
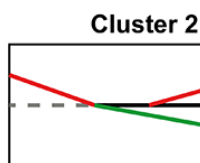
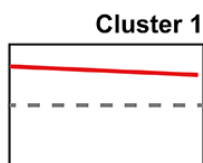
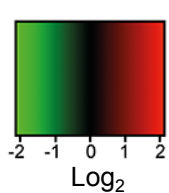


Figure 2.3 Changes in axoplasmic miRNA profiles in response to nerve injury.

Levels of axoplasmic miRNAs extracted from injured nerve at 1-, 4-, 7-, and 14-days after injury (DPI) were directly compared to that of uninjured, sham operated control (N = 3/group). The heatmap showed \log_2 transformed mean fold change values in levels of 63 different miRNAs that were differentially altered in response to nerve injury across all time points. Increased changes in miRNA level are represented in red and decreased changes are represented in green. Cluster dendrogram grouped axoplasmic miRNAs that responded similarly to injury. The insets on the top reflect three distinct clusters of changes in miRNA profiles. The dashed lines indicate miRNA levels in sham control.

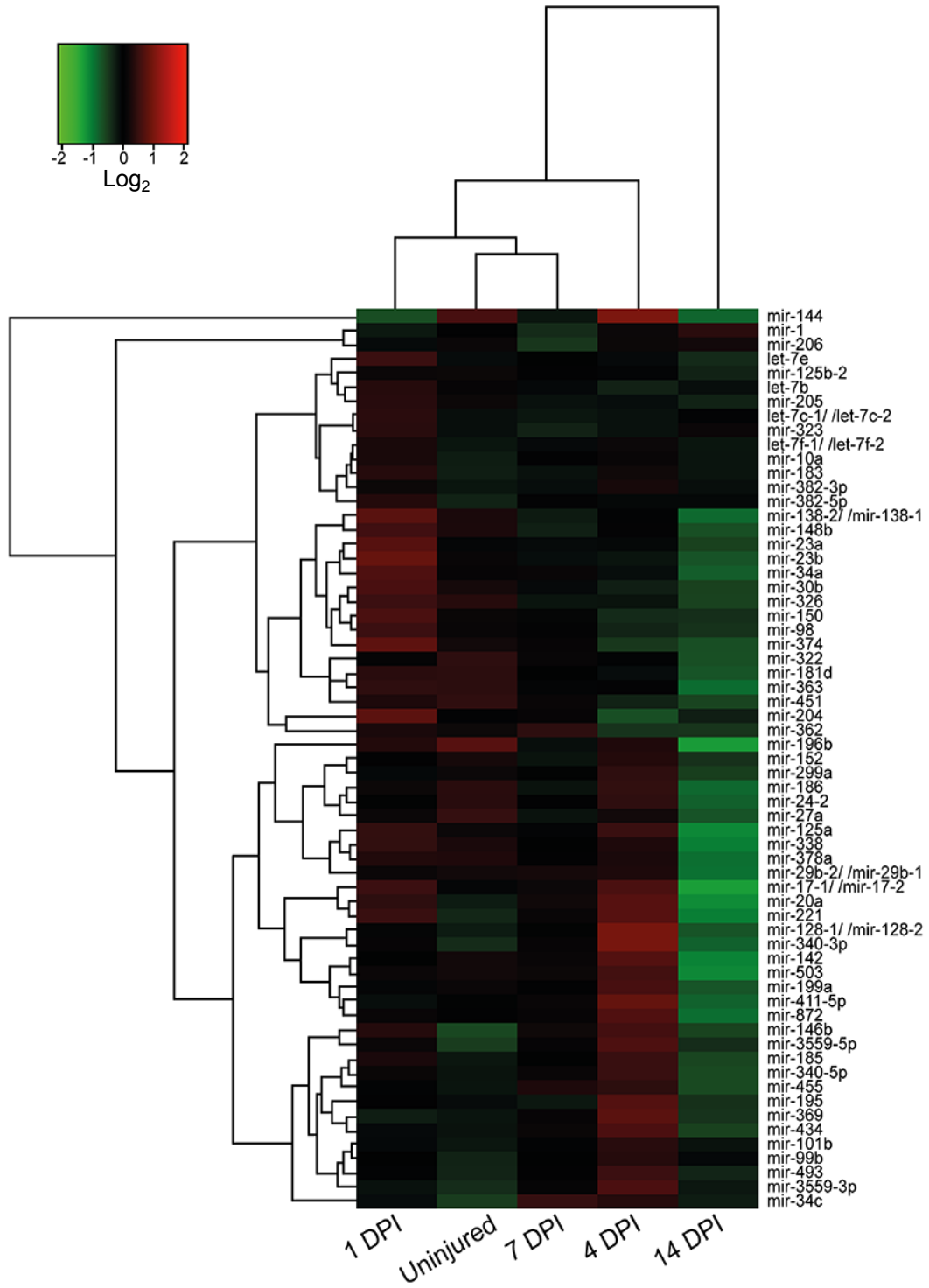


Figure 2.4 Changes in axoplasmic miRNA repertoires in response to nerve injury. To assess the relationship between miRNA profiles across the injury time points, two-way hierarchical clustering analysis was conducted on 63 miRNAs that showed differential changes in their levels at different time points after injury [1-, 4-, 7-, and 14- days post injury (DPI)]. The heatmap showed mean centered average read count for individual miRNAs in Log_2 -space. Red indicates increases in the level and green indicates decreases in the level of miRNA. Clustering analysis was carried out using Euclidean distance metric and average linkage method. Heatmap and cluster dendrogram indicate similarity between uninjured sham control, 1 DPI, and 7 DPI miRNA profiles. 4 DPI and 14 DPI miRNA profiles are considered as distinct clusters.

Absolute RT-qPCR analysis confirms accurate representation in the alteration of axoplasmic miRNAs levels observed by small-RNA sequencing

Although deep sequencing is one of the best methods used to profile gene expression at the transcriptional level, a potential bias associated with complex RNA-sequencing workflow warrants for a different approach to verify the results observed in sequencing datasets. Using miRNA-specific primer sets, I validated a subset of axoplasmic miRNAs by absolute RT-qPCR analysis. Since day 7 post-injury is considered as the peak period of axon regeneration response, differentially regulated eight miRNAs at 7 DPI (four up-regulated miR-146b-5p, -34c-5p, -20a-5p, and -455-5p and four down regulated miR-185-5p, -206-3p, -138-2-5p, and -148b-3p) were selected for RT-qPCR validation. These results indicated a strong correlation between datasets generated by small-RNA sequencing and RT-qPCR analysis (Fig. 2.5).

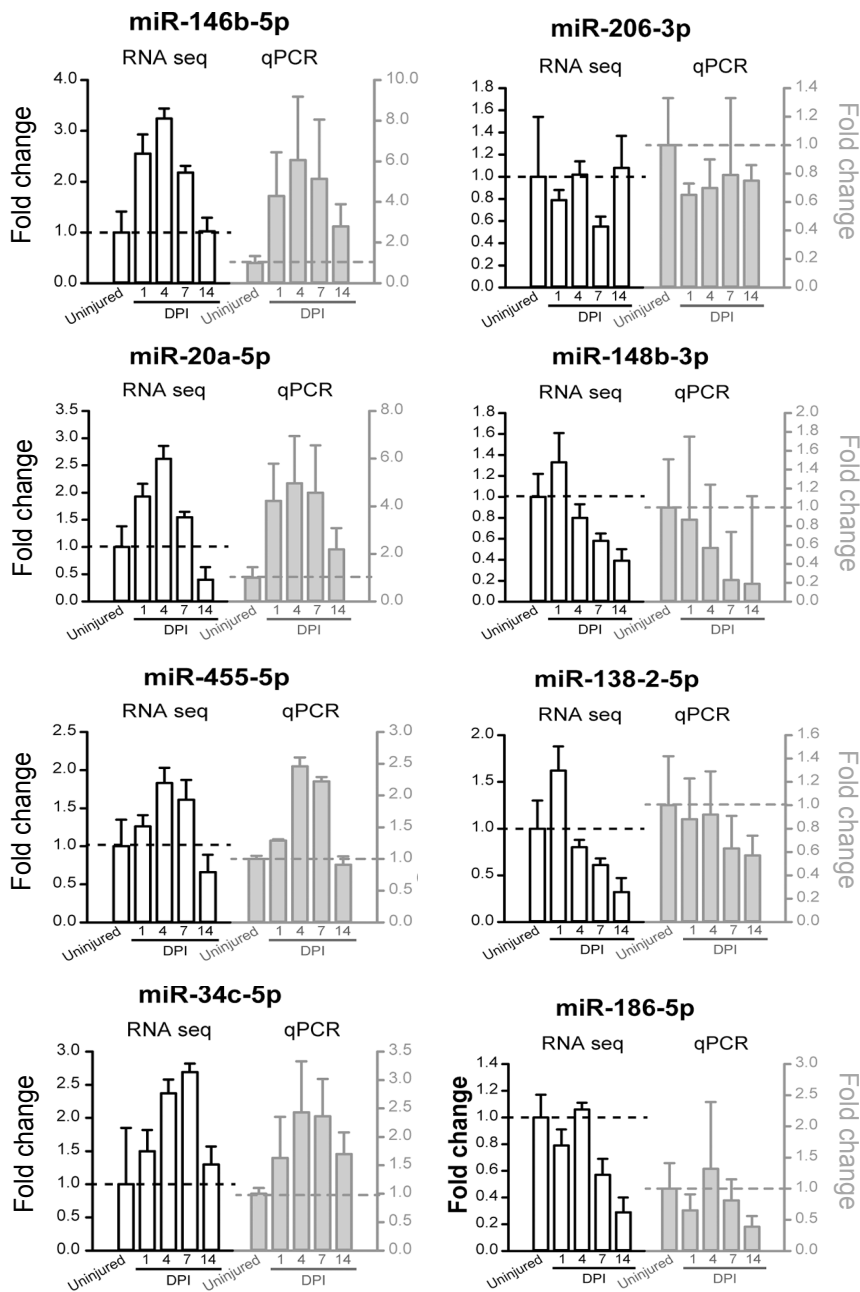


Figure 2.5 Validation of small miRNA sequencing data by absolute real time qPCR analysis. Bar graph shows averages \pm standard deviation of changes in levels of 8 different axoplasmic miRNAs at 1-, 4-, 7-, and 14-days post injury relative to that of uninjured control. Significantly up-regulated miRNAs are shown in the left panels and significantly down-regulated miRNAs are shown in the right panels.

Putative mRNA targets of significantly altered axoplasmic miRNAs show a strong association with multiple processes involved in neurological functions

To gain further insights into the biological functions of axoplasmic miRNAs that showed significant changes in response to nerve injury, I evaluated potential impacts of their mRNA targets in nerve regeneration. Since miRNA target prediction algorithms generate hundreds of possible mRNA target candidates, the following strategy was implemented to decrease false positives. In brief, TargetScan and miRanda-mirSVR were used to predict mRNA targets, and intersected target mRNAs were further overlapped with transcripts that are currently known to localize into axons of adult DRG neurons (Gumy et al., 2011) (Fig 2.6). In this analysis, I focused on the target transcripts for seven most up-regulated and eight most down-regulated miRNAs (FDR < 0.05, with minimum read >100) along the time series compared to uninjured control. My target prediction strategy yielded a total of 256 transcripts including 83 and 173 targets for significantly up-regulated and down-regulated miRNAs, respectively. Next, I sought to determine the function of these predicted genes using Gene Ontology (GO) enrichment and Ingenuity Pathway Analysis (IPA). GO term enrichment identified 240 GO functions ($p < 0.01$, # molecules > 5) that showed a significant enrichment by the predicted mRNA targets. To further understand the functional role of these genes in context of neuro-regeneration, IPA analysis was carried out to identify neurological functions that are relevant to nervous system injury. 92 out of 256 predicted mRNA targets showed a significant association with 34 distinct neurological functions ($p < 0.01$) (Fig 2.7) that are important in the

function and maintenance of neurons, nervous system development, and neurological diseases. Most importantly these bioinformatics analyses indicated that axoplasmic miRNAs that responded to nerve injury can affect numerous neuronal functions by modulating a variety of cellular activities such as ER stress response, microtubule dynamics, neurite outgrowth, and cell repairs (Fig 2.7).

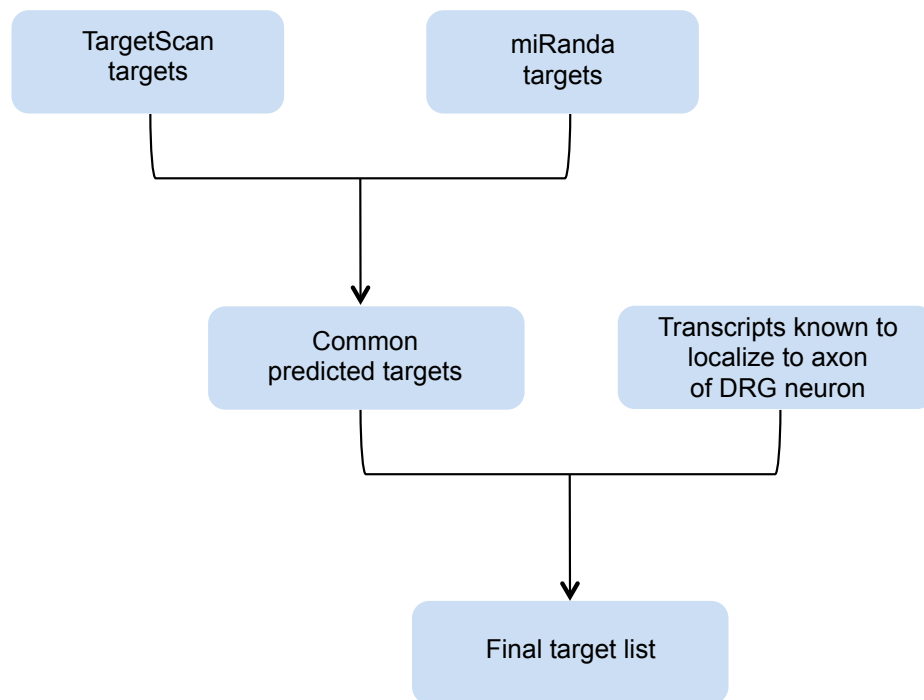


Figure 2.6 Strategy to identify axonally localized mRNA target(s) of differentially regulated axoplasmic miRNAs. TargetScan and miRanda miRNA target prediction algorithms were used to predict mRNA targets of 7 most up-regulated and 8 most down-regulated axoplasmic miRNAs. Common mRNA targets predicted by TargetScan and miRanda were then overlapped with transcripts that are known to localize to axons of adult DRG neurons.

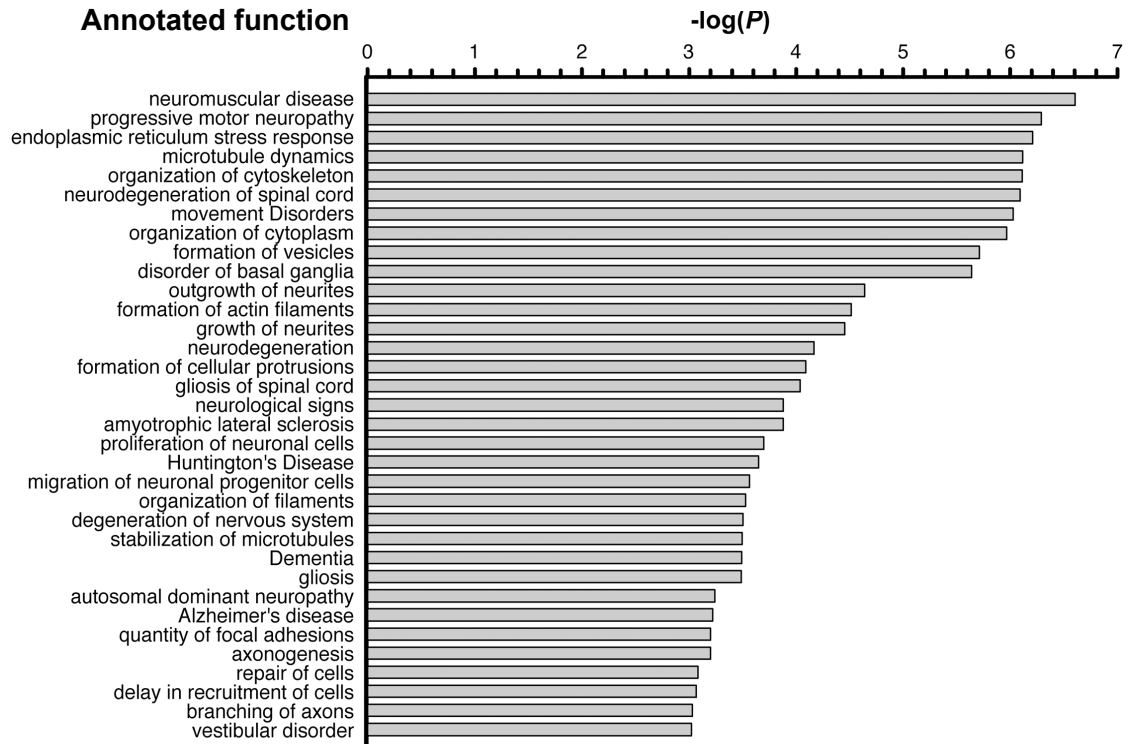


Figure 2.7 Ingenuity pathway analysis of mRNA targets of 7 up-regulated and 8 down-regulated axoplasmic miRNAs. The listed annotated functions were from nervous system and development function category. Only functions that associate with at least 3 or greater molecules are shown.

Discussion

Axon regeneration is one of the major factors that dictate the functional recovery after damages to the nervous system. In contrast to the limited capacity for CNS axons to regenerate, axons of PNS neurons can spontaneously regrow following injury (Huebner et al., 2010). The regenerative ability observed in PNS axons is due to its intrinsic capacity for local protein synthesis (Zheng et al., 2001). Studies have shown that varieties of proteins are locally translated at the site of injury to facilitate growth cone formation and signaling the cell body of axon damages. Axonally generated injury signals activate gene transcriptions that are necessary for neuronal survival and regenerative responses in the soma. While most studies have focused on understanding of transcriptional changes induced by axon injury, the mechanism underlying temporal regulation of injury induced intra-axonal protein synthesis remained largely unknown. Recently, the discovery of miRNAs along with the findings of key protein components of RISC complex in the axonal compartment have sparked interests in miRNA-mediated regulation of intra-axonal mRNA translation. Here, I used small-RNA sequencing to establish axoplasmic miRNA profiles in rat sciatic nerves following crush injury.

In the past years, similar studies have been carried out to profile miRNAs following nerve injury using RNA preparation from whole sciatic nerves. Due to anatomical structures of the spinal nerve, RNA preparation from whole sciatic nerve not only contains RNA from the axoplasm but also RNA from non-neuronal cells, particularly Schwann cells. This could be problematic when it comes to determining

how axon-specific miRNAs contribute to the regenerating process of damage nerve. In the present study, only RNA preparations free of non-neuronal and cell body contamination were subjected to deep sequencing to reduce biases introduced by non-neuronal RNA and increase the representation of axon-specific miRNAs. Using this approach, I directly contrasted the profiles of axoplasmic miRNAs in injured sciatic nerve at 1-, 4-, 7-, and 14-days post crush injury to that of uninjured nerves. Illumina sequencing of small RNA identified 141 different miRNAs in the axoplasm of rat sciatic nerves. 63 of these miRNAs exhibited significant changes in their levels following nerve injury. When I compared my findings to previous studies, only 51 out of 63 differentially altered miRNA in my data overlapped with 225 miRNA identified by Yu et al. (2011) to be differentially altered following nerve injury. Since axoplasmic RNA samples analyzed were free of contamination from non-neuronal cells, my study has uncovered an additional 12 axon-specific miRNAs that were missed by previous profiling studies.

To further understanding how injury affects global changes in the axoplasmic miRNA transcriptome during regeneration, I conducted hierarchical clustering of axoplasmic miRNA profiles at different time points following nerve injury. Based on the clustering of the datasets, miRNA profiles of uninjured nerve, 1 and 7 DPI were grouped into one cluster, while the profiles of 4 and 14 DPI were identified as separate clusters. My result was inconsistent with previous study by Yu et al. (2011) who used RNA isolated from whole sciatic nerve lysate and reported that miRNA profiles from injured sciatic nerves at 4, 7, and 14 DPI were clustered together and separate from the

cluster of the uninjured control and injured nerve at 1 DPI. Although the results from Yu et al (2011) study support the idea that changes in sciatic nerve miRNAs seems to correlate with the time course of nerve regeneration, my results indicated that temporal changes in axoplasmic small RNAs of injured sciatic nerve do not simply reflect the regenerative response but rather a complex and precisely control mechanism that are deployed as part of axonal post-injury responses.

To gain an in-depth understanding of how axoplasmic miRNAs respond to injury, I conducted another clustering analysis to group miRNAs that showed similar responses. This analysis revealed 3 distinct clusters of axoplasmic miRNAs. Since a miRNA can target hundreds of mRNAs and a single transcript can be targeted by multiple different and/or identical miRNAs, similarities in miRNAs' responses observed in the clustering analysis could suggest cooperative regulatory activity of axoplasmic miRNAs. Recent studies show that mRNAs that are targeted to the axon often have significantly longer 3'UTRs compared to the counterparts present in the cell body (Andreassi et al., 2017). Interestingly, multiples studies have indicated that transcripts with longer 3'UTRs usually contain higher density of miRNA binding sites (Osada and Takahashi, 2007; Sandberg et al., 2008; Chen et al., 2009). These findings suggest the involvement of multiple axoplasmic miRNAs working together in sync to regulate specific pathways during axon regeneration.

MicroRNA has been gaining intense research interests in neurobiology since it has the potential to regulate multiple pathways. It is becoming clear that not all miRNAs are of equal importance. Specific miRNAs such as miR-9 can regulate major

pathways that are important for neuronal differentiation and functions (Rajman and Schratt, 2017). This is reflected in a recent study showing that co-expression of miR-9 and miR-124 can induce conversion of human fibroblasts into functional neurons (Yoo et al., 2011). Therefore, I decided to focus on understanding functional pathways that are potentially regulated by axoplasmic miRNAs that exhibit at least a 2 fold change after nerve injury. IPA analysis revealed that 92 out of 256 predicted mRNA targets strongly associate with various neurological functions. These functions include ER stress response, cell repairs, axogenesis, and notably functions that are associated with neurodegenerative diseases such as amyotrophic lateral sclerosis, dementia, Alzheimer and Hunting disease. These findings suggest that axon-specific miRNAs that participate in nerve regeneration could play key roles in the etiology of neurological diseases. Hence, future work on molecular mechanisms underlying miRNA-mediated regulation of intra-axonal protein synthesis could be used to develop therapeutic strategies to treat both nervous system injury and neurological diseases.

While analyzing small-RNA sequences, I was surprised to find the presence of a different class of small regulatory non-coding RNAs called Piwi interacting RNA (piRNA) in the axoplasm of the regenerating nerves (Fig. 2.2). The most widely recognized function of piRNAs is silencing transposable genetic elements through the interaction with P-element induced wimpy testis (Piwi) protein (a member of AGO family). Interestingly, recent studies have uncovered other functions of piRNAs. These functions include euchromatin remodeling, epigenetic programming, modulating mRNA stability, and regulating translation (Akkouche et al., 2013; Ross et

al., 2014; Grivna et al., 2006; Lee et al., 2011). Although piRNAs were originally thought to be restricted in the germ cells where they play a role in preserving genomic integrity by suppressing mobile genetic elements, studies over the past years have uncovered the presence of piRNAs in various somatic cells (Yan et al., 2011; Peng and Lin, 2013). Particularly, piRNAs are highly abundant in neurons (Rajasethupathy et al., 2012; Lee et al., 2011; Zuo et al., 2016).

The present study is the first to report the presence of piRNA like molecules in mammalian axons during nerve regeneration. Subsequent studies in our lab further showed that small-RNA sequences that were annotated to piRNA bank displayed characteristic features of mammalian piRNAs and immunoprecipitated with Miwi (Phay et al., 2016). Bioinformatics analysis revealed that these axoplasmic piRNAs also exhibited temporal changes in their levels in response to nerve injury.

Additionally, RNAi knockdown of Miwi (mouse homolog of Piwi) protein in cultured sensory neurons preconditioned with nerve injury resulted in an increase of axon growth. These findings suggest that piRNAs could play a role in regulating intra-axonal protein synthesis in regenerating nerve. To date, mRNA targets of axoplasmic piRNAs have yet to be identified. Interestingly, a recent study has demonstrated that miRNAs and piRNAs can reciprocally regulate one another (Du et al., 2018). This finding led me to further examine the relationship between sequence reads that were annotated to miRNA and piRNA population in the sequencing dataset. Analysis of small RNA classification showed that the percentage of reads that were mapped to miRNA and piRNA at different injury time points is inversely proportional to each

other (Fig. 2.2C). This observation suggests the possibility that piRNA could play a role in regulating miRNA function during axon regeneration.

REFERENCES

- Abe N, Cavalli V (2008) Nerve injury signalling. *Curr Opin Neurobiol* 18:276-283.
- Akkouche A et al (2018) Maternally deposited germline piRNAs silence the transposon retrotransposon in somatic cells. *EMBO Rep* 14(5): 458-464.
- Aschrafi A, Schwechter AD, Mameza MG, Natera-Naranjo O, Gioio AE, Kaplan BB (2008) MicroRNA-338 regulates local cytochrome C oxidase IV mRNA and oxidative phosphorylation in the axons of sympathetic neurons. *J Neurosci* 28:12581-12590.
- Assouline JG, Bosch P, Lim R, Kim IS, Jensen R, Pantazis NJ (1987) Rat astrocytes and Schwann cells in culture synthesize nerve growth factor-like neurite-promoting factors. *Brain Res* 428:103-118.
- Ben-Yaakov K, Dagan SY, Segal-Ruder Y, Shalem O, Vuppalanchi D, Willis DE, Yudin D, Rishal I, Rother F, Bader M, Blesch A, Pilpel Y, Twiss JL, Fainzilber M (2012) Axonal transcription factors signal retrogradely in lesioned peripheral nerve. *EMBO J* 31:1350-1363.
- Bhatheja K, Field J (2006) Schwann cells: origins and role in axonal maintenance and regeneration. *Int J Biochem Cell Biol* 38:1995-1999.
- Cheng C, Bhardwaj N, Gerstein M (2009) The relationship between the evolution of microRNA targets and the length of their UTRs. *BMC Genomics* 10:431.
- David S, Aguayo AJ (1981) Axonal elongation into peripheral nervous system "bridges" after central nervous system injury in adult rats. *Science* 214:931-933.
- Du WW, Yang W, Xuan J, Gupta S, Krylov SN, Ma X, Yang Q, Yang BB (2016) Reciprocal regulation of miRNAs and piRNAs in embryonic development. In: *Cell Death Differ*, 1458-1470.
- Dun XP, Parkinson DB (2015) Visualizing peripheral nerve regeneration by whole mount staining. *PLoS One* 10:e0119168.

- Filbin MT (2003) Myelin-associated inhibitors of axonal regeneration in the adult mammalian CNS. *Nat Rev Neurosci* 4:703-713.
- Frade JM, Ovejero-Benito MC (2015) Neuronal cell cycle: the neuron itself and its circumstances. *Cell Cycle*, 712-720.
- GrandPre T, Nakamura F, Vartanian T, Strittmatter SM (2000) Identification of the Nogo inhibitor of axon regeneration as a Reticulon protein. *Nature* 403:439-444.
- Grivna ST, Beyret E, Wang Z, Lin H (2006) A novel class of small RNAs in mouse spermatogenic cells. *Genes Dev* 20:1709-1714.
- Hanz S, Fainzilber M (2006) Retrograde signaling in injured nerve--the axon reaction revisited. *J Neurochem* 99:13-19.
- Hanz S, Perlson E, Willis D, Zheng JQ, Massarwa R, Huerta JJ, Koltzenburg M, Kohler M, van-Minnen J, Twiss JL, Fainzilber M (2003) Axoplasmic importins enable retrograde injury signaling in lesioned nerve. *Neuron* 40:1095-1104.
- He Z, Jin Y (2016) Intrinsic Control of Axon Regeneration. *Neuron* 90:437-451.
- Hengst U, Cox LJ, Macosko EZ, Jaffrey SR (2006) Functional and selective RNA interference in developing axons and growth cones. *J Neurosci* 26:5727-5732.
- Huebner EA, Strittmatter SM (2009) Axon Regeneration in the Peripheral and Central Nervous Systems. *Results Probl Cell Differ* 48:339-351.
- Jessen KR, Mirsky R (2016) The repair Schwann cell and its function in regenerating nerves. *J Physiol*, 3521-3531.
- Ji B, Case LC, Liu K, Shao Z, Lee X, Yang Z, Wang J, Tian T, Shulga-Morskaya S, Scott M, He Z, Relton JK, Mi S (2008) Assessment of functional recovery and axonal sprouting in oligodendrocyte-myelin glycoprotein (OMgp) null mice after spinal cord injury. *Mol Cell Neurosci* 39:258-267.
- Lee EJ, Banerjee S, Zhou H, Jammalamadaka A, Arcila M, Manjunath B, Kosik KS (2011) Identification of piRNAs in the central nervous system. *RNA*, 1090-1099.

- Lemons ML, Howland DR, Anderson DK (1999) Chondroitin sulfate proteoglycan immunoreactivity increases following spinal cord injury and transplantation. *Exp Neurol* 160:51-65.
- Liu NK, Wang XF, Lu QB, Xu XM (2009) Altered microRNA expression following traumatic spinal cord injury. *Exp Neurol* 219:424-429.
- Ma TC, Willis DE (2015) What makes a RAG regeneration associated? *Front Mol Neurosci* 8:43.
- McKerracher L, Rosen KM (2015) MAG, myelin and overcoming growth inhibition in the CNS. *Front Mol Neurosci* 8.
- McKerracher L, David S, Jackson DL, Kottis V, Dunn RJ, Braun PE (1994) Identification of myelin-associated glycoprotein as a major myelin-derived inhibitor of neurite growth. *Neuron* 13:805-811.
- Moon LD, Asher RA, Rhodes KE, Fawcett JW (2002) Relationship between sprouting axons, proteoglycans and glial cells following unilateral nigrostriatal axotomy in the adult rat. *Neuroscience* 109:101-117.
- Mukhopadhyay G, Doherty P, Walsh FS, Crocker PR, Filbin MT (1994) A novel role for myelin-associated glycoprotein as an inhibitor of axonal regeneration. *Neuron* 13:757-767.
- Murashov AK, Chintalgattu V, Islamov RR, Lever TE, Pak ES, Sierpinski PL, Katwa LC, Van Scott MR (2007) RNAi pathway is functional in peripheral nerve axons. *FASEB J* 21:656-670.
- Nakanishi K, Nakasa T, Tanaka N, Ishikawa M, Yamada K, Yamasaki K, Kamei N, Izumi B, Adachi N, Miyaki S, Asahara H, Ochi M (2010) Responses of microRNAs 124a and 223 following spinal cord injury in mice. *Spinal Cord* 48:192-196.
- Natera-Naranjo O, Aschrafi A, Gioio AE, Kaplan BB (2010) Identification and quantitative analyses of microRNAs located in the distal axons of sympathetic neurons. *RNA*, 1516-1529.
- Ngeow WC (2010) Scar less: a review of methods of scar reduction at sites of peripheral nerve repair. *Oral Surg Oral Med Oral Pathol Oral Radiol Endod* 109:357-366.

- Osada H, Takahashi T (2007) MicroRNAs in biological processes and carcinogenesis. *Carcinogenesis* 28:2-12.
- Peng JC, Lin H (2013) Beyond transposons: the epigenetic and somatic functions of the Piwi-piRNA mechanism. *Curr Opin Cell Biol* 25:190-194.
- Perlson E, Hanz S, Ben-Yaakov K, Segal-Ruder Y, Seger R, Fainzilber M (2005) Vimentin-dependent spatial translocation of an activated MAP kinase in injured nerve. *Neuron* 45:715-726.
- Phay M, Kim HH, Yoo S (2018) Analysis of piRNA-Like Small Non-coding RNAs Present in Axons of Adult Sensory Neurons. *Mol Neurobiol* 55(1): 482-494
- Prinjha R, Moore SE, Vinson M, Blake S, Morrow R, Christie G, Michalovich D, Simmons DL, Walsh FS (2000) Inhibitor of neurite outgrowth in humans. *Nature* 403:383-384.
- Rajasethupathy P, Antonov I, Sheridan R, Frey S, Sander C, Tuschl T, Kandel ER (2012) A role for neuronal piRNAs in the epigenetic control of memory-related synaptic plasticity. *Cell* 149:693-707.
- Rajman M, Schrott G (2017) MicroRNAs in neural development: from master regulators to fine-tuners. *Development* 144:2310-2322.
- Richardson PM, McGuinness UM, Aguayo AJ (1980) Axons from CNS neurons regenerate into PNS grafts. *Nature* 284:264-265.
- Ross RJ, Weiner MM, Lin H (2014) PIWI proteins and PIWI-interacting RNAs in the soma. *Nature* 505:353-359.
- Sandberg R, Neilson JR, Sarma A, Sharp PA, Burge CB (2008) Proliferating cells express mRNAs with shortened 3' UTRs and fewer microRNA target sites#. *Science* 320:1643-1647.
- Stoll G, Muller HW (1999) Nerve injury, axonal degeneration and neural regeneration: basic insights. *Brain Pathol* 9:313-325.
- Stoll G, Jander S, Myers RR (2002) Degeneration and regeneration of the peripheral nervous system: from Augustus Waller's observations to neuroinflammation. *J Peripher Nerv Syst* 7:13-27.

- Taylor AM, Berchtold NC, Perreau VM, Tu CH, Jeon NL, Cotman CW (2009) Axonal mRNA in uninjured and regenerating cortical mammalian axons. *J Neurosci* 29:4697-4707.
- Vargas ME, Barres BA (2007) Why is Wallerian degeneration in the CNS so slow? *Annu Rev Neurosci* 30:153-179.
- Wang B, Bao L (2017) Axonal microRNAs: localization, function and regulatory mechanism during axon development. *J Mol Cell Biol*, 82-90.
- Willis DE, van Niekerk EA, Sasaki Y, Mesngon M, Merianda TT, Williams GG, Kendall M, Smith DS, Bassell GJ, Twiss JL (2007) Extracellular stimuli specifically regulate localized levels of individual neuronal mRNAs. *J Cell Biol* 178:965-980.
- Yan Z, Hu HY, Jiang X, Maierhofer V, Neb E, He L, Hu Y, Hu H, Li N, Chen W, Khaitovich P (2011) Widespread expression of piRNA-like molecules in somatic tissues. *Nucleic Acids Res* 39:6596-6607.
- Yoo AS, Sun AX, Li L, Shcheglovitov A, Portmann T, Li Y, Lee-Messer C, Dolmetsch RE, Tsien RW, Crabtree GR (2011) MicroRNA-mediated conversion of human fibroblasts to neurons. *Nature* 476:228-231.
- Yu B, Zhou S, Wang Y, Ding G, Ding F, Gu X (2011) Profile of MicroRNAs following Rat Sciatic Nerve Injury by Deep Sequencing: Implication for Mechanisms of Nerve Regeneration. *PLoS One*
doi.org/10.1371/journal.pone.0024612
- Yudin D, Hanz S, Yoo S, Iavnilovitch E, Willis D, Gradus T, Vuppalanchi D, Segal-Ruder Y, Ben-Yaakov K, Hieda M, Yoneda Y, Twiss JL, Fainzilber M (2008) Localized regulation of axonal RanGTPase controls retrograde injury signaling in peripheral nerve. *Neuron* 59:241-252.
- Zheng JQ, Kelly TK, Chang B, Ryazantsev S, Rajasekaran AK, Martin KC, Twiss JL (2001) A functional role for intra-axonal protein synthesis during axonal regeneration from adult sensory neurons. *J Neurosci* 21:9291-9303.
- Zhou S, Yu B, Qian T, Yao D, Wang Y, Ding F, Gu X (2011) Early changes of microRNAs expression in the dorsal root ganglia following rat sciatic nerve transection. *Neurosci Lett* 494:89-93.
- Zuo L, Wang Z, Tan Y, Chen X, Luo X (2016) piRNAs and Their Functions in the Brain. *Int J Hum Genet* 16:53-60.

Chapter 3

AXONAL LOCALIZATION AND LOCAL MATURATION OF SPECIFIC SUBSETS OF PRECURSOR MICRORNAS AND THEIR BIOLOGICAL ROLES IN RERENERGATING AXONS

Introduction

Local translation of specific mRNAs transported subcellularly is a conserved mechanism that allows cells to spatially and temporally control protein expression. This mechanism not only provides a basis for establishing molecular asymmetry that is important for many biological processes but also enables rapid changes in local cellular proteome without having to first signal the nucleus to induce transcription followed by translation and subsequent transport of individual protein (Piper and Holt, 2004; Jung et al., 2012). Thus, molecular understanding of how localized mRNA translation is precisely regulated is an important question in diverse biological context.

Given that a single transcript can produce multiple proteins, local translation of localizing mRNAs is a very efficient way for cells to generate protein asymmetry. The resultant asymmetrical distribution of proteins contributes to the development and dynamics of polarity in many different cell types, including epithelia cells, migrating

cells, and neural cells (neurons and glial cells). During the formation of basal-apical cellular architecture, transcripts encoding polarity proteins such as Stardust and Crumbs are localized apically in *Drosophila* follicle epithelial cells and embryonic epithelial cells, where their local protein production is required to specify the apical domain (Tepass et al., 1990; Bachmann et al., 2001; Barr et al., 2016). In a migrating fibroblast, mRNA encoding β -actin (cytoskeletal protein) is localized to the leading edge, where a high concentration of β -actin monomer is generated by local translation to facilitate polarized cell movement (Kislauskis et al., 1997). In neurons, differential targeting of mRNAs encoding microtubule-associated protein 2 (MAP2) to dendrites and Tau to axons contributes to directional localization of cytoskeletal proteins that maintain neuronal transport systems (Garner et al., 1988; Litman et al., 1994; Hirokawa et al., 1996).

Another advantage of local translation of mRNAs after their localization is to prevent the activity of proteins with special local function in an inappropriate region of the cell. For example, myelin basic protein (MBP) is a component of the myelin sheath (extension of glial cell membrane that insulates neuronal axons) that binds non-discriminately to membranes and causes them to collapse. To prevent other regions of glial cell membrane from collapsing, *MBP* mRNA is localized to the plasma membrane and undergoes local translation only at the axon-glia contact site (Muller et al., 2013).

Neurons are extremely polarized cells with specialized dendritic and axonal compartments that respond rapidly to local stimuli. Since the length of some dendrites

and axons can exceed more than ten- to one thousand-fold the diameter of the neuronal cell body, coupling of mRNA localization and local protein synthesis enables dendrites and axons to autonomously respond to external stimuli (including injury). Intra-dendritic protein synthesis of localized mRNAs has been implicated in the formation of synapses and activity dependent synaptic plasticity (Holt and Shuman, 2013). For example, local translation of dendritic mRNA encoding brain derived neurotrophic factor (BDNF) induces selective translation of activity-regulated cytoskeletal protein (Arc) in the synapto-dendritic compartment (Kang and Schuman, 1996; Yin et al., 2012). These locally generated Arc proteins then modulate synaptic efficacy by altering the spine size (Peebles et al., 2010) and regulate the endocytosis of AMPA-type glutamate receptors (AMPA) (Chowdhury et al., 2006; Rial Verde et al., 2006). Synaptic stimulation has also been shown to induce local translation of *calcium-calmodulin-dependent protein kinase II (CaMKII)* mRNA, which increases the size of post-synaptic (dendritic) spines to mediate long-term potentiation (LTP) (Bagni et al., 2000; Lisman et al., 2012; Hell, 2014). Similarly in axons, locally translated protein is crucial in providing navigational direction for the growth cone during axon pathfinding (Spaulding and Burgess, 2017). *β -actin* mRNA is one of the first transcripts to be identified in the growth cones of developing axons (Bassell et al., 1998; Eng et al., 1999). In response to attractive chemotropic cues such as netrin-1, intra-axonal *β -actin* mRNA is translated into proteins to facilitate attractive growth cone turning (Leung et al., 2006), whereas repulsive chemotropic cues such as slit 2 triggers rapid local production of cofilin, a protein that destabilizes actin polymer and

causes growth cone collapse, resulting in growth cone turning (Piper et al., 2006). In addition, several recent studies showed that intra-axonal protein synthesis plays a crucial role in degenerative and regenerative responses following injury. For example, nerve injury triggers rapid mRNA translation of a variety of proteins including a transcription factor STAT3 and transporting protein components such as ran binding protein 1 (RanBP1) and importin- β 1 that provide retrograde injury signals to the cell body (Ben-Yaakov et al., 2012; Hanz et al., 2003; Yudin et al., 2008). Locally synthesized proteins that retrogradely transport injury signals to the cell body consequently trigger robust cell body responses that are necessary for successful regeneration.

It is now known that intra-axonal protein synthesis is important for many aspects of neurophysiological functions. However, little is known about the molecular mechanisms underlying the regulation of intra-axonal translation. Spatial control over intra-axonal protein expression can be achieved by regulating mRNA transport, since axonal mRNA transport can dynamically contribute to the contents of an axonal transcriptome and, subsequently, proteome by local translation. mRNA transport is accomplished through the recognition of *cis*-acting localization elements (LEs) typically located in the 3' untranslated region (UTR) of mRNAs by *trans*-acting factors such as an RNA binding protein (RBP). For example, a 54 nts *cis*-acting LE in the 3'UTR of *β -actin* mRNA, called “zipcode”, is required for the localization of this transcript into cellular periphery of a migrating fibroblasts or into dendrites and axons of neurons (Rodriguez et al., 2008; Zheng et al., 1999; Tiruchinapalli et al., 2003).

The zipcode element is recognized by a RBP called zipcode binding protein 1 (ZBP1) that regulates the transport of β -actin mRNA to its final destination. Since localizing mRNAs need to be translationally silenced *en route* to the final destination, the binding of ZBP1 stabilizes β -actin mRNA and inhibits premature translation. Upon arrival to the final destination, specific signal(s) are necessary for de-repressing translation to synthesize new proteins. For example, BDNF signals to phosphorylate the ZBP1 by Src-family kinase, triggering conformational changes that releases the bound β -actin mRNA for translational initiation machinery (Huttelmaier et al., 2005; Sasaki et al., 2010). For example, application of netrin-1 to axonal growth cones promotes both the translocation of ZBP1 bound to β -actin mRNA to the site of stimulation and local protein expression partially facilitated by asymmetrical activation of mammalian target of rapamycin (mTOR) pathway to mediate attractive growth cone turning (Leung et al., 2006). Although mRNA localization and activity-dependent translation provide spatial control over local protein expression in axons, the mechanism underlying temporal control of intra-axonal mRNA translation is still unclear. A recently discovered class of non-coding small RNAs called microRNAs has been shown to negatively regulate gene expression at the post-transcriptional level. These small regulatory RNAs could potentially serve as a temporal regulator that represses specific *de novo* synthesis of axonal proteins that are no longer required for particular neurological function.

MicroRNAs are single stranded non-coding RNAs of 18 – 24 nucleotides in length that modulate gene expression at a post-transcriptional level by promoting

transcript degradation and/or inducing translational repression (Bartel, 2004). In animal cells, the generation of mature miRNA starts in the nucleus with the transcription of a miRNA gene by RNA polymerase II into a long primary miRNA (pri-miRNA) transcript. Once transcribed, pri-miRNA is processed by an RNase III enzyme, Drosha, together with its cofactor DiGeorge Syndrome Critical Region 8 (DGCR8) into a ~70 nts hairpin structure precursor miRNA (pre-miRNA). Pre-miRNA is then exported into the cytosol, where another RNase III enzyme, Dicer, together with its cofactor the HIV-1 transactivating response RNA-binding protein (TRBP), processes it into a ~22 nts duplex. The resultant miRNA:miRNA* duplex (passenger strand is designated with asterisk) is loaded into Argonaute (AGO) protein and the strand with the thermodynamically less stable 5' end is selected to serve as a guide (mature miRNA) for the miRNA-induced silencing complex (miRISC), while the opposing strand (miRNA*) is degraded. Although the formation of the miRISC recruits other effectors of translational repression and/or mRNA degradation that are necessary for miRNA-mediated gene silencing, the core components of the miRISC containing just small RNA bound to Argonaute protein is necessary and sufficient for mRNA target recognition and gene silencing (Rivas et al., 2005).

Functionally active mature miRNA relies heavily on Watson-Crick base pairing between the seed region (2-8 nt residues from the 5' proximal end) of mature miRNA and its cognate target mRNAs for target recognition. This recognition site is typically located within the 3'UTR of target mRNAs. Upon recognition, miRNA associated RNA-induced silencing complex (miRISC) represses translation in one of

two ways, depending on the nature and the degree of miRNA:mRNA base pairing. MicroRNA-directed mRNA cleavage (mRNA degradation) occurs when there is an extensive miRNA:mRNA complementarity (100% complementarity or base-pairing over the seed region plus 10-17 nts of mature miRNA). In contrast, imperfect base pairing downstream of the seed region complementary to the target mRNA leads to translational inhibition. In mammalian cells, most mature miRNAs form imperfect base pairing downstream of the seed region with their mRNA targets and thus decrease the amount of protein output without substantially affecting the mRNA level (Bartel, 2004; Wightman et al., 1993).

Since its initial discovery in 1993, hundreds of miRNAs have been identified in variety of organisms. Studies over the past two decades revealed that miRNAs play an important regulatory role in many biological processes including development timing and tissue maintenance (Bartel, 2004; Ambros, 2011; Hwang and Mendell, 2006). Evolutionarily conserved miRNAs such *lin-4*/miR-125 and *let-7* are essential in orchestrating key developmental events (Ambros, 2011). Early studies in *C. elegans* showed that *lin-4* and *let-7* control cell fate progression and differentiation throughout development by gradually down-regulating the expression of key transcription factors such as LIN-14 and LIN-41, respectively (Zhang and Fire, 2010; Hammell et al., 2009; Slack et al., 2000). In adult animals, miRNAs have been shown to precisely regulate cell proliferation and apoptosis. For example, in *Drosophila*, *Bantam* miRNA stimulates cell proliferation and blocks apoptosis by silencing the expression of pro-apoptotic gene, *hid* (Brennecke et al., 2003). On the other hand,

miR-497 has been shown to suppress cell proliferation and induce apoptosis by negatively regulating the expression of cell survival protein Bcl2 to promote the activity of caspase-9/3 (Yanget al., 2016; Wu et al., 2016). Given the importance of its regulatory roles in cellular functions, aberrant levels of miRNAs have been linked to various diseases such as cancer and neurological diseases (Alzheimer, Parkinson, Huntington, amyotrophic lateral sclerosis, schizophrenia, and autism) (Peng, 2016; Ma et al., 2015).

Recently, miRNAs have emerged as a crucial regulator in the nervous system. The role of miRNAs in the nervous system was first observed in early miRNA-pathway knockout experiments (Giraldez et al. 2005; Kawase-koga et al., 2009; Davis et al., 2008). For example, knockout of pre-miRNA processing enzyme dicer severely affected brain development by impairing the formation of neurocoel and neural tube in Zebrafish embryo (Giraldez et al., 2005). Since then, individual miRNAs such as miR-134 and miR-184 have been implicated in neural progenitor maintenance and proliferation. Contemporaneously, let-7 family (let-7a/let-7b) and several highly abundant miRNAs in the brain such as miR-9 and miR-124 have been shown to promote neuronal differentiation (Stappert et al., 2015; Bian et al., 2013).

In adult neurons, miRNAs are differentially distributed into dendrites and axons where they play a role in regulating different neuronal functions. Dendritic miRNAs have been shown to regulate morphology and functions of the synapse in an activity dependent manner. For example, dendritically localized miR-134 regulates spine development by negatively inhibiting local translation of mRNA encoding

LIMK1, a protein that promotes spine outgrowth by controlling actin filament dynamics (Schratt et al., 2006). In axons, miRNAs have been shown to regulate energy metabolism and activity of local protein synthesis. For example, miR-338 regulates axonal mitochondria function and ATP production by modulating the expression of nuclear-encoded mitochondria proteins cytochrome c-oxidase (CoxIV) and ATP synthase (ATP5G1) (Aschrafi et al., 2008). More recently, axonally localized miR-16 has been demonstrated to regulate intra-axonal protein synthesis activity by inhibiting local translation of mRNA encoding eukaryotic translation initiation factors eIF2B2 and eIF4G2 (Kar et al., 2013).

Although it is now clear that miRNAs play essential regulatory roles in dendrites and axons, there is a lack of understanding of how small RNAs are transported into the distal region of these neuronal compartments. Recent studies in the Schratt laboratory have demonstrated that precursor miR-134 is targeted to synapto-dendritic compartment by DEAH-box helicase (DHX36) (Bicker et al., 2013). Direct association of DHX36 with the terminal loop region of pre-miR-134 is not only important for the dendritic localization but also protects the precursor miRNA from Dicer-mediated cleavage (Bicker et al., 2013). This finding suggests that dendritically localized pre-miRNAs could provide local sources of mature miRNAs. Very recently, study in the Schuman laboratory has demonstrated that dendritically localized pre-miRNAs are locally processed by Dicer into their corresponding mature miRNAs in an activity dependent manner (Sambandan et al., 2017). Yet, the molecular mechanism underlying axonal targeting of miRNAs remains largely unknown.

Previous work in our laboratory has shown that subsets of miRNA precursors are selectively localized into distal axons of sensory neurons. We also showed that components of miRNA biogenesis machinery such as dicer and KSRP (proteins that promote maturation of a subset of pre-miRNAs) also localized to axons and growth cones. Based on these findings, ***I hypothesized that particular groups of precursor miRNAs are selectively localized to distal axons, where the corresponding mature miRNAs are generated in an activity dependent manner via local processing to regulate specific intra-axonal mRNA translation.*** Localization of pre-miRNAs would not only provide axons with local sources of functionally active mature miRNA, but also enable precise control over specific miRNA activity by regulating local processing of the precursors. This is extremely important as abnormal activities and levels of miRNAs have been shown to strongly associate with impairment in numerous neurological functions (Wang et al., 2012; Ma et al., 2015).

Previous work in our laboratory showed that miR-433 precursor (pre-miR-433) is present in axons of cultured DRG neurons and in rat sciatic nerve (Kim et al., 2015). Interestingly, the levels of both axonal pre-miR-433 and mature miR-433-3p showed significant increases on day 7 after nerve injury. Since 7 days following nerve injury is considered as the apex of axonal regenerative response (Yi et al., 2015; Dun and Parkinson, 2015), the regulatory role of functionally active miR-433-3p could provide further insight into molecular pathways that facilitate axon regeneration. To further dissect the mechanism underlying selective targeting of pre-miR-433 into axons, I utilized an RNA reporter system and systematically identified the terminal loop region

of pre-miR-433 structure as a *cis*-element that strongly governs the transport of reporter mRNAs into distal axons. In addition, I showed that axonally localized pre-miR-433 is locally processed into mature miR-433-3p in the absence of the neuronal cell body. Using bioinformatics tools, functionally active mature miR-433-3p was predicted to target axonally localized *Ran binding protein 1 (RanBP1)* mRNA, whose intra-axonal translation at the injury site is essential for the retrograde injury signaling in distal axons (Yudin et al., 2008). To test whether miR-433-3p recognizes target sequences in the 3'UTR of RanBP1 mRNA, as predicted by bioinformatics tools, the interaction of miR-433-3p and its targeting sequences was assessed using a dual luciferase reporter assay and then confirmed in primary DRG neurons in culture. Here, I showed that overexpression of miR-433-3p in cultured DRG neurons reduced the level of RanBP1 in axons/growth cones and caused attenuation in axon growth. Together, these findings provide a mechanism for axons to generate a local source of biologically active mature miRNAs as well as providing evidence for the regulatory role of miR-433-3p in axon regeneration.

Material and Methods

Dissociated DRG culture and transfection

All animal procedures described in this chapter were conducted under protocols approved by the Institutional Animal Care and Use Committee (IACUC) of Alfred I. duPont Hospital for Children. Adult male *Sprague Dawley* rats (150 – 250g) were euthanized by asphyxiation under CO₂ gas, and dorsal root ganglion (DRG) neurons from L2-L6 were collected in ice cold Hibernate A medium (Gibco). Collected ganglia were sterilized by multiple washes in Hibernate A medium containing penicillin and streptomycin, and dissociated for 40 minutes with collagenase at 37 °C in DRG culture media containing DMEM/F12 media (Gibco), 5% horse serum (Hyclone), 5% fetal bovine serum (Sigma), 25 mM HEPES, 2 mM L-Glutamine, 1X N1 supplement (Sigma), and 10 µM Cytosine Arabinoside (Ara C), followed by several rounds of trituration using fire polished glass pipettes. To aid in the trituration steps, DNase I was added to the cell suspension. After dissociation, the cells were washed three times with DRG culture media and plated at a low density on to glass cover slips (FISH/IF experiments) or on glass bottom dishes (for FRAP experiment) coated with poly-L-lysine (10 µg/cm², Sigma) and laminin (5 µg/mL, Millipore). For the compartmentalization culture of DRG neurons, dissociated ganglia were plated on porous (8 µm) polyethylene tetrathalate (PET) membrane inserts (BD Falcon) coated with poly-L-lysine and laminin. Cytosine Arabinoside (Ara C, 10 µM) was added to the culture media daily to prevent glia cell proliferation.

4D Nucleofector® device (Lonza) was used for transfections. Briefly, dissociated DRGs were suspended in Amaxa™ P3 4D Nucleofector® containing P3 supplement and subsequently transferred to the electroporation cuvette containing either 2.5 - 5 µg of DNA plasmid or 10 nM – 200 nM of synthetic small RNA. The cell suspension was then gently mixed with the DNA construct or the synthetic small RNA, and electroporated using CA 138 parameters. After transfection, cells were plated at a low density in the appropriate culture vessel and incubated at 37 °C with 5% CO₂.

Fluorescence in situ hybridization and Immunofluorescence

Pre-miRNA FISH

Digoxigenin (DIG) labeled locked nucleic acid (LNA) probe specific to the terminal loop region of the pre-miR-433, pre-miR-138-1, and scrambled probe (Exiqon) were used for hybridization to detect precursor miRNAs in sensory neurons. DRG neurons were cultured on glass coverslips and used for pre-miRNA FISH at 3 days in culture. In brief, coverslips were rinsed twice with phosphate buffer saline (PBS), fixed in 2% paraformaldehyde (PFA) for 15 minutes, and permeabilized with 0.3% triton X-100 in (tris buffer with 50% saline) TBS₅₀ for 8 minutes. The samples were equilibrated in 1X (15 mM sodium citrate, 150 mM sodium chloride) sodium saline citrate (SSC) followed by a 5 minutes wash with 50% deionize formamide and then hybridized in 100 nM DIG-labeled miRCURY™ LNA probes in hybridization buffer (5X SSC, 20% Dextran sulphate, 50% formamide, 0.25 mg/mL ssDNA, 0.25

mg/mL tRNA and 1X Denhardt's) for 3 hours at 60°C in a humidified chamber. After hybridization, coverslips were washed twice with 50% deionized formamide in 1X SSC for 15 minutes followed by multiple rounds of washes with SSC in an increasing stringency (twice in 2X SSC for 5 minutes, twice in 1X SSC for 5 minutes, and twice in 0.5X SSC for 5 minutes) and processed for immunodetection. Coverslips were blocked with immunofluorescence (IF) buffer containing 3% heat shock bovine serum albumin (BSA) (Roche), 3% FBS (Gibco), 0.3% triton X-100 in TBS₅₀ for 1 hour at room temperature, followed by overnight incubation with the primary antibody [1:200 sheep anti-DIG (Roche, 11333089001), 1:200 chicken anti-neurofilament heavy chain (Millipore, AB5539), and 1:2000 anti-neurofilament light chain (Novus biological, NBP1-05219)] diluted in IF buffer at 4°C. After primary antibody incubation, coverslips were washed three times in TBS₅₀ for 5 minutes followed by incubation with Alexa 488-conjugated secondary anti-sheep and Alexa 555 conjugated secondary anti-chicken for 1 hour at room temperature. After several rounds of washes with TBS₅₀, samples were stained with DAPI diluted in PBS and mounted using mounting buffer containing n-propyl gallate to reduce fading of fluorescence signal. Fluorescent signals were detected by epifluorescence microscope (Zeiss AxioImager M2p equipped with AxioCam camera) and all images from each experiment were matched for exposure, gain, and offset to that of scrambled LNA probe control.

eGFP mRNA FISH

DIG-labeled antisense Riboprobes for *eGFP* mRNA were used to detect the reporter mRNA in DRG neurons transfected with eGFP^{myr}-pre-miR433, eGFP^{myr}-pre-miR-138-1, eGFP^{myr}-(S433 + L138-1), or eGFP^{myr}-(S138-1 + L433) construct. These Ribopobes were generated by *in vitro* transcription of linearized pcDNA2-EGFP with DIG RNA labeling mix (Roche). After the elimination of linearized pcCDNA-EGFP templates with DNase TURBO treatment, unincorporated nucleotides were removed using Mini Quick Spin RNA column (Roche). DIG-labeled *eGFP* mRNA antisense strands were alkaline hydrolyzed into ~100 – 150 fragments, ethanol precipitated, resuspended in nuclease free water, and quantified using Quant-iT RiboGreen RNA Assay Kit (Invitrogen). Transfected DRG neurons cultured on glass coverslips were rinsed twice in PBS, fixed with 2% PFA for 15 minutes at 3 days in culture and permeabilized with 0.3% triton X-100 in TBS₅₀ for 8 minutes. The samples were then equilibrated in 1X SSC, followed by brief wash in 50% deionized formamide in 1X SSC and then hybridized with Riboprobe (5 ng/μL) in hybridization buffer (5X SSC, 20% dextran sulfate, 50% formamide, 0.25 mg/mL ssDNA, 0.25 mg/mL tRNA and 1X Denhardts) in a humidified chamber for 3 hours at 50 °C. After hybridization, the coverslips were washed with 50% formamide in 1X SSC, followed by washes in 1X SSC (3 times for 5 minutes each), and processed for immunodetection. In brief, samples were blocked in IF blocking buffer for 1 hour at room temperature, incubated in primary sheep anti-DIG antibody diluted in blocking buffer over night at 4°C, followed by three rounds of washes with TBS₅₀ for 5 minutes each, and an incubation

in Alexa 555-conjugated secondary anti-sheep (1:200) diluted in blocking buffer for 1 hour at room temperature. After washes with TBS₅₀ and stained with DAPI, the samples were mounted as previously described, and FISH signals were detected by epifluorescence microscope (Zeiss AxioImager M2p equipped with AxioCam camera). All images from individual experiment were matched for exposure, gain, and offset to that of sense control probe.

Animal surgery and procedures

150 - 200g of *Sprague Dawley* male rats were used for all survival studies. Animals were anesthetized with intraperitoneal injection of ketamine and xylazine cocktail. Loss of consciousness was verified by cornea reflex and response to hind leg pinch. Surgical sites were prepared by removing hair from both hindquarters followed by application of 70% ethanol and Betadine disinfection solution. Right and left sciatic nerves were exposed at mid-thigh level by gluteal muscle-splitting incision. Crush injury was induced to the left sciatic nerve with twice for 15 seconds using fine forceps. Contralateral sciatic nerve (right) was left intact to serve as sham operated uninjured control. Incision sites were closed with 4-0 Ethion sutures followed by application of 70% ethanol. The animals were then placed on a heating pad to recover until awake and returned to the cage. On day 1, 4, 7, and 14 following injury, animals were euthanized by asphyxiation with CO₂ and sciatic nerves were carefully removed and subsequently processed for RNA extraction.

Axoplasmic RNA extraction from rat sciatic nerve

For *in vivo* studies examining the axonal levels of pre-miRNAs and mature miRNAs, the axoplasm was extracted from rat sciatic nerve using a modified mechanical squeeze method. In brief, sciatic nerves were carefully isolated and dissected out without damaging surrounding blood vessels from 150 – 250g euthanized *Sprague Dawley* rats and placed into microfuge tubes chilled on dry ice. The nerve segments were then washed with RNase free phosphate buffered saline (PBS) for several times and then transferred to a plastic dish containing at least 2 mL of RNase free PBS. Residual connective tissues around the nerve were carefully removed, and the nerve segment was further cut into 0.5 cm fragments and transferred to a new dish containing at least 2 mL of RNase free PBS. Nerve fragments were then transferred into a 1.5 mL RNase free microfuge tube containing 200 μ L of Trizol (Invitrogen) and gently squeezed with an RNase free plastic pestle to extract the axoplasm. No more than seven nerve fragments were squeezed into 200 μ L of Trizol. Extracted axoplasm in Trizol was then processed for RNA purification according to manufacturing protocol. RNA from the axoplasmic isolate was then quantified by fluorimetry using Quant-iT RiboGreen RNA Assay Kit (Invitrogen). 50 ng of the total axoplasmic RNA isolate was reverse transcribed to cDNA using iScript RT kit (BioRad) and subsequently used to test for RNA contaminations from the neuronal cell body and non-neuronal cells including glial cells by polymerase chain reaction (PCR). Primers for β -*actin* mRNA were used as a positive control for RNA amplification from the isolated axoplasm, primers for *MAP2* mRNA were used to test

for contamination from the neuronal cell body, and primers for *ErBb3*, *GFAP*, and *HIF0* mRNAs were used to test for contamination from glial cells and non-neuronal cells. The resultant RT-PCR amplicons were subjected to 1% agarose gel electrophoresis and analyzed by ethidium bromide staining. Only highly enriched axoplasmic RNA free of contaminants were used in downstream analysis with quantitative RT-PCR.

Axonal RNA isolation from compartmentalized primary DRG neuronal culture

L2-L6 DRGs from 150 – 250g male *Sprague Dawley* rats were dissociated as previously described and plated onto PET membrane inserts (BD Falcon) etched with 8 μ m pores coated with poly-L-lysine and laminin. DRG neurons were cultured for 3 days and 10 μ M of Ara C was added to the culture media daily to reduce proliferation of glial cells. To isolate the axonal fraction, both the top and bottom surfaces of the membrane were carefully rinsed in ice cold RNase free PBS three times before repeatedly scrapping the center of the bottom membrane surface containing the axonal compartment with a cell scrapper into Trizol (Invitrogen). After the axonal fraction was isolated, the top surface of the membrane insert was scrapped with a new cell scrapper to collect the cell body compartment into Trizol. The axonal fraction and cell body fraction were then processed for RNA purification according to the manufacturing protocol.

For the *in vitro* studies on intra-axonal processing of pre-miRNAs, DRG neurons were cultured as described above and the experiments were carried out at 3

days in culture. First, the top of the membrane containing the cell body compartment was carefully rinsed twice with RNase free PBS. Then, the cell body compartment was physically removed by using a cell scraper to repeatedly scrap the top surface of the membrane. Once the cell body fraction was removed and collected, the top of the membrane was rinsed twice with RNase free PBS and the inserts containing severed anucleate axons in the bottom of the membrane were placed back into culture media. The culture vessels were then placed back into the incubator (37°C, 5% CO₂) until harvesting the axonal fraction. The axonal fraction was collected as followed. First, both the top and bottom of the membrane inserts were rinsed 3 times with ice cold RNase Free PBS. Then, a cell scraper was used to repeatedly scrap the center of the bottom membrane surface to collect the axonal fraction into Trizol.

Purified axonal RNA was quantified using Quant-iT RiboGreen RNA Assay Kit (Invitrogen) and 50 ng of the RNA isolate was reverse transcribed into cDNA and subjected to extended PCR analysis previously described to determine the purity of axonal RNA isolate purity. Only highly enriched axonal RNA free of contamination of the cell body and glial cells was used for downstream analysis.

***Quantification of RNA by quantitative real time polymerase chain reaction
(RT-qPCR)***

Quantification of axonal pre-miR-433 and pre-miR-138-1

To compare levels of pre-miR-433 and pre-miR-138-1 in the axonal compartment vs. cell body compartment, RNA samples were isolated from DRG tissue and sciatic nerve axoplasm to examine the levels of these precursors *in vivo*. For the *in vitro* study, RNA samples were purified from the axonal fraction and the cell body fraction of DRG neurons that had been cultured in the Boyden chambers for 3 days. After checking RNA purity with extended RT-PCR, RNA samples were converted into cDNA using miR-X miRNA First Strand Synthesis Kit (Clontech). Subsequent RT-qPCR reaction was carried out using SYBR Advantage® qPCR Premix (Clontech) and primers specific to pre-miR-433 and pre-miR-138-1. U6 snRNA was used as an internal control since our previous *in vivo* and *in vitro* studies showed consistent expression of this RNA in both the cell body and axons. First, the level of pre-miRNAs was normalized to that of U6 [$\Delta C_t = C_t(\text{pre-miRNA}) - C_t(\text{U6})$]. Then, relative levels of axoplasmic/axonal pre-miRNAs were compared to that of the DRG/cell body fraction and expressed as the ratio of relative axonal pre-miRNA level to the relative cell body pre-miRNA level using the following calculation;

$$2^{-\Delta\Delta C_t} = 2^{-[\Delta C(\text{axon}) - \Delta C(\text{cell body})]}$$

Quantification of eGFP reporter mRNAs in the axon fraction of DRG neurons transfected with the reporter construct

Using iScript RT kit (BioRad), cDNA templates were generated from RNA samples isolated from the axonal fraction and cell body fraction of DRG neurons transfected with one of the following constructs; eGFP-pre-miR-433, eGFP-pre-miR-138-1, eGFP-(S433 + L138-1), and eGFP-(S138-1 + L433). Relative RT-qPCR analysis was carried out using EXPRESS[®] SYBR GreenER[™] and primers specific to the coding region of *eGFP* reporter mRNA. *GAPDH* mRNA was used as a reference control. First, relative level of *eGFP* mRNA to that of *GAPDH* mRNA (ΔC_t) was calculated as followed, $\Delta C_t = C_t(\text{eGFP}) - C_t(\text{GAPDH})$.

Then, RT-qPCR results are expressed as the ratio of relative axonal *eGFP* mRNA level to relative cell body *eGFP* mRNA level ($2^{-\Delta\Delta C_t}$) by using the following method;

$$2^{-\Delta\Delta C_t} = 2^{-[\Delta C(\text{axon}) - \Delta C(\text{cell body})]}$$

Quantification of pre-miR-433 and mature miR-433-3p in the axoplasm of regenerating nerve

Highly enriched axoplasmic RNA samples isolated from sham operated (uninjured control) nerves and injured sciatic nerves at 1-, 4-, 7-, and 14- days post injury were reverse transcribed into cDNA using miR-X miRNA First Strand Synthesis Kit (Clontech). The resulting cDNA was used as a template to determine the copy number of pre-miR-433 and mature miR-433-3p in the axoplasmic RNA

samples by absolute qPCR method. Quantitative PCR reactions were carried out using SYBR Advantage® qPCR Premix (Clontech) and standard curve for absolute qPCR analysis was generated using known concentrations of double stranded β -actin DNA templates. The standard curve was determined by plotting the C_t values against the corresponding Log transformed copy number of β -actin templates [C_t vs. Log(β -actin copy number)]. Using the following equation, $E = 10^{(-1/\text{slope}) - 1}$, the efficiency of β -actin primers was determined to be 101% and thus confirming the doubling of β -actin RT-qPCR product for every amplification cycle. The copy numbers of pre-miR-433 and mature miR-433-3p were extrapolated from the standard curve using the following calculation; Copy number = $10^{(C_t - y)/\text{-slope}}$.

Quantification of pre-miRNAs and mature miRNAs in severed anucleate axons

RNA purified from the axonal fraction harvested at 0 hr, 2 hrs, and 6 hrs after removing the cell body was spiked with 0.05 ng of *in vitro* transcribed *eGFP* mRNA. *eGFP* mRNA was added to serve as a reference control since the level of U6 was inconsistent between the axonal fraction collected at different time points after anucleation. RNA samples were converted into cDNA using miR-X miRNA First Strand Synthesis Kit (Clontech). Then, RT-qPCR reaction was carried out using SYBR Advantage® qPCR Premix. Pre-miRNA was detected using either forward and reverse primers specific to each precursor or forward primer specific to the terminal loop region of the precursors and a universal reverse primer included in miR-X

miRNA First Strand Synthesis Kit (Clontech). Mature miRNAs were detected using forward primer specific to each mature miRNA of interest and universal reverse primer. Levels of pre-miRNAs and mature miRNAs were first normalized to the level of spiked *eGFP* mRNA (ΔC_t) as followed, $\Delta C_t = C_t(\text{pre-miRNA or mature miRNA}) - C_t(\text{eGFP})$. Then relative levels of mature miRNAs to their corresponding pre-miRNAs ($2^{-\Delta\Delta C_t}$) were calculated as followed,

$$2^{-\Delta\Delta C_t} = 2^{-[\Delta C(\text{mature miRNA}) - \Delta C(\text{pre-miRNA})]}$$

Quantification of mature miR-433-3p and RanBP1 mRNA in DRG neurons transfected with synthetic small RNAs.

RNA sample isolated from DRG neurons (cultured for 2 days) transfected with mimic control, miR-433-3p mimic, or antisense miR-433-3p mimic was reverse transcribed into cDNA using miR-X miRNA First Strand Synthesis Kit (Clontech). The resulting cDNA was then used as a template for RT-qPCR analysis using Advantage® qPCR Premix. Primers specific to the coding region of *RanBP1* mRNA was used to detect both the short and the extended form of *RanBP1* mRNA's 3'UTR variants. Primers specific to the extended 3'UTR of *RanBP1* mRNA was used to exclusively detect *RanBP1* mRNA containing an extended 3'UTR. Forward primer specific to miR-433-3p and universal reverse primer included in miR-X miRNA First Strand Synthesis Kit (Clontech) was used to detect mature miR-433-3p. In the RT-

qPCR analysis, U6 was used as a reference control for miR-433-3p and *GAPDH* mRNA was used as a reference control for *RanBP1* mRNAs. Relative levels of miR-433-3p to that of U6 was calculated [$\Delta C_t = C_t(\text{miR-433-3p}) - C_t(\text{U6})$] and subsequently normalized to the relative level of miR-433-3p in mimic control $2^{-\Delta\Delta C_t} = 2^{-[\Delta C(\text{indicated small synthetic RNAs}) - \Delta C(\text{mimic control})]}$. Similarly, relative level of *RanBP1* mRNA to that of *GAPDH* mRNA was calculated [$\Delta C_t = C_t(\text{RanBP1}) - C_t(\text{GAPDH})$] and then normalized to the relative level of *RanBP1* mRNA in mimic control $2^{-\Delta\Delta C_t} = 2^{-[\Delta C(\text{indicated small synthetic RNAs}) - \Delta C(\text{mimic control})]}$.

Fluorescence recovery after photobleaching (FRAP)

DRG neurons were transfected with indicated eGFP^{myr} reporter constructs and plated at low density onto a 35 mm glass-bottom dish coated with poly-L-lysine and laminin as previously described. 48-72 hours after transfection, neurons expressing GFP were selected for FRAP analysis. To minimize the diffusion of eGFP proteins, a myristoylation tag (myr) was added to the N-terminus of eGFP protein to anchor newly synthesized eGFP^{myr} to the adjacent plasma membrane. In addition, axonal terminals measured at least 500 μm or greater from the cell body were carefully selected to further minimize the diffusion. FRAP experiments were performed using a Zeiss LSM 880 confocal microscope fitted with environment chamber (37 °C), 40X oil immersion objective, and 488 nm laser line for eGFP excitation and

photobleaching. Prior to photobleaching (prebleach), terminal axons were imaged for every 15 seconds over 1 minute to establish baseline for fluorescence intensity. A region of interest (ROI) containing 100 – 150 μm of the terminal axon was then exposed to 488 nm laser line set to 100% power for 50 frames at 1-second intervals (bleach). Recovery of eGFP^{myr} fluorescence signals were monitored every 15 seconds over 20 minutes using the same 488 nm laser line setting for prebleach image acquisition (postbleach). To ensure that eGFP^{myr} fluorescence recovery was due to intra-axonal translation, the culture was pretreated with a protein synthesis inhibitor Cycloheximide (100 $\mu\text{g}/\text{mL}$) or Anisomycin (10 mM) for at least 20 minutes before imaging. The image processing tool in Zen Black was used to determine the fluorescence intensity in the ROIs of raw confocal images. These values were then normalized to prebleach baseline intensity to calculate for percent recovery. For statistical analysis, two-way ANOVA with repeated measures was used to compare fluorescence recovery in DMSO *vs.* protein synthesis inhibitor treated group. If the DMSO treated group was statistically different from the protein synthesis inhibitor group, one-way ANOVA followed by Bonferroni post hoc test was used to compare fluorescence intensity of each postbleach time point with $t = 0$ minute.

Plasmid constructs

eGFP reporter constructs

Diffusion limited GFP^{myr} construct was used to test the ability of specific RNA sequence/structure of interest to localize *eGFP* reporter mRNA to distal axons.

gBlocks Gene Fragments (Integrated DNA Technologies) containing pre-miR-433, pre-miR-138-1, pre-(S433 + L138-1), or pre-(S138-1 + L433) sequence were clone into pCRTM Blunt II TOPO. These constructs were subsequently used as templates to PCR amplified pre-miR-433, pre-miR-138-1, pre-(S433 + L138-1), or pre-(S138-1 + L433) with terminal NotI and XhoI recognition sequences with the following primer sets. All constructs were sequence validated prior to use.

NotI-pre-miR-433-XhoI

Sense: 5'-AAATATGCGGCCGCCCGGGGAGAAGTACGGTGAG-3'

Antisense: 5'-CCGCTCGAGCCTGGAGAACACCGAGGAGC-3'

NotI-pre-miR-138-1-XhoI

Sense: 5'-AAATATGCGGCCGCCTCTGGCATGGTGTGTTGTGGGA-3'

Antisense: 5'-CCGCTCGAGCCTGCAGTGCAGTGAGACC-3'

NotI-pre-(S433 + L138-1)-XhoI

Sense: 5' AAATATGCGGCCGCCCGGGGAGAAGTACGGTGAG-3'

Antisense: 5'-CCGCTCGAGCCTGGAGAACACCGAGGAGC-3'

NotI-pre-(S138-1 + L433)-XhoI

Sense: 5'-AAATATGCGGCCGCCTCTGGCATGGTGTGTTGTGGGA-3'

Antisense: 5'-CCGCTCGAGCCTGCAGTGCAGTGAGACC-3'

PCR products were then cloned into NotI and XhoI site of GFP^{myr} expression constructs located immediately downstream of eGFP^{myr} coding sequence.

Dual luciferase reporter constructs

pGL4.18 Renilla construct was used to validate RanBP1 extended 3'UTR as a target for miR-433-3p. Extended 3'UTR sequences of rat RanBP1 mRNA (GenBank: EU146304.1) with terminal *NotI* and *XhoI* was PCR amplified and cloned into *NotI* and *XhoI* site immediately downstream of Renilla luciferase open reading frame. Construct was sequence validated prior to use.

Dual luciferase reporter assay

An *in vitro* assay for miR-433-3p target validation was carried out in the F11 cell line using reporter constructs and miRNA mimic. MiRNA mimics are chemically modified RNA molecules that designed to mimic endogenous mature miRNAs when transfected into cells. First, F11 cells were plated at low density (8000 cells/cm²) in growth medium (DMEM/F11 medium containing 10% FBS, 2 mM glutamine, and 1X penicillin and streptomycin) on 100 mm plastic dish coated with poly-L-lysine. 24 hours after plating, cells were co-transfected with Firefly construct (internal control) and Renilla-RanBP1 extended 3'UTR construct using lipofectamine 2000 (Invitrogen) according to manufacture protocol, and cultured in penicillin and streptomycin free growth medium. 24 hours after initial transfection, F11 cells were replated at 8000

cells/cm² in poly-L-lysine coated 6 well plate and cultured in antibiotic free growth medium for 8 hours. The cell were then transfected again with miRNA mimic control, anti-Firefly siRNA duplex, anti-Renilla duplex, miR-433-3p mimic, seed mismatched miR-433-3p, or antisense miR-433-3p using Lipofectamine 2000 and cultured in antibiotic free growth medium. The cells were harvested at 48 hours after the second transfection and lysed with passive lysis buffer (Promega). The resulting lysate was then used to measure Firefly and Renilla luciferase activities using Dual-Luciferase Reporter 1000 Assay System (Promega). Luminescence signal of from Renilla (reporter) was first, normalized to Firefly (internal control), and relative Renilla to Firefly signal was then, normalized to that of control mimic.

Analysis of axonal growth

DRG neurons were co-transfected with a GFP construct (pMax GFP construct supplied by Lonza) and miR-433-3p mimic, antisense miR-433-3p, or mimic control and cultured on glass cover slips coated with poly-L-lysine and laminin. After 48 hours, cultures were fixed with 2% PFA, stained with DAPI, and the coverslips were mounted on a slide. Lengths of the longest axonal projection of neurons expressing GFP were imaged and measured. Only the longest axons whose length measured at least three times the diameter of the cell body were considered for these experiments.

Results

Pre-miR-433 is selectively localized to distal axons of DRG neurons.

Using RT-qPCR approach, pre-miR-433 was previously shown to be present in distal axons of sensory neurons (Kim et al., 2015). To visualize endogenous pre-miR-433 in distal axons, I performed fluorescence *in situ* hybridization (FISH) using locked nucleic acid (LNA) probe specific for pre-miR-433. Since mature miR-433 sequences overlapped extensively with the stem region of pre-miR-433, LNA FISH probe specific for the terminal loop region of the precursor was used to distinguish the pre-miRNA from its corresponding mature miRNA. In cultured DRG neurons, pre-miR-433 FISH signal was detected in both the cell body (asterisk) and axons (arrows) (Fig. 3.1A). As a negative control, I also performed FISH using LNA probe specific for the terminal loop region of pre-miR-138-1 since our previous PCR results showed the absence of pre-miR-138-1 in axons of DRG neurons (Kim et al., 2015). In line with our previous finding, other studies have reported localization of miR-138 to somatodendrites (Siegel et al., 2009; Pichardo-Casas et al., 2012). As expected, FISH signal for pre-miR-138-1 was detected in the cell body (asterisk) but not in axons (Fig. 3.1B). Consistent with these FISH results, RT-qPCR analysis of the axoplasmic RNA extracted from sciatic nerves (*in vivo*) and axon fractions isolated from DRG neurons cultured in the Boyden chambers (*in vitro*) showed comparable levels of pre-miR-433 in axons to those in DRG/cell body (level in axoplasm/DRG, 1.38; level in axon preparation/cell body, 0.97; not statistically significant) (Fig. 3.1C-D). As anticipated, levels of pre-miR-138-1 (cell body restricted pre-miRNA) detected in both the sciatic

nerve axoplasm and the axonal fraction of cultured DRG neurons were significantly lower compared to those in DRG/cell body (level in axoplasm/DRG, 0.23; level in axon preparation/cell body, 0.17; $p < 0.001$ and $p < 0.01$, respectively) (Fig. 3.1C-D). Residual levels of pre-miR-138-1 detected by RT-qPCR analysis of axoplasm/axon fraction samples were likely linked to contamination from proximal axonal segment adjacent to the cell body. Collectively, these results suggest that pre-miR-433 is selectively targeted to distal axons of DRG neurons.

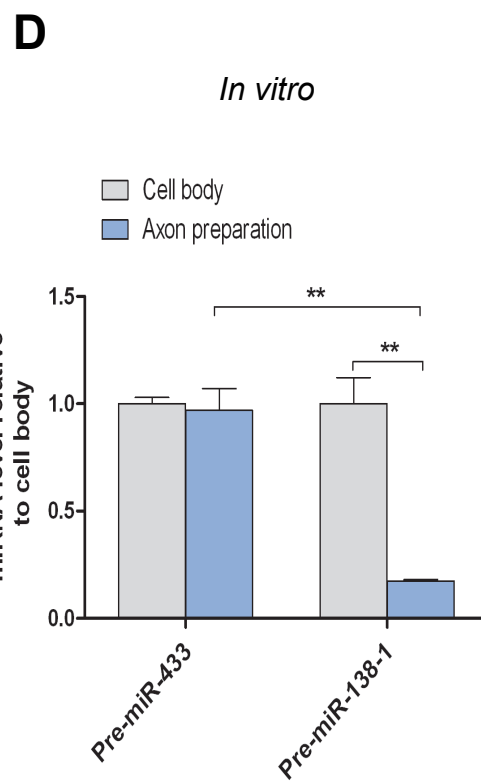
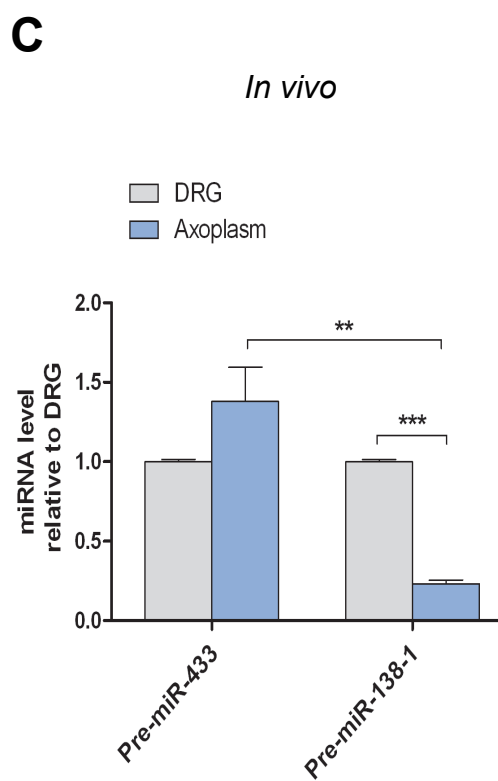
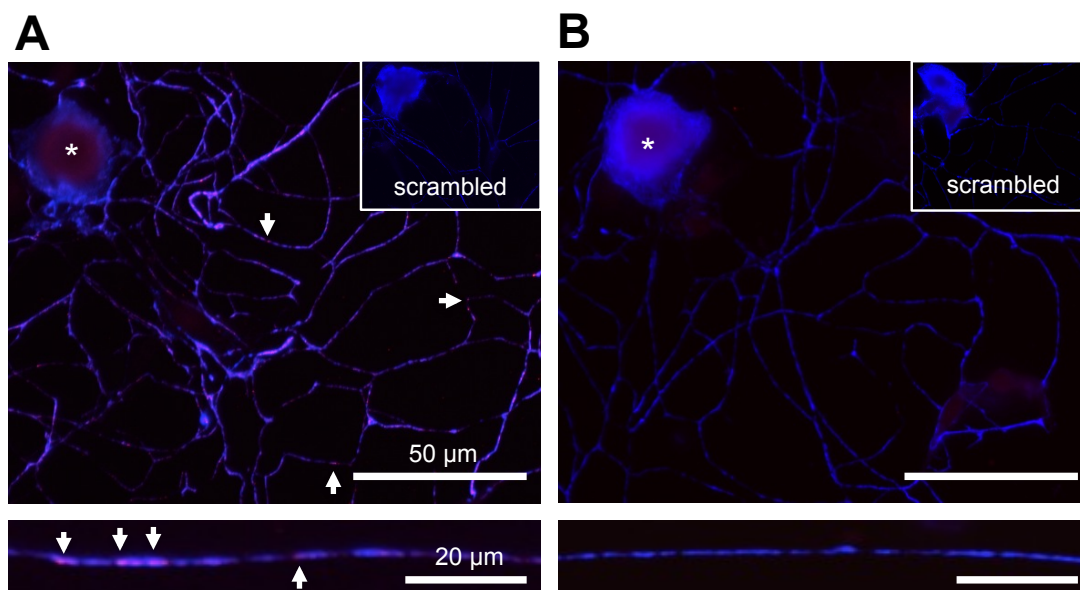


Figure 3.1 Pre-miR-433 is selectively localized to distal axons of sensory neurons. FISH was performed on cultured DRG neurons using LNA probe against the terminal loop regions of (A) pre-miR-433 and (B) pre-miR-138-1. Immunofluorescence for neurofilament (NF, blue) was performed to indicate neuronal cells. In the top panels, the asterisks mark the cell body and the arrows indicate FISH signals (red) in axons of DRG neurons. Exposure matched scrambled controls are shown in inset panels. The bottom panels represent high magnification of distal axons showing pre-miRNA FISH signals (arrows) and NF (blue). RT-qPCR analysis using primers specific to pre-miR-433 and pre-miR-138-1 was performed on DRG tissues and axoplasm extracted from sciatic nerves (C), and cell body fractions and axon fractions of DRG neurons cultured in the Boyden chambers (D). Student's T-test was used for RT-qPCR analysis of pre-miRNAs (**, $p < 0.01$; ***, $p < 0.001$).

The terminal loop region of pre-miR-433 structure is sufficient to drive the localization of eGFP reporter mRNA into axons of DRG neurons.

To identify *cis*-element(s) within the axonally localizing pre-miR-433 that direct its transport into axons, I used an RNA reporter system in combination with FISH, RT-qPCR, and fluorescence recovery after photobleaching (FRAP) methods to probe different structural regions of pre-miR-433 and examined its ability to localize *eGFP* reporter mRNA into distal axons of culture DRG neurons. First, I generated an *eGFP* construct carrying full sequence of pre-miR-433 in the 3'UTR (*eGFP^{myr}-pre-miR-433*) and determined whether pre-miR-433 can drive the localization of *eGFP* reporter mRNA into distal axons. As a negative control, an *eGFP* construct carrying full sequence of cell body restricted pre-miR-138-1 in the 3'UTR (*eGFP^{myr}-pre-miR-138-1*) was generated. DRG neurons were transfected with either *eGFP^{myr}-pre-miR-433* or *eGFP^{myr}-pre-miR-138-1* construct and *eGFP* reporter mRNA was visualized by FISH at 3 days in culture. In the transfected DRG neurons expressing *eGFP^{myr}-pre-miR-433* mRNA, FISH signal was detected both in the cell body and in axons (arrows) (Fig 3.2A). In contrast, FISH signal was detected only in the cell body of transfected DRG neurons expressing *eGFP^{myr}-pre-miR-138-1* (Fig 3.2B). To confirm these results, I quantified the levels of the reporter mRNA separately in the cell body and in axon using RT-qPCR. DRG neurons transfected with either *eGFP^{myr}-pre-miR-433* or *eGFP^{myr}-pre-miR-138-1* construct were cultured in the Boyden chambers. After 3 days in culture, the cell body compartment and axonal compartment were physically separated by scraping and the resultant cell body fraction and axonal fraction were

processed for RNA purification. Prior to RT-qPCR, RNA isolated from the axonal fraction was subjected to RNA purity analysis by extended RT-PCR to detect the presence of *MAP2* (cell body restricted mRNA) and *GFAP* (mRNA expressed in glia cells) mRNAs. This is to ensure that the resultant axonal fractions are relatively free of cell body and glial cell contamination. RT-qPCR showed that the normalized level of *eGFP^{myr}-pre-miR-433* mRNA to the endogenous *GAPDH* mRNA was ~1.4-fold higher in the axonal fraction than in the cell body fraction (Student's T-test, $p < 0.001$). In contrast, the normalized levels of *eGFP* reporter transcripts carrying its own 3'UTR or cell body restricted pre-miR-138-1 in the 3'UTR were significantly lower in the axonal fractions compared to those in the cell body fractions (Fig 3.2C, $p < 0.001$).

To further support the results showing the ability of pre-miR-433 to drive the localization of *eGFP* reporter mRNA, I utilized fluorescence recovery after photobleaching (FRAP) approach. Since axonal mRNA must be first localized before being translated, FRAP has been used to determine the localization of transcript of interests as well as the translatability of the localized mRNAs. In brief, both localization of the reporter mRNA and subsequent intra-axonal translation can be assessed by observing the recovery of *eGFP^{myr}* fluorescence signal after photobleaching the terminal axons within the region of interest (ROIs). Typically, the terminal axonal growth cone region measured at least $\geq 500 \mu\text{m}$ from the cell body was selected and utilized for FRAP experiments. In addition, protein synthesis inhibitors such as cycloheximide and anisomycin were used to ensure that recovery of *eGFP^{myr}* signal is due to local translation since active transport and diffusion can also

contribute to signal recovery. To limit diffusion of the fluorescent protein, myristoylation tag (myr) was added to the N-terminus of eGFP protein to anchor newly synthesized myristoylated eGFP (eGFP^{myr}) to the adjacent plasma membrane and prevent its diffusion.

When terminal growth cones of DRG neurons transfected with eGFP^{myr}-pre-miR-433 construct were photobleached, eGFP^{myr} fluorescence signal showed a significant recovery over 20 minutes after having been bleached (Fig 3.3A-B). Upon treatment of protein synthesis inhibitor (cycloheximide), photobleached growth cones of these transfected neurons did not show significant recovery of eGFP^{myr} fluorescence signal. These results indicate that the recovery of eGFP^{myr} fluorescence signal in photobleached growth cones of DRG neurons transfected with eGFP^{myr}-pre-miR-433 construct was primarily due to intra-axonal translation of the localized reporter mRNAs. In contrast, no significant eGFP^{myr} signal was recovered in photobleached growth cone of DRG neurons transfected with eGFP^{myr}-pre-miR-138-1 (Fig. 3.4A-B). Taken together, these results indicate that full sequence of pre-miR-433 was sufficient for the localization of *eGFP* reporter mRNA into axons of cultured DRG neurons.

To further dissect the localization *cis*-element(s) within pre-miR-433, I considered the hairpin loop secondary structure that occurs in pre-miR-433 and divided it into two regions, the terminal loop region (L) and the stem region (S) (Fig. 3.5). The terminal loop region (L) of pre-miRNAs includes the terminal loop and immediate adjacent structure that are cleaved off after Dicer processing. The

remaining structure containing the miRNA:miRNA* duplex and the precursor base stem (base stem is also cleaved off after Dicer processing) are considered as the stem region (S). Since the stem region is formed by base-pairing between two sections of the same RNA strand (RNA folding) that also generated a loop structure, it was practically impossible to incorporate only the stem region into the reporter construct. Therefore, I decided to generate reporter constructs carrying chimeric pre-miRNAs that contain either the terminal loop region of cell body restricted pre-miR-138-1 (L138-1) in the backbone (stem region of pre-miR-433) of axonally localizing pre-miR-433 (S433) or the terminal loop region of axonally localizing pre-miR-433 (L433) in the backbone (stem region of pre-miR-138-1) of cell body restricted pre-miR-138-1 (S138-1) (Fig. 3.5). Using thermodynamic prediction of RNA structure, I further showed that the resultant chimeric pre-miRNAs maintained the secondary structure of the terminal loop regions and the stem regions of both pre-miR-433 and pre-miR-138-1 (Fig. 3.5).

First, to determine whether the stem region of pre-miR-433 structure (S433) contained *cis*-acting axon localization element(s), eGFP reporter construct carrying a chimeric pre-miRNA structure that contains the stem region of pre-miR-433 and the terminal loop region of pre-miR-138-1 [eGFP^{myr}-(S433 + L138-1)] was examined using FISH and RT-qPCR approaches. In DRG neurons transfected with eGFP^{myr}-(S433 + L138-1), FISH signals for *eGFP* reporter mRNA was detected in the cell body but not in distal axons (Fig 3.6A). In addition, RT-qPCR showed that axonal fraction contained significantly lower level of the reporter transcript (only ~35%

compared to that in the cell body fraction, one-way ANOVA, $p < 0.01$) (Fig. 3.6C). Consistent with these results, FRAP experimental data showed that photobleached growth cones of DRG neurons transfected with eGFP^{myr}-(S433 + L138-1)] construct did not show significant recovery of eGFP^{myr} fluorescence signal over 20 minutes after bleached (Fig. 3.7A-B). Taken together, these results indicate that the stem region of pre-miR-433 (S433) was not sufficient as a *cis*-acting element for axonal localization.

Next, I asked whether axon localization *cis*-element(s) are located within the terminal loop structure of pre-miR-433 (L433). To address this question, I transfected DRG neurons with an eGFP reporter construct carrying a chimeric pre-miRNA structure that contain the stem region of pre-miR-138-1 and the terminal loop region of pre-miR-433 [eGFP^{myr}-(S138-1 + L433)] and assessed the localization of the reporter mRNA using FISH, RT-qPCR, and FRAP approaches. Cultured DRG neurons transfected with eGFP^{myr}-(S138-1 + L433) construct showed detectable FISH signal for *eGFP* reporter mRNA both in the cell body and in axons (arrows) (Fig. 3.6B). In addition, RT-qPCR analysis showed that the axonal level of eGFP^{myr}-(S138-1 + L433) transcript was comparable to that in the cell body (Fig. 3.6C). Given previous RT-qPCR results of the axonal level of the control eGFP^{myr} transcript lacking pre-miRNA sequences (eGFP^{myr} in Fig. 3.2C), this cell body comparable level of eGFP^{myr}-(S138-1 + L433) mRNA in the axonal fraction indicates selective axon localization, rather than homogenous distribution presumably due to concentration gradient-dependent diffusion. It is also noteworthy that the axonal level of eGFP^{myr}-(S138-1 + L433) mRNA was significantly higher than that of axonal eGFP^{myr}-(S433 +

L138-1) (Fig. 3.6C; one-way ANOVA, $p < 0.01$). In line with these results, FRAP analysis of growth cones of DRG neurons transfected with eGFP^{myr}-(S138-1 + L433) construct showed a significant eGFP^{myr} fluorescence recovery after photobleaching (Fig. 3.8). Further, addition of cycloheximide (protein synthesis inhibitor) was shown to inhibit this fluorescence recovery (Fig. 3.8A-B). Altogether, these findings indicate that the terminal loop region of pre-miR-433 structure (L433) contained *cis*-element(s) that strongly govern the localization of the reporter mRNA into distal axons of DRG neurons.

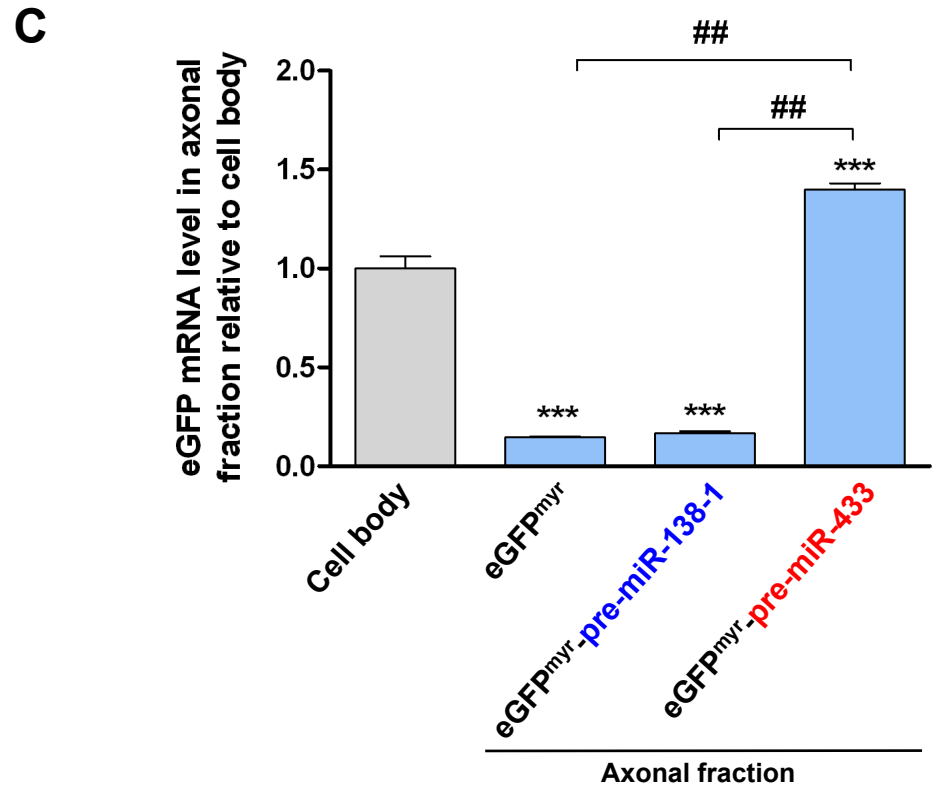
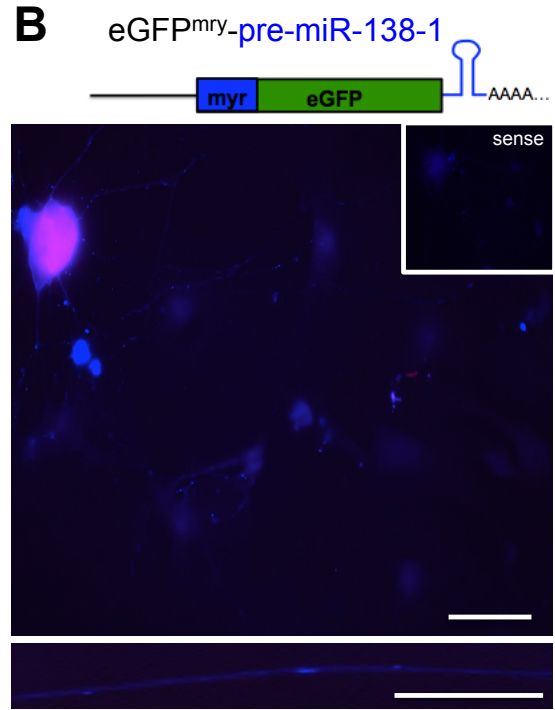
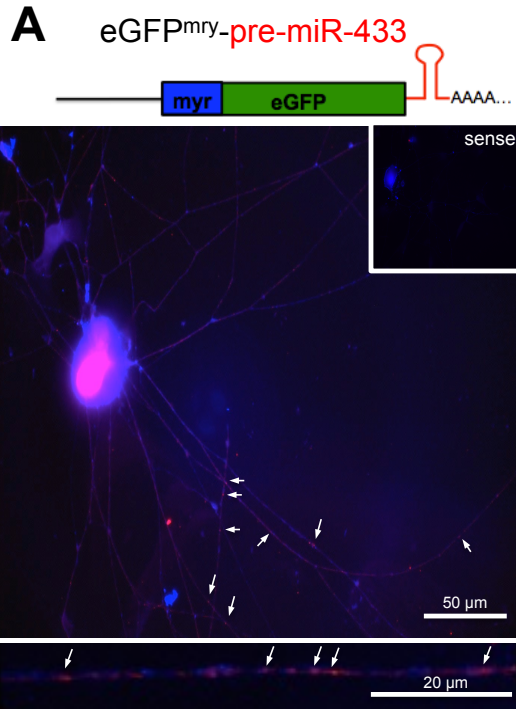


Figure 3.2 Pre-miR-433 can drive the localization of *eGFP* reporter mRNA into distal axon of DRG neurons.

FISH for eGFP mRNA was performed in DRG neurons transfected with either (A) eGFP^{myr}-pre-miR-433 or (B) eGFP^{myr}-pre-miR-138-1 construct (expression of GFP fluorescence signals is shown in blue). The arrows indicate FISH signals (red) in axons and exposure matched sense controls are shown in the inset panels. The bottom panels represent high magnification of distal axon showing *eGFP* mRNA FISH signals (arrows). Quantification of normalized level of *eGFP* reporter mRNA to endogenous *GAPDH* mRNA in the axonal fraction relative to that in the cell body was measured using RT-qPCR method (C). For statistical comparison analysis, one-way ANOVA followed by Benferroni post-hoc test was used (***, $p < 0.001$, compared to cell body; ##, $p < 0.01$, compared between indicated groups).

Figure 3.3 eGFP^{myr}-pre-miR-433 mRNA is localized to distal axons and intra-axonally translatable.

Panel **A** is a representative time-lapse image sequences of FRAP showing the recovery of eGFP^{myr} fluorescence signals in growth cones of DRG neurons transfected with eGFP^{myr}-pre-miR-433 construct. Bleached axonal region of interest (ROI) is indicated in white boxes. Panel **B** shows quantitative analysis of FRAP data. Protein synthesis inhibitor Cycloheximide was used to ensure that fluorescence recovery was due to local translation of localized mRNAs. Normalized fluorescence intensity to time t=0 after photobleaching is represented as average \pm SEM ($N \geq 5$) for each condition; **, $p < 0.01$ and ***, $p < 0.001$ indicate time points vs. t = 0 min by one-way ANOVA analysis followed by analysis of variance with Bonferroni post-hoc test.

A

eGFP^{myr}-pre-miR-138-1: 

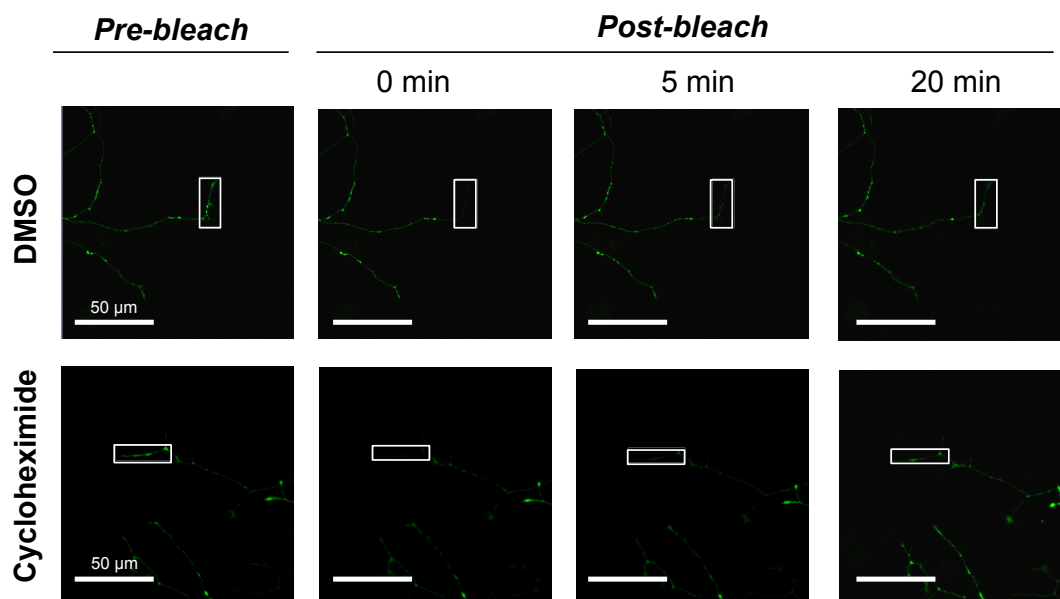
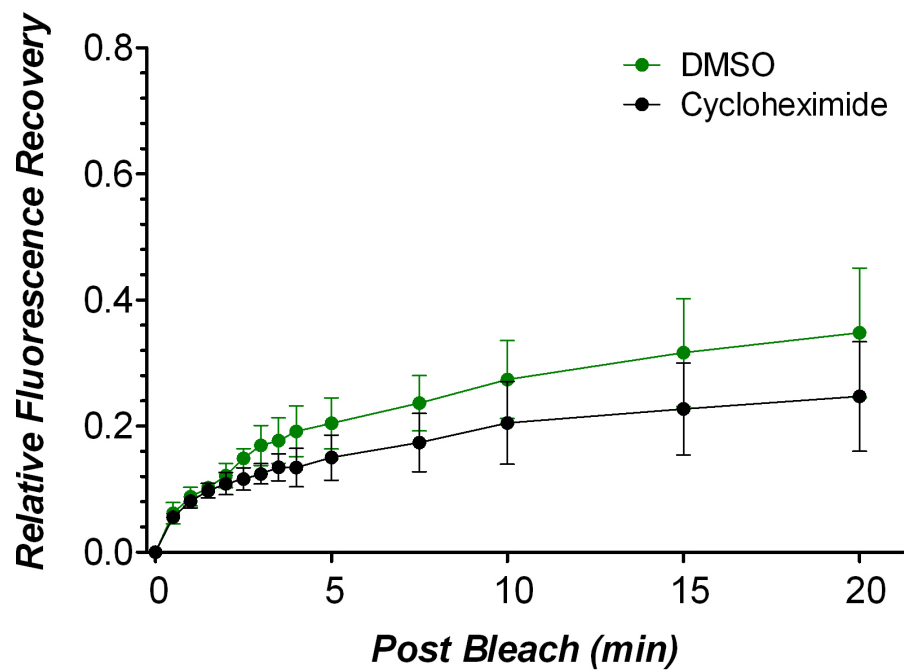
**B**

Figure 3.4 eGFP^{myr}-pre-miR-138-1 mRNA does not localize to axons of DRG neurons.

Panel **A** is a representative time-lapse image sequences of FRAP showing no recovery of eGFP^{myr} signals in the photobleached growth cones of DRG neurons transfected with eGFP^{myr}-pre-miR-138-1 construct. Bleached axonal region of interest (ROI) is indicated in white boxes. Panel **B** shows the quantitative analysis of FRAP data. Cycloheximide was used to inhibit local translation. Normalized fluorescence intensity to t=0 after photobleaching is represented as average \pm SEM (N \geq 5) for each condition.

- Pre-miR-433 structures that are cleaved off after Dicer processing
 - miR-433 miRNA:miRNA* duplex
- Pre-miR-138-1 structures that are cleaved off after Dicer processing
 - miR-138-1 miRNA:miRNA* duplex

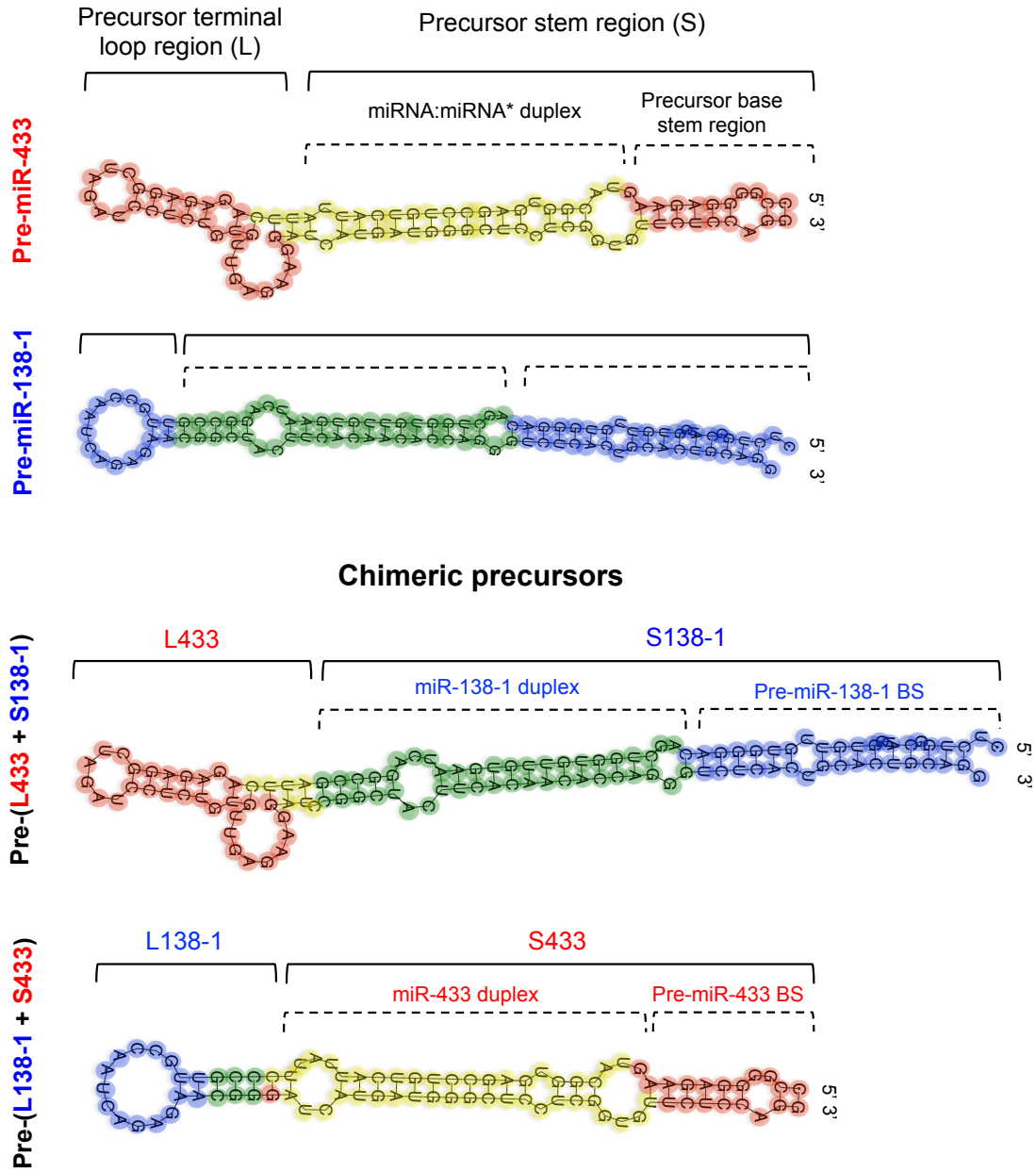


Figure 3.5 Prediction of precursor miRNA structure based on thermodynamic.

The secondary structure of indicated pre-miRNAs was predicted based on minimum free energy (M-fold). Structures within precursor miRNAs are grouped into two regions, the terminal loop region (L) and the stem region (S). The terminal loop region contains both the terminal loop and adjacent structure that are cleaved off after Dicer processing. The stem region refers to the rest of the precursor structures that contains the miRNA:miRNA* duplex and precursor base stem (the base stem structure is also cleaved off after Dicer processing). Thermodynamic structure prediction showed a conservation of both the secondary structures of the terminal loop region (L) of pre-miR-433 and pre-miR-138-1 in the chimeric pre-miRNAs.

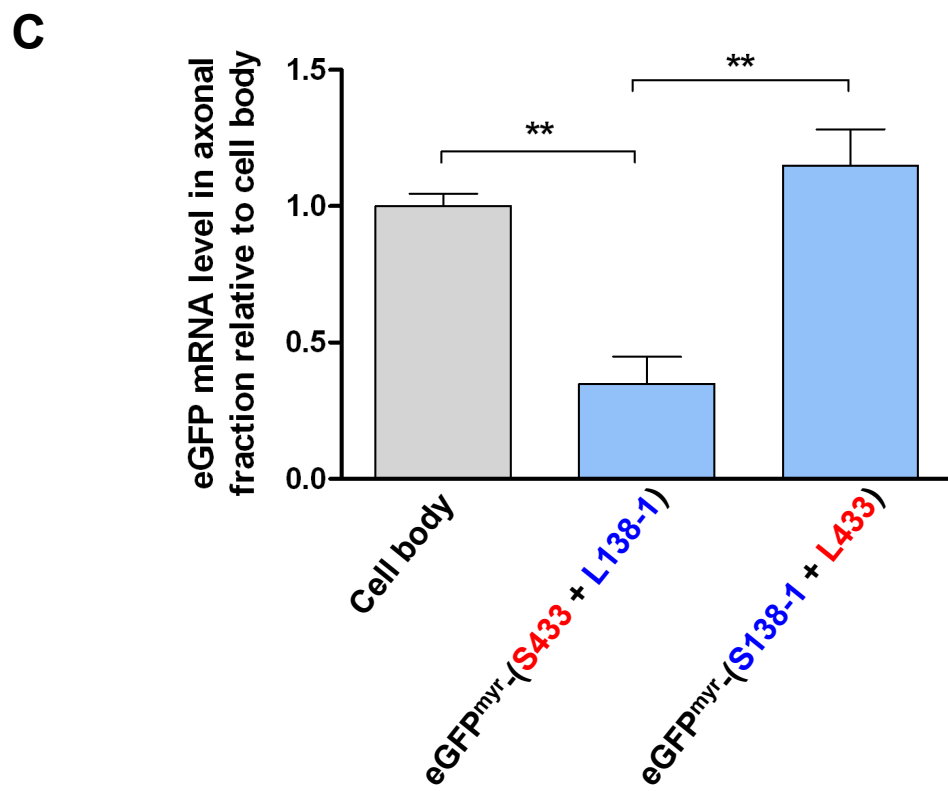
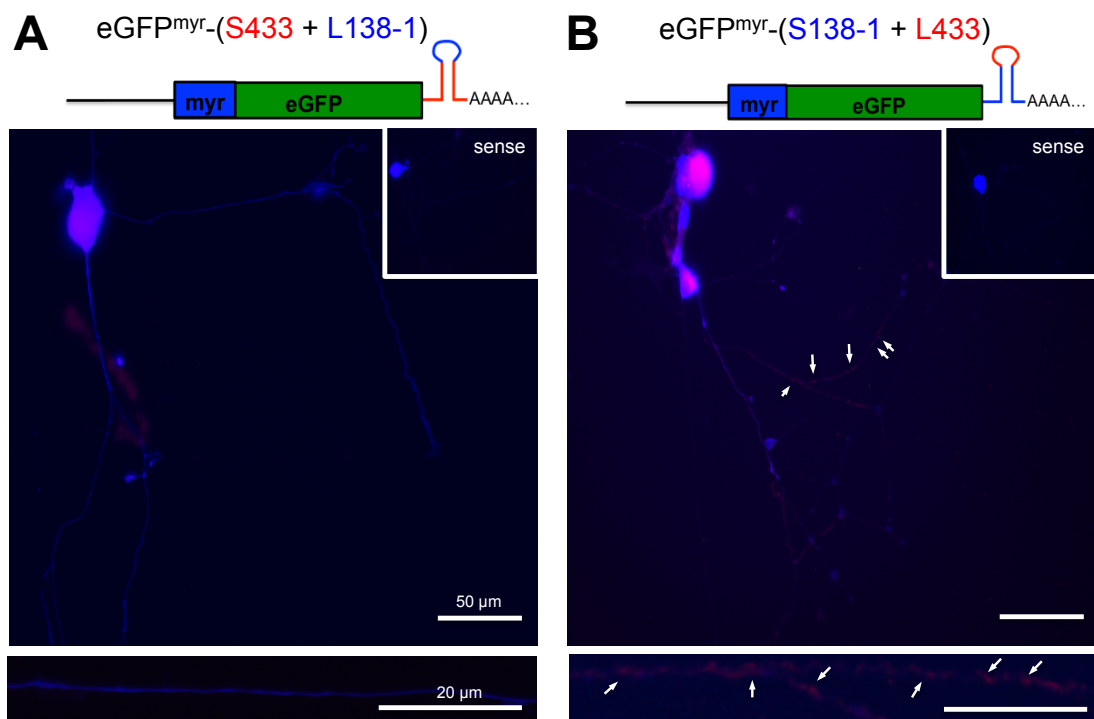


Figure 3.6 The terminal loop region of pre-miR-433 structure strongly governs the localization of eGFP reporter mRNA into axons.

eGFP mRNA FISH was performed in DRG neurons transfected with either an *eGFP* construct carrying a chimeric pre-miRNA containing the stem region of pre-miR-433 (S433) and the terminal loop region of pre-miR-138-1 (L138-1) [eGFP^{myr}-(S433 + L138-1)] (**A**) or a construct carrying chimeric pre-miRNA containing the stem region of pre-miR-138-1 (S138-1) and the terminal loop region of pre-miR-433 (L433) [eGFP^{myr}-(S138-1 + L433)] (**B**) (mRNA FISH signals in red; GFP^{myr} fluorescence signal in blue). The arrows indicate FISH signals in axons and exposure matched sense control are shown in the inset panels. The bottom panels show high magnification of *eGFP* mRNA FISH images in the distal axon. RT-qPCR data (**C**) show relative levels of the *eGFP* reporter mRNAs in axonal fraction of DRG neurons transfected with indicated constructs compared to those measured in the cell body fraction. One-way ANOVA followed by Bonferroni post-hoc test was used for all statistical analysis (**, p<0.01).

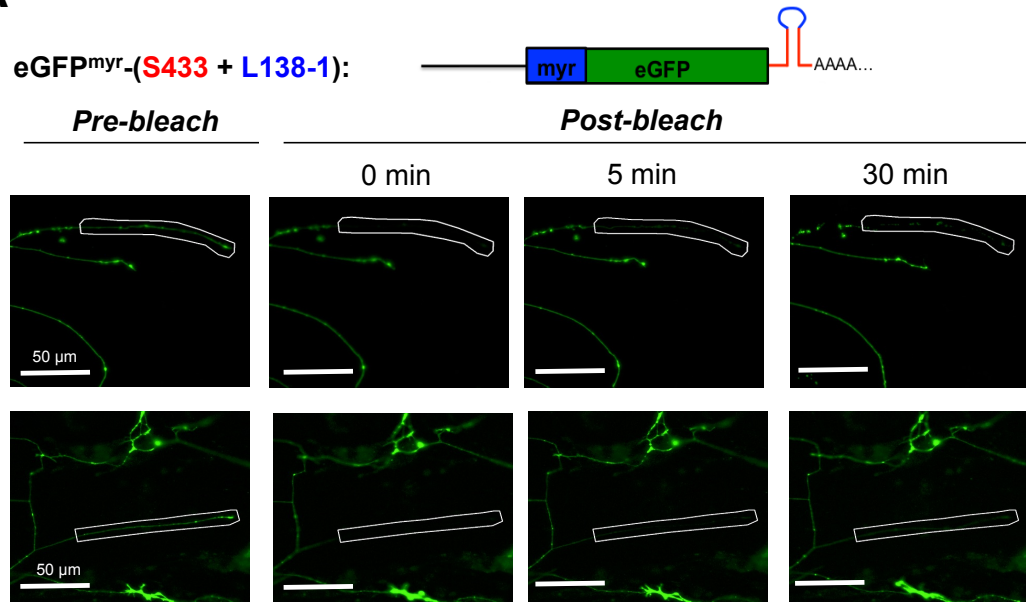
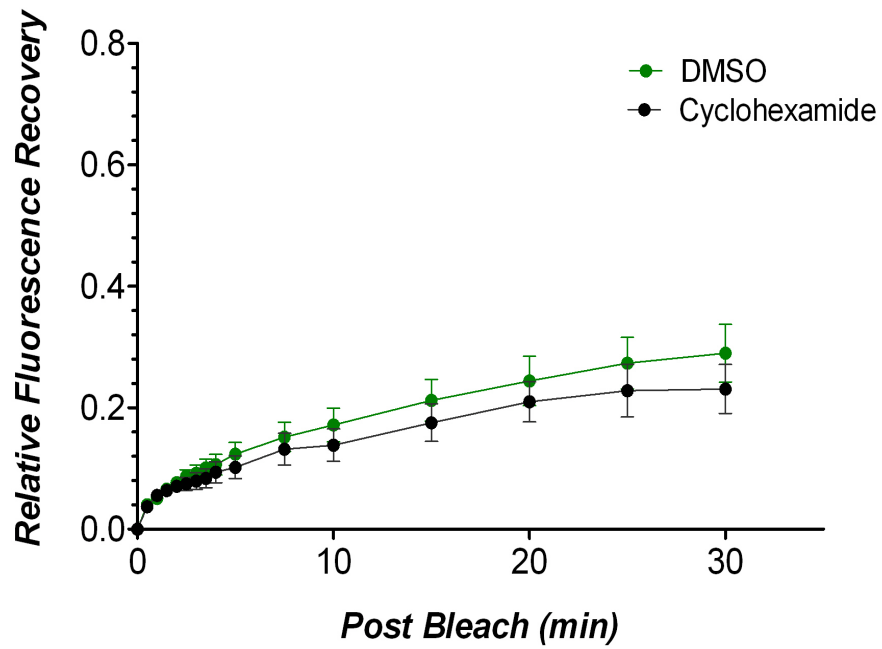
A**B**

Figure 3.7 Stem region of pre-miR-433 structure alone is not sufficient to localize *eGFP* reporter mRNA into axons.

Panel **A** is a representative time-lapse image sequences of FRAP showing no recovery of $eGFP^{myr}$ fluorescence signals in growth cones of DRG neurons transfected with a construct carrying a chimeric pre-miRNA containing the stem region of pre-miR-433 (S433) and terminal stem loop region of pre-miR-138-1 (L138-1) in the 3'UTR [$eGFP^{myr}$ -(S433 + L138-1)]. Bleached axonal region of interest (ROI) is indicated in white boxes. Panel **B** shows quantitative data analysis of FRAP experiments. Protein synthesis inhibitor Cycloheximide was used to ensure that fluorescence recovery was due to local translation. Normalized fluorescence is represented as average \pm SEM ($N \geq 5$) for each condition.

A

eGFP^{myr}-(S138-1 + L433): 

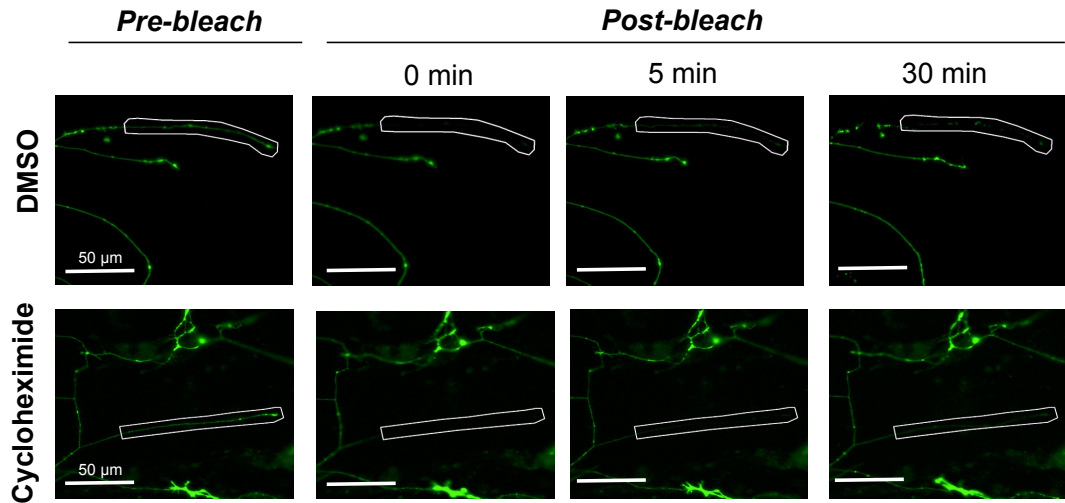
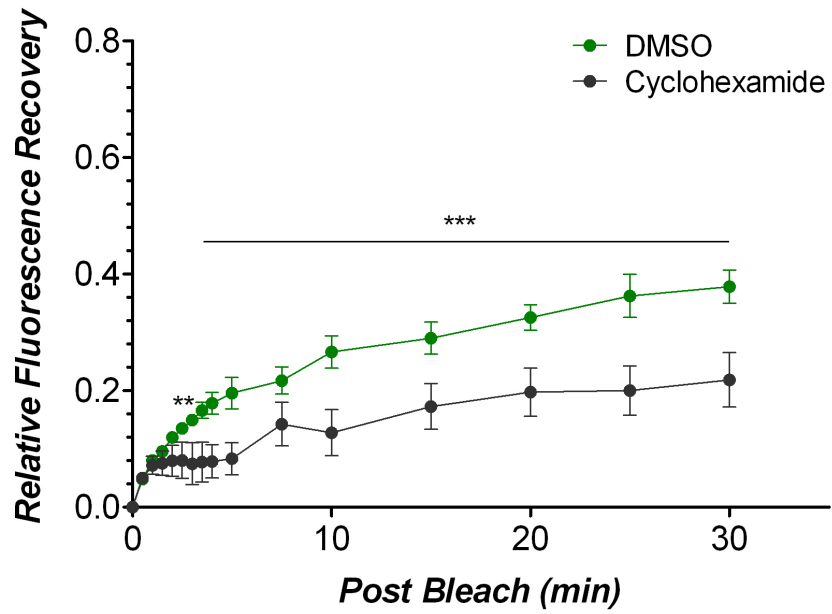
**B**

Figure 3.8 Reporter *eGFP* mRNA is driven into distal axons by the terminal loop region of pre-miR-433 structure and is locally translated.

Panel **A** is a representative time-lapse image sequences of FRAP showing the recovery of eGFP^{myr} fluorescence signals in growth cones of DRG neuron transfected with a construct carrying a chimeric pre-miRNA containing the stem region of pre-miR-138-1 (S138-1) and terminal stem loop region of pre-miR-433 (L433) in the 3'UTR [eGFP^{myr}-(S138-1 + TSL433)]. Bleached axonal region of interest (ROI) is indicated in white boxes. Panel **B** shows quantitative data analysis of FRAP experiments. Protein synthesis inhibitor Cycloheximide was used to ensure that fluorescence recovery was due to local translation. Normalized fluorescence is represented as average \pm SEM ($N \geq 5$) for each condition; **, $p < 0.01$ and ***, $p < 0.001$ indicate time points vs. $t = 0$ min by one-way ANOVA analysis followed by analysis of variance with Bonferroni post-hoc test.

Specific endogenous miRNA precursors localized in distal axons are processed to give rise to corresponding mature miRNAs.

To determine whether pre-miR-433 is locally processed into mature miR-433-3p *in vivo* in response to axon injury, I first measured levels of axoplasmic pre-miR-433 and mature miR-433-3p at 1-, 4-, 7-, and 14-days after sciatic nerve crush injury using RT-qPCR. Inconsistent with my previous small-RNA sequencing data, the statistical analysis of RT-qPCR data showed a significant up-regulation in the levels of both pre-miR-433 and mature miR-433-3p at 4- and 7-days post injury (DPI) compared to sham operated (uninjured) control with a positive correlation between the two - the precursor and the mature miRNAs (Fig. 3.9A-B). The increase in the levels of axoplasmic pre-miR-433 and mature miR-433-3p at 4 DPI and 7 DPI could be explained by an increase in the anterograde transport of the RNAs from the cell body after injury. In addition to the increased anterograde transport after injury, I hypothesized that the axoplasmic level of mature miR-433-3p could be increased by local maturation of the localized pre-miR-433. To test this possibility, I utilized the Boyden chamber approach to eliminate anterograde transport from the soma to the axon.

To observe exclusive temporal dynamics of pre-miRNA processing in axons, DRG neurons were cultured in the Boyden chamber and the levels of subsets of pre-miRNAs and their corresponding mature miRNAs were quantified in the axonal fraction by RT-qPCR as a function of time (at t= 0, 2, and 6 hours) after the removal

of the cell bodies (ARC). By removing the cell bodies, I eliminated a possible somatic contribution of the precursors and the mature miRNAs through anterograde active transport. Since axon can survive for 6 hours in the absence of the cell body before rapid axonal degeneration (Zheng et al., 2001; Barrientos et al., 2011), this gave me a time window to assess whether endogenous axonal pre-miRNAs are locally processed into their corresponding mature miRNAs independently from the neuronal cell body. In addition to pre-miR-433, other axoplasmic precursors such as pre-miR-27a, pre-miR-146b, pre-miR-21, let-7b, and pre-miR-20a were selected for these experiments based on my previous sequencing data showing differential changes in the levels of mature miRNAs in response to nerve injury. RT-qPCR analysis of the axonal fraction at 2 hrs ARC and 6 hrs ARC revealed a significant increase in the levels of mature miR-433-3p (2 hrs ARC: 2 fold, 6 hrs ARC: 3 fold) and mature miR-27a-3p (2 hrs ARC: 1.4 fold, 6 hrs ARC: 2 fold) compared to those at 0 hr (Fig. 3.10). In contrast, the levels of miR-146b-3p and miR-21a-5p showed statistically no significant changes in the axonal fraction after anucleation (Fig. 3.10). The levels of mature let-7b-5p and miR-20a-5p showed no significant changes at 2 hrs ARC, but by 6 hrs ARC they were significantly reduced by ~17% (let-7b-5p) and ~ 20% (miR-20a-5p), respectively, when compared to those at 0 hr (Fig. 3.10). Taken together, these results suggest that axons are capable of locally processing specific miRNA precursors independently from the neuronal cell body. It is noteworthy that not all axonally localized precursors are locally processed after the cell body is removed.

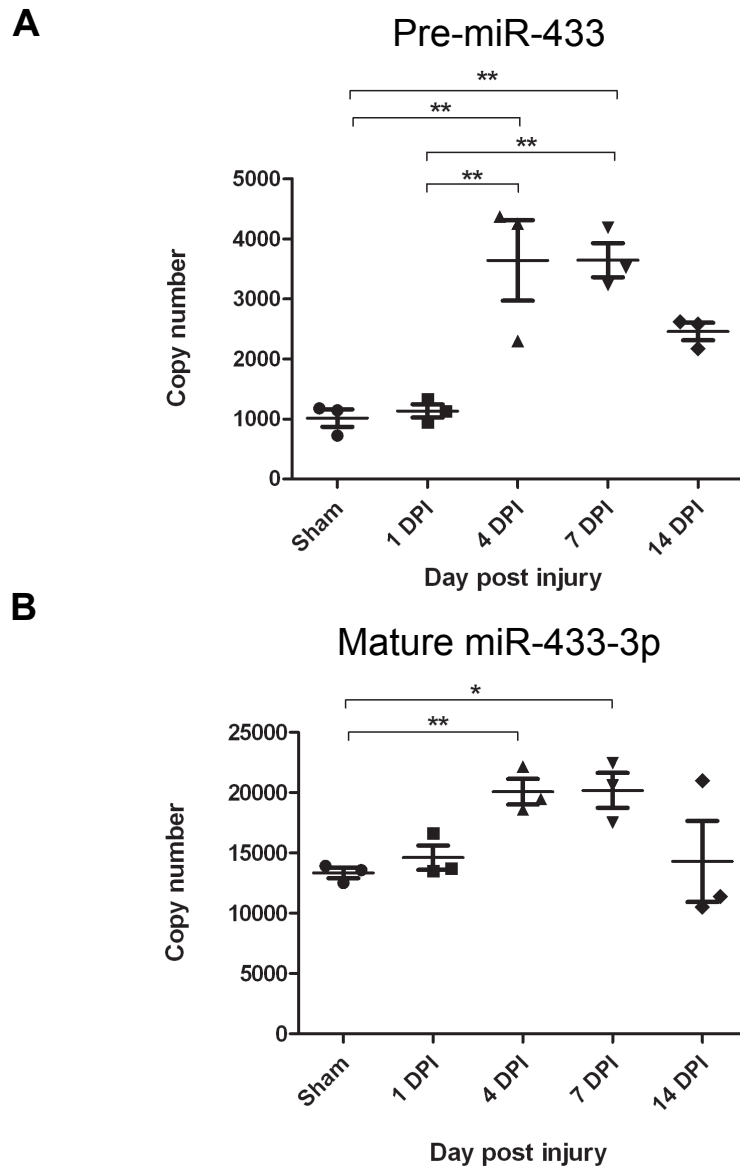


Figure 3.9 Axoplasmic levels of pre-miR-433 and mature miR-433-3p *in vivo* are increased after nerve injury.

Highly enriched axoplasmic RNA extracted from rat sciatic nerves at different times following crush injury was subjected to RT-qPCR experiments to quantify levels of pre-miR-433 (A) and its corresponding mature miR-433-3p (B). Standard curves were generated and used to calculate average copy number \pm SEM in the axoplasm from 3 different animals (N=3). A statistical analysis was carried out using one-way ANOVA followed by Bonferroni post hoc test (*, $p < 0.05$; **, $p < 0.01$).

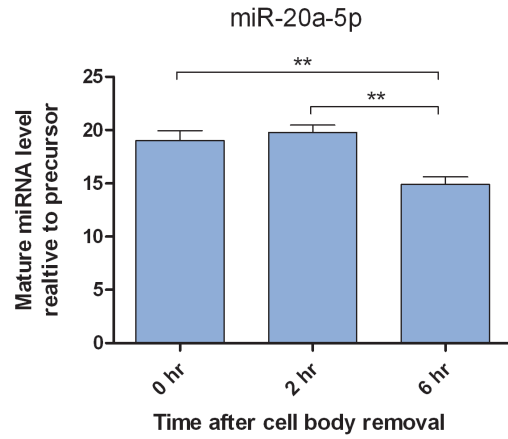
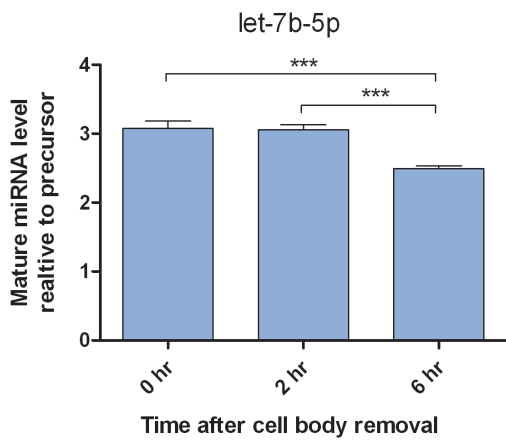
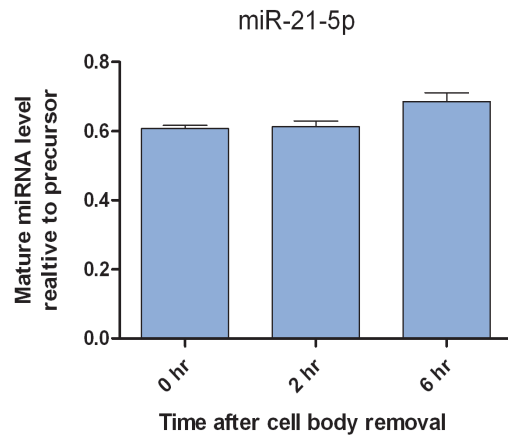
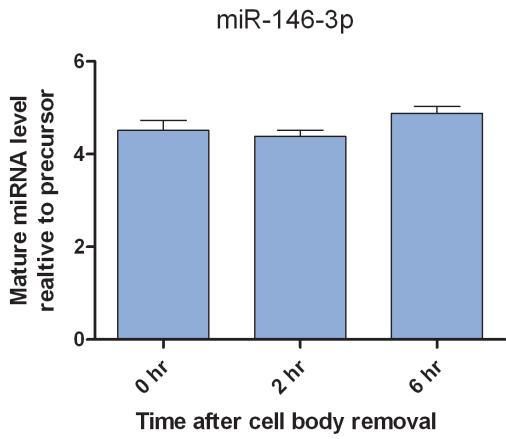
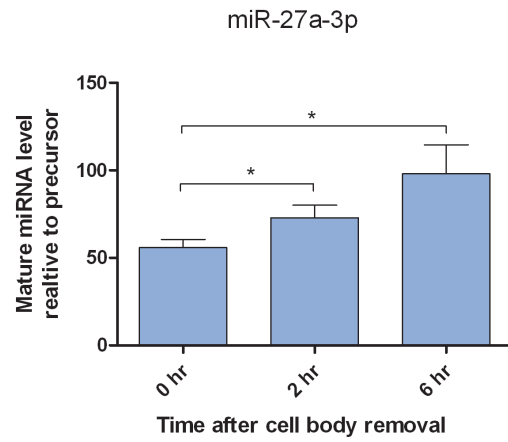
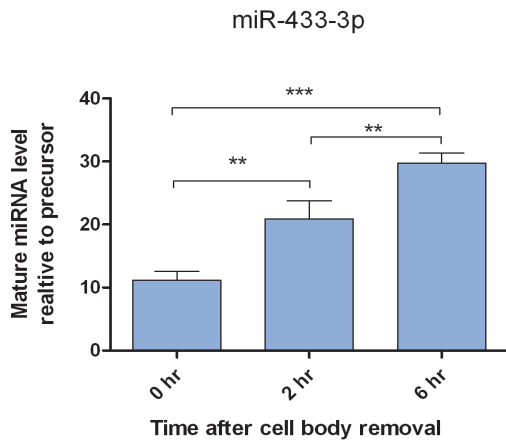


Figure 3.10 Specific axonal miRNA precursors are processed into their corresponding mature miRNAs independently from the neuronal cell body.

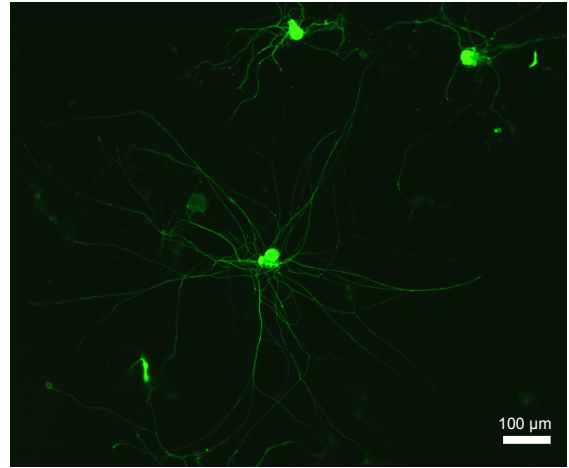
Axon fractions of DRG neurons cultured in Boyden chambers for 3 days were harvested at 0 hr, 2 hrs, and 6 hrs after removing the cell body fraction by cell scrapper. RNA isolated from these axon fractions was spiked with *in vitro* transcribed *eGFP* mRNA that subsequently used for normalization between axonal fraction samples and for calculation of ΔC_t values. $2^{-(\Delta C_t \text{ mature miRNA} - \Delta C_t \text{ precursor})}$ was used in the determination of the average relative level of mature miRNA to pre-miRNA \pm SEM. One-way ANOVA was used for all statistical analysis followed by analysis of variance with Bonferroni post-hoc test (*, $p < 0.05$; **, $p < 0.01$; ***, $p < 0.001$).

Overexpression of miR-433-3p attenuates axon growth in vitro.

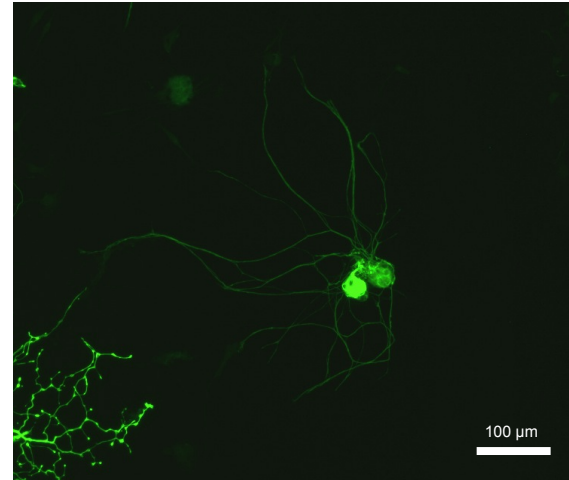
To determine the biological function of mature miR-433-3p, I transfected miR-433-3p mimic and antisense miR-433-3p in DRG neurons and examined the morphological outcomes. Transfection of miR-433-3p mimic decreased axon length by ~22% compared to mimic control (Fig. 3.11A-B). These results indicate that biologically functional mature miR-433-3p plays a regulatory role in axon growth *in vitro*.

A

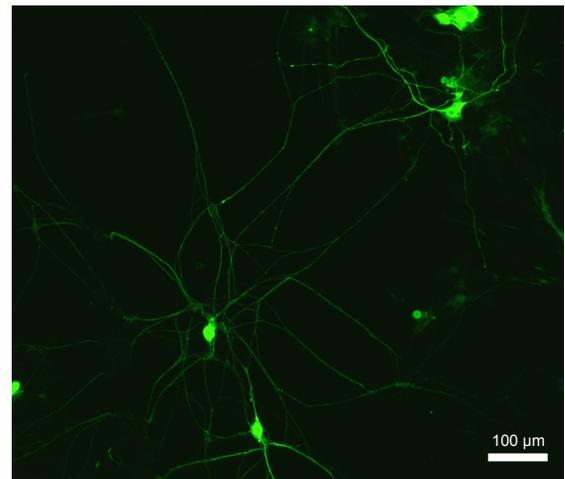
**Mimic
control**



**200 nM
Mimic
miR-433-3p**



**200 nM
Antisense
miR-433-3p**



B

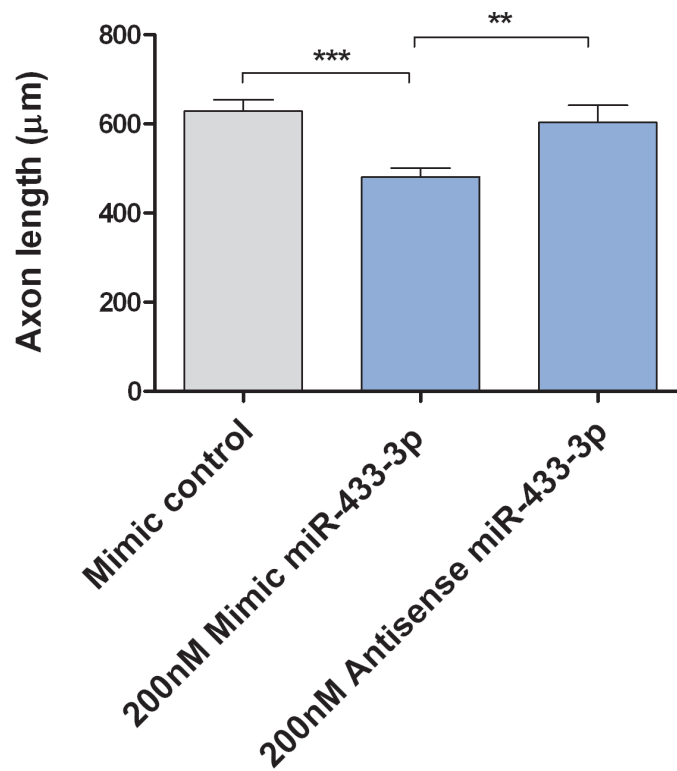


Figure 3.11 Transient transfection of miR-433-3p mimic attenuates axon growth in DRG neurons.

DRG neurons were co-transfected with GFP construct and indicated small synthetic RNAs. Representative images showing the effect of the indicated small synthetic RNAs in DRG neurons were taken 2 days after transfection (A). The effect of miR-433-3p on axon length was quantified as average axon length \pm SEM ($N \geq 60$) (B). Overexpression of miR-433-3p reduced axon length by ~22%. A statistical analysis was carried out using Student's T-test (**, $p < 0.01$; ***, $p < 0.001$).

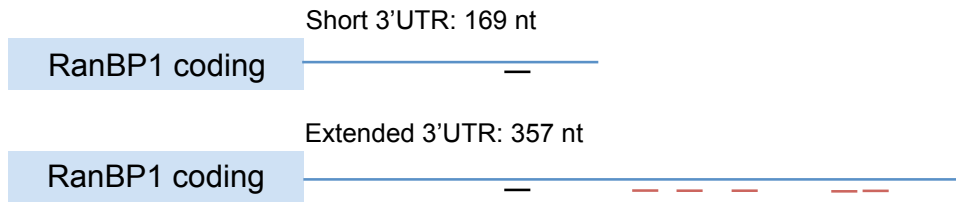
Mature miR-433-3p regulates the translation of RanBP1 mRNA containing an extended 3'UTR.

Using several miRNA prediction algorithms such as TargetScan and PITA, axonally localized *RanBP1* mRNA carrying an extended 3'UTR was predicted to contain a total of 6 binding sites (5 of which are exclusively located on the extended 3'UTR) for miR-433-3p (Fig. 3.12A-B). Three (positions at 244, 309, and 216) out of the five predicted miR-433-3p binding sites showed favorable ddG scores, which measure the accessibility of miRNA to the mRNA binding site [ddG measures the difference in hybridization energy of the miRNA to the binding site (dGduplex) and the energy required to open the local RNA secondary structure surrounding the binding site (dGopen)] (Fig. 3.12A-B). First, I checked to see whether *RanBP1* mRNA containing an extended 3'UTR is targeted by miR-433-3p utilizing dual luciferase reporter assay system. In brief, the extended 3'UTR of *RanBP1* mRNA was cloned into the 3'UTR of a pGL4 construct encoding Renilla luciferase (*Renilla-RanBP1 extended 3'UTR*). The construct encoding firefly luciferase was co-transfected and used as an internal control. As shown in figure 3.12C, transfection of miR-433-3p mimic significantly reduced Renilla activity by ~33% compared to the mimic scrambled control. When base mismatched within the seed region of miR-433-3p was introduced, this reduction in Renilla activity was abolished, further confirming the binding specificity of miR-433-3p to *RanBP1*'s extended 3'UTR. Similar to the miR-433-3p mismatched, antisense miR-433-3p also showed no significant effects on Renilla activity when compared to control mimic (Fig. 3.12C).

To determine whether miR-433-3p negatively regulates axonal RanBP1 expression in neurons, I co-transfected miR-433-3p mimic with a construct expressing GFP in DRG neurons and quantified the level of RanBP1 protein in GFP positive axonal growth cones by immunofluorescence. Since adult DRG neurons are quite difficult to transfect, GFP serves as an indicator for positive transfection of miR-433-3p mimic. Immunofluorescence analysis showed that miR-433-3p mimic caused 37% reduction in the level of RanBP1 protein expression in the growth cone compared to mimic control (Fig. 3.13). In contrast, antisense miR-433-3p showed no effect on the growth cone level of RanBP1 protein (Fig. 3.13). These results indicate that overexpression of miR-433-3p represses the expression of RanBP1 protein in axons.

To determine whether miR-433-3p mediated repression of RanBP1 protein expression was exerted at the level of mRNA degradation, I transfected DRG neurons with control mimic, miR-433-3p mimic, or antisense miR-433-3p and quantified the levels of RanBP1 mRNA carrying the extended 3'UTR by RT-qPCR. First, I confirmed that addition of miR-433-3p mimic resulted in an increase in the cellular level of mature miR-433-3p. RT-qPCR analysis for mature miR-433-3p showed that miR-433-3p was increased in DRG neurons transfected with miR-433-3p mimic (Fig. 3.14A). In contrast, the level of mature miR-433-3p was significantly reduced after transfection with antisense miR-433-3p (Fig. 3.14A). As shown in figure 3.14B, ~70% of axoplasmic *RanBP1* transcript were the extended 3'UTR variant of *RanBP1* mRNA, suggesting this is the predominant form in neurons. A primer set specific to the coding region of *RanBP1* mRNA was used to quantify overall *RanBP1* transcripts

representing both the short and the extended 3'UTR variants, whereas a primer set specific to the extended 3'UTR was used to exclusively quantify the level of *RanBP1* mRNA with an extended 3'UTR. RT-qPCR analysis revealed that overexpression of miR-433-3p resulted in 32% reduction in *RanBP1* transcript containing the extended 3'UTR (Fig. 3.14C). Taken all together, these results showed that miR-433-3p silenced the expression of RanBP1 protein by binding the extended 3'UTR of *RanBP1* mRNA and caused transcript degradation.

A**B**

Position	Seed	dGduplex	dGopen	ddG
133	6:1:1	-7.2	-8.72	1.52
202	6:1:1	-3.7	-3.66	-0.036
216	7:1:1	-8.4	-6.53	-1.86
244	6:0:0	-15.6	-8.37	-7.22
300	6:1:0	-7.9	-9.34	1.44
309	7:1:1	-7.04	-4.95	-2.08

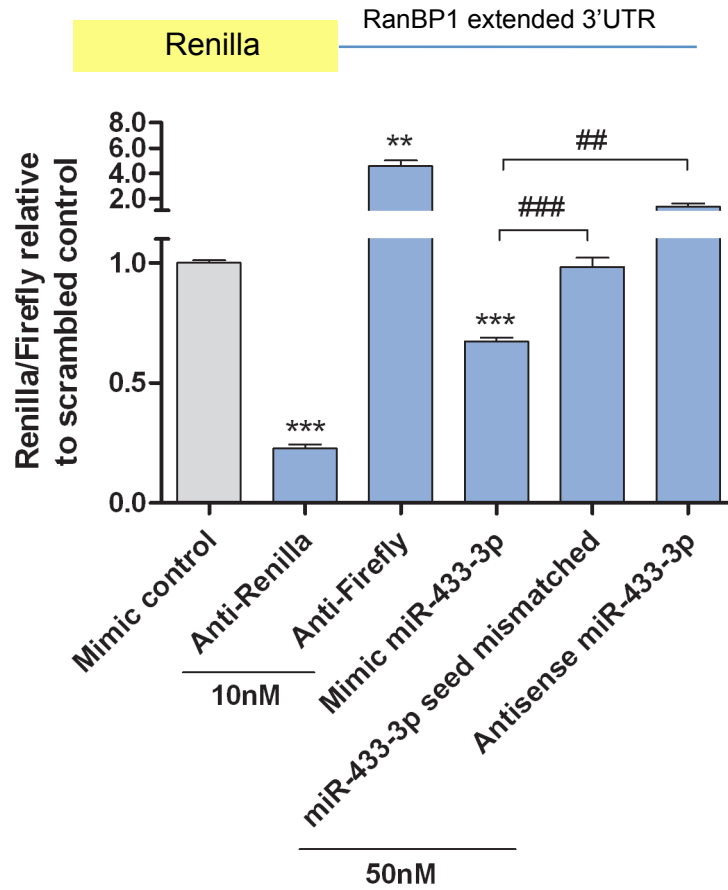
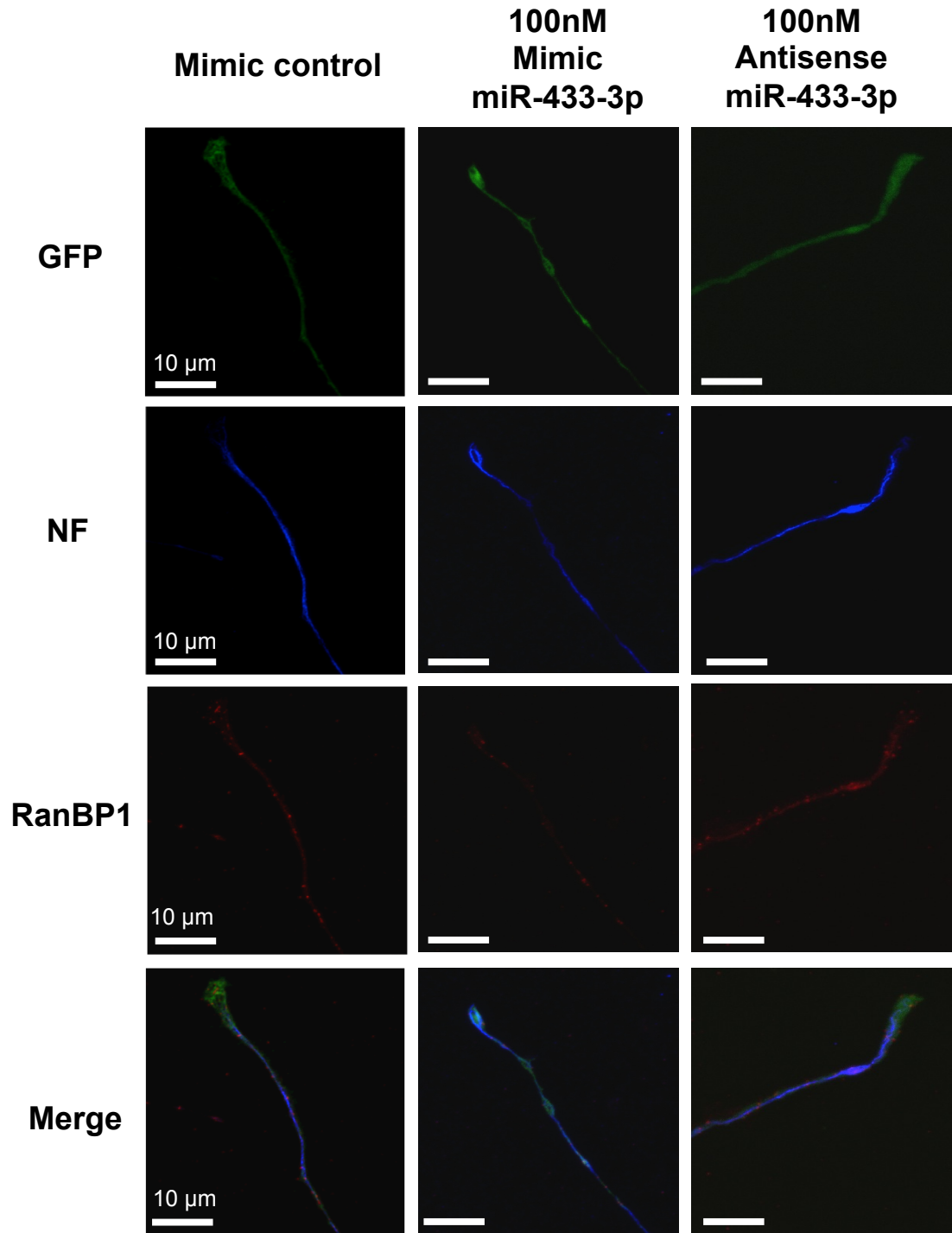
C

Figure 3.12 miR-433-3p targets an mRNA encoding Ran binding protein 1.

Ran binding protein 1 (RanBP1) mRNA has two different 3'UTR variants (a short or an extended 3'UTR) (A). *RanBP1* mRNA carrying a short 3'UTR is predicted to contain only one binding site for miR-433-3p, whereas *RanBP1* mRNA carrying the extended 3'UTR is predicted to contain 6 miR-433-p binding sites (B). The binding sites for miR-433-3p was predicted by PITA miRNA target prediction algorithm that also accounts the accessibility of miRNA to the binding site on the target mRNA in addition to seed match score in the scoring parameters. PITA indicates the interaction of mature miRNA to the see matched region on the mRNA as X:Y:Z, in which X represents the seed size, Y represents the number of mismatched, and Z represents the number of G:U wobble pairs. The accessibility of mature miRNA to the binding site on the mRNA is determined by ddG ($ddG = dG_{duplex} - dG_{open}$, in which dG_{duplex} is defined as free energy gain from the formation of miRNA:target duplex and dG_{open} is defined as the energy cost required to open local RNA secondary structure around the binding site). Predicted *RanBP1* mRNA target was validated using dual luciferase assay system using miR-433-3p mimic in F11 cell line (C). Overexpression of miR-433-3p significantly reduced Renilla luciferase activity (~ 33% reduction) compared to mimic control. Student's T-test was used for all statistical analysis. * represents statistically significant p-values comparing relative Renilla activity to mimic control (**, $p < 0.01$; ***, $p < 0.001$) and # represents statistically significant p-values comparing relative Renilla activity between samples (##, $p < 0.01$; ###, $p < 0.001$).

A



B

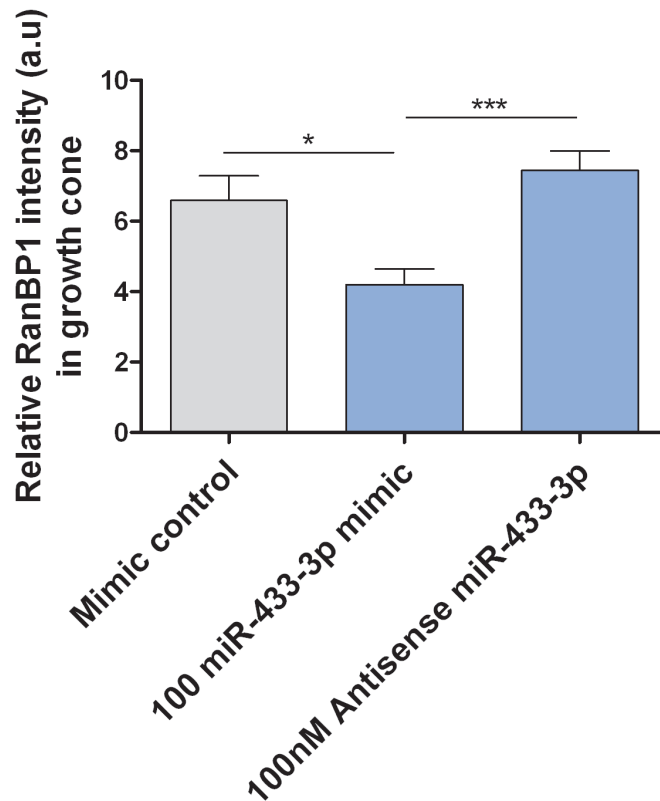
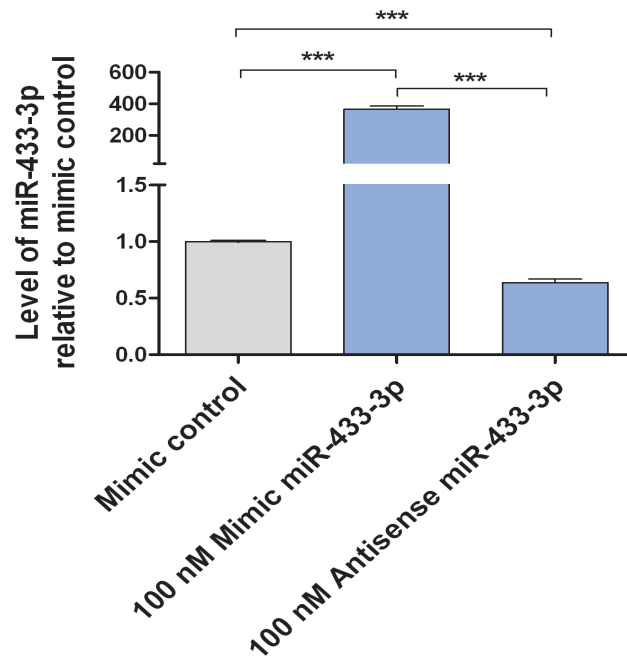
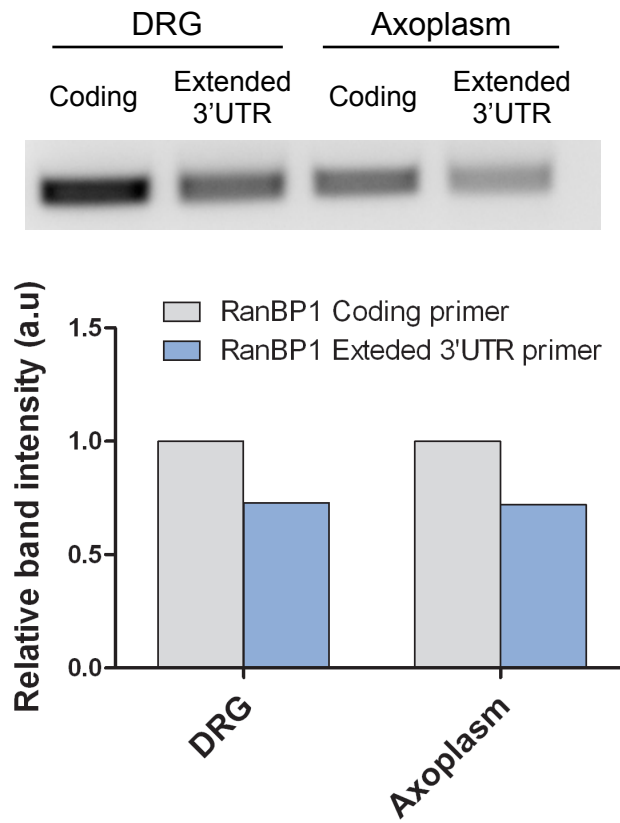


Figure 3.13 miR-433-3p negatively regulates RanBP1 expression in distal axons. DRG neurons were co-transfected a GFP construct and indicated synthetic small RNAs. Immunofluorescence for RanBP1 (red) and Neurofilament (NF, blue) in growth cones and distal axon shafts of transfected DRG neurons confirmed the effect of miR-433-3p on RanBP1 expression (A). Relative RanBP1 intensity (RanBP1 relative to neurofilament) in the growth cones ($N \geq 20$ neurons/condition) showed that miR-433-3p significantly reduced the expression of RanBP1 protein (~37% reduction) (B). Statistical analysis was carried out using one-way ANOVA followed by Bonferroni post-hoc test. A statistically significant p-values are represented by * (*, $p < 0.05$; ***, $p < 0.001$).

A**B**

C

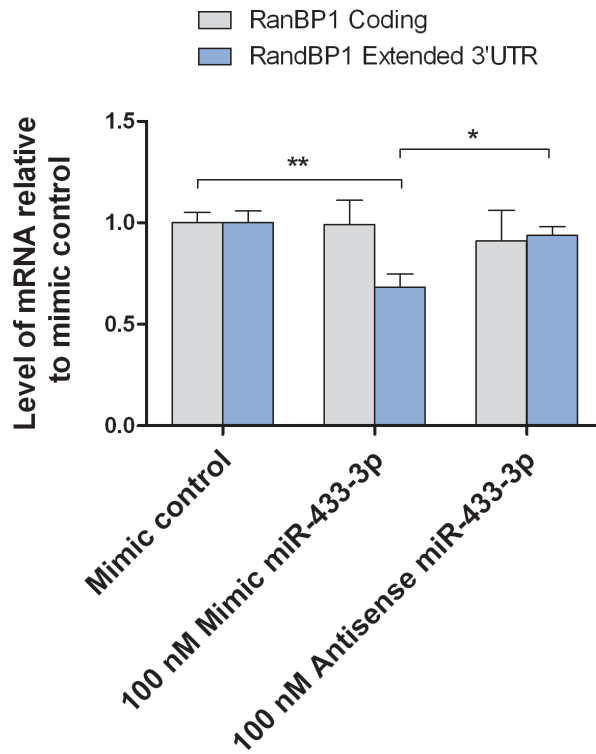


Figure 3.14 miR-433-3p mediates silencing of RanBP1 expression by inducing transcript degradation.

(A) RT-qPCR indicates the level of miR-433-3p in DRG neurons transfected with indicated synthetic RNAs. DRG neurons transfected with miR-433-3p mimic showed a significant increase in the level of mature miR-433-3p. (B) Agarose gel electrophoresis analysis of PCR amplicons of *RanBP1* mRNA in DRG tissues and sciatic nerve axoplasm using primers specific for the coding region and primers specific for the extended 3'UTR region revealed that ~ 70% of RanBP1 transcripts carry an extended 3'UTR. (C) RT-qPCR analysis of *RanBP1* mRNA in transfected DRG neurons showed that miR-433-3p significantly decreased the level of RanBP1 transcript containing the extended 3'UTR (~32% reduction). A statistically analysis was carried out using Student's T-test and statistically significant p-values are represented by * (*, $p < 0.05$; **, $p < 0.01$; ***, $p < 0.0001$).

Discussion

A number of studies have demonstrated that miRNAs are differentially distributed to axons, where they could play a role in regulating various axonal functions (Natera-Naranjo et al., 2010; Sasaki et al., 2014). However, it is unclear how these small regulatory RNAs are localized to distal axons. Multiple hypothetical models have been proposed for the selective transport of miRNAs to neuronal processes; 1) transport of biologically active mature miRNAs, 2) co-transport of miRNA bound to its target mRNAs via RNA transport granules (“hitch-hiking model), and 3) transport of miRNA precursors followed by local processing of pre-miRNAs into functionally active mature miRNAs (Kosik, 2006; Kaplan et al., 2013). Supporting the third hypothesis, previous studies in our laboratory and others showed that both miRNA precursors and components of their processing machinery such as Dicer and KSRP are localized to distal axons of sensory neurons (Kim et al., 2015, Vargas et al., 2016, Hengst et al., 2006, Murashov et al., 2007). These findings raise an important cellular/molecular question as to how pre-miRNAs are selectively transported into axons. In addition to this unresolved question, it is unknown whether axonally localized endogenous pre-miRNAs are processed into their corresponding functional mature miRNAs. In the present study, I identified a structural region within axonally localizing pre-miRNA-433 that strongly governs the localization of the precursor miRNA into distal axons of DRG neurons. Further, I demonstrated that

axonal pre-miRNAs are selectively processed into the corresponding mature miRNAs where they play a role in regulating axon growth.

Using an RNA reporter system in combination with FISH, RT-qPCR, and FRAP methods, I first demonstrated that pre-miR-433 contains *cis*-element(s) that drive the localization of *eGFP* reporter mRNA into distal axons of DRG neurons. Next, I examined whether axon localization element(s) exist within either the stem region or the terminal loop region of the pre-miR-433 structure by generating reporter constructs that carry a chimeric pre-miRNA that contains either the terminal loop region of axonally localizing pre-miR-433 structure in the backbone of cell body restricted pre-miR-138-1 [*eGFP^{myr}*-(L433 + S138-1)] or the terminal loop region of pre-miR-138-1 in the backbone of pre-miR-433 [*eGFP^{myr}*-(L138-1 + S433)]. As predicted, *eGFP^{myr}*-(L433 + S138-1) mRNA is selectively localized into distal axons of DRG neurons. In contrast, *eGFP^{myr}*-(L138-1 + S433) mRNA was not localized, indicating a lack of *cis* localization element(s) needed for its transport into distal axons. Together these results indicate that the terminal loop region within axonally localizing pre-miR-433 structure (L433) is an important determinant for the localization of the reporter mRNA into axons of DRG neurons. Similar to my findings, recent study reported by Bicker et al. (2013) has also implicated the importance of the terminal loop region within dendritically localizing pre-miR-134 in directing the localization of pre-miRNAs into dendrites. It is not surprising that the terminal loop regions of pre-miRNAs play an important role in determining the localization of pre-miRNAs in neurons since the geometrical structure of pre-miRNAs

makes this region easily accessible to an RNA binding proteins (RBPs). Many RBPs including dicer, KSRP, DHX36, and MCPIP1 have been demonstrated to bind the terminal loop regions of pre-miRNAs and regulate the processing and turn over of miRNA precursors (Zhang and Zeng, 2010; Trabucchi et al., 2009; Viswanathan et al., 2008; Bicker et al., 2010; Bajan and Hutvagner, 2011). Even though I showed that the terminal loop region of pre-miR-433 structure is important for axon localization, further studies are needed to determine exact primary sequences and/or structure(s) (e.g., terminal loop, stem, internal loop, and bulge) within the terminal loop region of pre-miR-433 that are essential for axon localization. Given the important roles of RBPs in axon localization of mRNAs, future studies will also be needed to address the identity of *trans*-acting RBPs that mediate the transport of pre-miRNAs into axons.

Despite many recent studies showing localization of pre-miRNAs and components of their processing machinery in axons, no studies have investigated whether axonally localized endogenous precursor miRNAs are autonomously processed into functionally active corresponding mature miRNAs. Using the Boyden chamber compartmentalized culture system, I was able to physically separate neuronal cell bodies from axons and showed that specific pre-miRNAs are processed to give rise to the corresponding mature miRNAs within the severed anucleate axons using RT-qPCR method. Removal of neuronal cell bodies from the compartmentalized cell culture system serves two purposes; 1) disruption of connectivity between axons and neuronal cell bodies blocks active anterograde transport and eliminates somatic contribution of RNAs to axons and 2) severance of axons from the cell bodies mimics

injury induced axonal stimulation. My results showed a statistically significant increase in the levels of mature miR-433-3p and miR-27a-3p in severed axons at 6 hours after anucleation, but no changes in the axonal levels of miR-146-3p and miR-21-5p. The fact that there were no changes in the levels of miR-146-3p and miR-21-5p in severed axons suggests that the significant increase in the levels of miR-433-3p and miR-27a-3p resulted from local processing of highly selective precursors in response to axon injury, rather than a general degradation of miRNA precursors. It is noteworthy that since severing the axon from the cell body compromises axonal membrane integrity, local processing of pre-miR-433 and pre-miR-27a in severed anucleate axons could be triggered by rapid influx of calcium and other ions. In agreement with my data showing that axonal stimulus induced processing of specific pre-miRNAs into corresponding mature miRNAs, a recent study reported by Sambandan et al. (2017) revealed that processing of dendritically localized pre-miR-181a is triggered by a low frequency synaptic stimulation. Taken together, my results suggest that intra-axonal miRNA maturation pathway may be regulated in a signal-specific manner.

Due to regulatory functions in specific target mRNA metabolism of miRNAs, I further investigated functional roles of mature miR-433-3p in DRG neurons. Using miRNA target prediction algorithms and dual luciferase reporter assay, I identified and validated *Ran binding protein 1 (RanBP1)* mRNA carrying an extended 3'UTR variant as a target of miR-433-3p. RanBP1 is a ran GTPase effector protein that regulates the interaction of cargo protein with importin α/β heterodimer, a complex

that shuttles the cargo protein into the nucleus. The transports of cargo between the cytosol and the nucleus relies on gradients of a small GTPase Ran that cycles between GTP bound form in the nucleus (Ran-GTP) and GDP bound form (Ran-GDP) in the cytosol. Since Ran-GDP does not bind to importins, high level of Ran-GDP in the cytosol allows importins α/β complex to interact with cargo protein and imports it into the nucleus. Due to high concentration of Ran-GTP in the nucleus, an interaction of Ran-GTP with the importins causes the release of the cargo protein from the complex. Importins bound to Ran-GTP is subsequently exported back into the cytosol, where a competitive binding of RanBP1 stimulates the release of Ran-GTP from importins and enables importin subunits to once again interact with cargo protein. Interestingly, previous studies showed that *RanBP1* mRNA carrying the extended 3'UTR variant is locally translated at the site of axonal injury, where it facilitates the formation of importins-injury signal cargo complex that retrogradely transports the signal to the cell body of damaged axons (Yudin et al., 2008). Herein, I showed that overexpression of miR-433-3p in cultured DRG neurons not only significantly reduced the level of RanBP1 protein expression in growth cone of cultured DRG neurons, but also decreased the level of *RanBP1-extended 3'UTR* transcript. This suggests that miR-433-3p negatively regulates RanBP1 expression by binding to the extended 3'UTR of *RanBP1* mRNA and causes transcript degradation. Most importantly, transient transfection of miR-433-3p mimic in cultured DRG neurons significantly reduced axon growth. The attenuation in axon growth is consistent with a previous report by Yudin et al. (2008) demonstrating that DRG neurons of RanBP1 knock out mice

cultured after conditioning lesion exhibit decreased neurite outgrowth and reduced axon length. Collectively, these results suggest that pre-miR-433 is locally processed to give rise to mature miR-433-3p at the site of axon injury, where it negatively regulates intra-axonal translation of *RanBP1-extended 3'UTR* mRNA when it is no longer required.

REFERENCES

- Ambros V (2011) MicroRNAs and developmental timing. *Curr Opin Genet Dev* 21:511-517.
- Aschrafi A, Schwechter AD, Mameza MG, Natera-Naranjo O, Gioio AE, Kaplan BB (2008) MicroRNA-338 regulates local cytochrome C oxidase mRNA levels and oxidative phosphorylation in the axons of sympathetic neurons. *J Neurosci* 28:12581-12590.
- Bachmann A, Schneider M, Theilenberg E, Grawe F, Knust E (2001) *Drosophila* Stardust is a partner of Crumbs in the control of epithelial cell polarity. *Nature* 414:638-643.
- Bagni C, Mannucci L, Dotti CG, Amaldi F (2000) Chemical stimulation of synaptosomes modulates alpha-Ca²⁺/calmodulin-dependent protein kinase II mRNA association to polysomes. *J Neurosci* 20:Rc76.
- Bajan S, Hutvagner G (2011) Another "loophole" in miRNA processing. *Mol Cell* 44:345-347.
- Barr J, Yakovlev KV, Shidlovskii Y, Schedl P (2016) Establishing and maintaining cell polarity with mRNA localization in *Drosophila*. *Bioessays* 38:244-253.
- Bartel DP (2004) MicroRNAs: genomics, biogenesis, mechanism, and function. *Cell* 116:281-297.
- Bassell GJ, Zhang H, Byrd AL, Femino AM, Singer RH, Taneja KL, Lifshitz LM, Herman IM, Kosik KS (1998) Sorting of beta-actin mRNA and protein to neurites and growth cones in culture. *J Neurosci* 18:251-265.
- Ben-Yaakov K, Dagan SY, Segal-Ruder Y, Shalem O, Vuppalanchi D, Willis DE, Yudin D, Rishal I, Rother F, Bader M, Blesch A, Pilpel Y, Twiss JL, Fainzilber M (2012) Axonal transcription factors signal retrogradely in lesioned peripheral nerve. *EMBO J* 31:1350-1363.
- Bian S, Hong J, Li Q, Schebelle L, Pollock A, Knauss JL, Garg V, Sun T (2013) MicroRNA cluster miR-17-92 regulates neural stem cell expansion and

transition to intermediate progenitors in the developing mouse neocortex. *Cell Rep* 3:1398-1406.

Bicker S, Khudayberdiev S, Weiß K, Zocher K, Baumeister S, Schrott G (2013) The DEAH-box helicase DHX36 mediates dendritic localization of the neuronal precursor-microRNA-134. *Genes Dev* 27:991-996.

Brennecke J, Hipfner DR, Stark A, Russell RB, Cohen SM (2003) bantam encodes a developmentally regulated microRNA that controls cell proliferation and regulates the proapoptotic gene *hid* in *Drosophila*. *Cell* 113:25-36.

Chowdhury S, Shepherd JD, Okuno H, Lyford G, Petralia RS, Plath N, Kuhl D, Hagan RL, Worley PF (2006) Arc/Arg3.1 interacts with the endocytic machinery to regulate AMPA receptor trafficking. *Neuron* 52:445-459.

Davis TH, Cuellar TL, Koch SM, Barker AJ, Harfe BD, McManus MT, Ullian EM (2008) Conditional loss of Dicer disrupts cellular and tissue morphogenesis in the cortex and hippocampus. *J Neurosci* 28:4322-4330.

Eng H, Lund K, Campenot RB (1999) Synthesis of beta-tubulin, actin, and other proteins in axons of sympathetic neurons in compartmented cultures. *J Neurosci* 19:1-9.

Garner CC, Tucker RP, Matus A (1988) Selective localization of messenger RNA for cytoskeletal protein MAP2 in dendrites. *Nature* 336:674-677.

Giraldez AJ, Cinalli RM, Glasner ME, Enright AJ, Thomson JM, Baskerville S, Hammond SM, Bartel DP, Schier AF (2005) MicroRNAs regulate brain morphogenesis in zebrafish. *Science* 308:833-838.

Hammell CM, Karp X, Ambros V (2009) A feedback circuit involving let-7-family miRNAs and DAF-12 integrates environmental signals and developmental timing in *Caenorhabditis elegans*. *Proc Natl Acad Sci U S A* 106:18668-18673.

Hanz S, Perlson E, Willis D, Zheng JQ, Massarwa R, Huerta JJ, Koltzenburg M, Kohler M, van-Minnen J, Twiss JL, Fainzilber M (2003) Axoplasmic importins enable retrograde injury signaling in lesioned nerve. *Neuron* 40:1095-1104.

Hell JW (2014) CaMKII: Claiming Center Stage in Postsynaptic Function and Organization. *Neuron* 81:249-265.

- Hengst U, Cox LJ, Macosko EZ, Jaffrey SR (2006) Functional and selective RNA interference in developing axons and growth cones. *J Neurosci* 26:5727-5732.
- Hirokawa N, Funakoshi T, Sato-Harada R, Kanai Y (1996) Selective stabilization of tau in axons and microtubule-associated protein 2C in cell bodies and dendrites contributes to polarized localization of cytoskeletal proteins in mature neurons. *J Cell Biol* 132:667-679.
- Holt CE, Schuman EM (2013) The central dogma decentralized: new perspectives on RNA function and local translation in neurons. *Neuron* 80:648-657.
- Huttelmaier S, Zenklusen D, Lederer M, Dichtenberg J, Lorenz M, Meng X, Bassell GJ, Condeelis J, Singer RH (2005) Spatial regulation of beta-actin translation by Src-dependent phosphorylation of ZBP1. *Nature* 438:512-515.
- Jung H, Yoon BC, Holt CE Axonal mRNA localization and local protein synthesis in nervous system assembly, maintenance and repair. *Nat Rev Neurosci* 13:308-324.
- Kamal MA, Mushtaq G, Greig NH (2015) Current Update on Synopsis of miRNA Dysregulation in Neurological Disorders. *CNS Neurol Disord Drug Targets* 14:492-501.
- Kang H, Schuman EM (1996) A requirement for local protein synthesis in neurotrophin-induced hippocampal synaptic plasticity. *Science* 273:1402-1406.
- Kaplan BB, Kar AN, Gioio AE, Aschrafi A (2013) MicroRNAs in the axon and presynaptic nerve terminal. *Front Cell Neurosci* 7.
- Kar AN, MacGibeny MA, Gervasi NM, Gioio AE, Kaplan BB (2013) Intra-axonal synthesis of eukaryotic translation initiation factors regulates local protein synthesis and axon growth in rat sympathetic neurons. *J Neurosci* 33:7165-7174.
- Kawase-Koga Y, Otaegi G, Sun T (2009) Different timings of Dicer deletion affect neurogenesis and gliogenesis in the developing mouse central nervous system. *Dev Dyn* 238:2800-2812.
- Kim HH, Kim P, Phay M, Yoo S (2015) Identification of precursor microRNAs within distal axons of sensory neuron. *J Neurochem* 134:193-199.

- Kislauskis EH, Zhu X, Singer RH (1997) beta-Actin messenger RNA localization and protein synthesis augment cell motility. *J Cell Biol* 136:1263-1270.
- Kosik KS (2006) The neuronal microRNA system. *Nat Rev Neurosci* 7:911-920.
- Leung KM, van Horck FP, Lin AC, Allison R, Standart N, Holt CE (2006) Asymmetrical beta-actin mRNA translation in growth cones mediates attractive turning to netrin-1. *Nat Neurosci* 9:1247-1256.
- Lisman J, Yasuda R, Raghavachari S (2012) Mechanisms of CaMKII action in long-term potentiation. *Nat Rev Neurosci* 13:169-182.
- Litman P, Barg J, Ginzburg I (1994) Microtubules are involved in the localization of tau mRNA in primary neuronal cell cultures. *Neuron* 13:1463-1474.
- Medioni C, Mowry K, Besse F (2012) Principles and roles of mRNA localization in animal development. *Development* 139:3263-3276.
- Muller C, Bauer NM, Schafer I, White R (2013) Making myelin basic protein -from mRNA transport to localized translation. *Front Cell Neurosci* 7:169.
- Murashov AK, Chintalgattu V, Islamov RR, Lever TE, Pak ES, Sierpinski PL, Katwa LC, Van Scott MR (2007) RNAi pathway is functional in peripheral nerve axons. *FASEB J* 21:656-670.
- Natera-Naranjo O, Aschrafi A, Gioio AE, Kaplan BB (2010) Identification and quantitative analyses of microRNAs located in the distal axons of sympathetic neurons. *RNA*,1516-1529.
- Peebles CL, Yoo J, Thwin MT, Palop JJ, Noebels JL, Finkbeiner S (2010) Arc regulates spine morphology and maintains network stability in vivo. *Proc Natl Acad Sci U S A* 107:18173-18178.
- Peng Y, Croce CM (2016) The role of MicroRNAs in human cancer. *Signal Transduction and Targeted Therapy* 1:15004.
- Piper M, Holt C (2004) RNA Translation in Axons. *Annu Rev Cell Dev Biol* 20:505-523.
- Piper M, Anderson R, Dwivedy A, Weigl C, van Horck F, Leung KM, Cogill E, Holt C (2006) Signaling mechanisms underlying Slit2-induced collapse of *Xenopus* retinal growth cones. *Neuron* 49:215-228.

- Rial Verde EM, Lee-Osbourne J, Worley PF, Malinow R, Cline HT (2006) Increased expression of the immediate-early gene *arc/arg3.1* reduces AMPA receptor-mediated synaptic transmission. *Neuron* 52:461-474.
- Rivas FV, Tolia NH, Song JJ, Aragon JP, Liu J, Hannon GJ, Joshua-Tor L (2005) Purified Argonaute2 and an siRNA form recombinant human RISC. *Nat Struct Mol Biol* 12:340-349.
- Rodriguez AJ, Czaplinski K, Condeelis JS, Singer RH (2008) Mechanisms and cellular roles of local protein synthesis in mammalian cells. *Curr Opin Cell Biol* 20:144-149.
- Sambandan S, Akbalik G, Kochen L, Rinne J, Kahlstatt J, Glock C, Tushev G, Alvarez-Castelao B, Heckel A, Schuman EM (2017) Activity-dependent spatially localized miRNA maturation in neuronal dendrites. *Science* 355:634-637.
- Sasaki Y, Gross C, Xing L, Goshima Y, Bassell GJ (2014) Identification of Axon-Enriched MicroRNAs Localized to Growth Cones of Cortical Neurons. *Dev Neurobiol* 74:397-406.
- Sasaki Y, Welshhans K, Wen Z, Yao J, Xu M, Goshima Y, Zheng JQ, Bassell GJ (2010) Phosphorylation of zipcode binding protein 1 is required for brain-derived neurotrophic factor signaling of local beta-actin synthesis and growth cone turning. *J Neurosci* 30:9349-9358.
- Schratt GM, Tuebing F, Nigh EA, Kane CG, Sabatini ME, Kiebler M, Greenberg ME (2006) A brain-specific microRNA regulates dendritic spine development. *Nature* 439:283-289.
- Slack FJ, Basson M, Liu Z, Ambros V, Horvitz HR, Ruvkun G (2000) The *lin-41* RBCC gene acts in the *C. elegans* heterochronic pathway between the *let-7* regulatory RNA and the *LIN-29* transcription factor. *Mol Cell* 5:659-669.
- Spaulding EL, Burgess RW (2017) Accumulating Evidence for Axonal Translation in Neuronal Homeostasis. *Front Neurosci* doi: 10.3389/finin.2017.00312
- Stappert L, Roesse-Koerner B, Brüstle O (2015) The role of microRNAs in human neural stem cells, neuronal differentiation and subtype specification. *Cell Tissue Res*, 47-64.
- Stokin GB, Lillo C, Falzone TL, Brusch RG, Rockenstein E, Mount SL, Raman R, Davies P, Masliah E, Williams DS, Goldstein LSB (2005) Axonopathy and

- Transport Deficits Early in the Pathogenesis of Alzheimer's Disease. *Science* 307(5713): 1282-1288.
- Tepass U, Theres C, Knust E (1990) crumbs encodes an EGF-like protein expressed on apical membranes of *Drosophila* epithelial cells and required for organization of epithelia. *Cell* 61:787-799.
- Tiruchinapalli DM, Oleynikov Y, Kelic S, Shenoy SM, Hartley A, Stanton PK, Singer RH, Bassell GJ (2003) Activity-dependent trafficking and dynamic localization of zipcode binding protein 1 and beta-actin mRNA in dendrites and spines of hippocampal neurons. *J Neurosci* 23:3251-3261.
- Trabucchi M, Briata P, Garcia-Mayoral M, Haase AD, Filipowicz W, Ramos A, Gherzi R, Rosenfeld MG (2009) The RNA-binding protein KSRP promotes the biogenesis of a subset of microRNAs. *Nature* 459:1010-1014.
- Vargas JN, Kar AN, Kowalak JA, Gale JR, Aschrafi A, Chen CY, Gioio AE, Kaplan BB (2016) Axonal localization and mitochondrial association of precursor microRNA 338. *Cell Mol Life Sci* 73:4327-4340.
- Viswanathan SR, Daley GQ, Gregory RI (2008) Selective blockade of microRNA processing by Lin28. *Science* 320:97-100.
- Wang W, Kwon EJ, Tsai L-H (2012) MicroRNAs in learning, memory, and neurological diseases. *Learn Mem.* 19:359-368.
- Wightman B, Ha I, Ruvkun G (1993) Posttranscriptional regulation of the heterochronic gene *lin-14* by *lin-4* mediates temporal pattern formation in *C. elegans*. *Cell* 75:855-862.
- Wu Z, Cai X, Huang C, Xu J, Liu A (2016) miR-497 suppresses angiogenesis in breast carcinoma by targeting HIF-1alpha. *Oncol Rep* 35:1696-1702.
- Yang G, Xiong G, Cao Z, Zheng S, You L, Zhang T, Zhao Y (2016) miR-497 expression, function and clinical application in cancer. *Oncotarget*, 55900-55911.
- Yin Y, Edelman GM, Vanderklish PW (2002) The brain-derived neurotrophic factor enhances synthesis of Arc in synaptoneuroosomes. *Proc Natl Acad Sci U S A* 99:2368-2373.
- Yudin D, Hanz S, Yoo S, Iavnilovitch E, Willis D, Gradus T, Vuppalachchi D, Segal-Ruder Y, Ben-Yaakov K, Hieda M, Yoneda Y, Twiss JL, Fainzilber M (2008)

Localized regulation of axonal RanGTPase controls retrograde injury signaling in peripheral nerve. *Neuron* 59:241-252.

Zhang H, Fire AZ (2010) Cell autonomous specification of temporal identity by *Caenorhabditis elegans* microRNA *lin-4*. *Dev Biol* 344:603-610.

Zhang HL, Singer RH, Bassell GJ (1999) Neurotrophin regulation of beta-actin mRNA and protein localization within growth cones. *J Cell Biol* 147:59-70.

Zhang X, Zeng Y (2010) The terminal loop region controls microRNA processing by Drosha and Dicer. *Nucleic Acids Res* 38:7689-7697.

Chapter 4

CONCLUSION AND PERSPECTIVE

Up until about twenty years ago, it was thought that all axonal proteins are delivered from the neuronal cell body after being produced. With major advances in molecular biology and microscopy techniques, numerous studies have unequivocally demonstrated that invertebrate and vertebrate axons are capable of synthesizing proteins locally (Jung and Holt, 2012). Intra-axonal translations of localized mRNAs have been implicated in a variety of axonal functions including axon growth, pathfinding, rapid injury response, and regeneration (Yoo et al., 2010). Despite the emerging functional importance of axonally synthesized proteins, many questions regarding the control over intra-axonal protein synthesis remain unanswered. A class of small non-coding RNAs, microRNAs (miRNAs), has recently been recognized as a prominent player in post-transcriptional regulation of gene expression. These small regulatory RNAs could play a role in spatiotemporal regulation of intra-axonal protein synthesis and the identification and validation of their axonal mRNA targets are being extensively investigated. Although subsets of miRNAs are known to be enriched in distal axons, the mechanism underlying the transport of specific miRNAs into distal axon remains largely unknown. In the conclusion chapter of my dissertation, I will

discuss the contribution of my studies toward the understanding of how miRNAs are selectively localized into distal axons and the role of miRNAs in axon regeneration.

Establishing axon-specific miRNA profiles in regenerating nerves

Studies in the field of neural repair over the past century have consistently showed that axons of mature mammalian CNS neurons do not spontaneously regenerate after injury, whereas adult PNS neurons can readily regenerate their damaged axons (Huebner and Strittmatter, 2009). Intra-axonal protein synthesis has been directly linked to the robust regenerative response in PNS neurons. Upon peripheral nerve lesions, a variety of proteins including importin- β , vimentin, RanBP1, and STAT3 are locally synthesized at the axonal injury site (Yoo et al., 2010). These locally synthesized proteins provide retrograde injury signals to the neuronal cell body and activate gene transcriptions that are necessary for the regenerative response. Intra-axonal mRNA translation not only provides a means to communicate essential information concerning the axonal injury to the cell body, but also provides local sources of proteins that are required for the reformation of the axonal growth cone, which is a crucial prerequisite for successful axon regeneration (Zheng et al., 2001; Verma et al., 2005). Translation is an energetically costly process and therefore intra-axonal protein synthesis induced by axon injury must be silenced when it is no longer required. To date, mechanisms underlying this post-transcriptional silencing in axons are largely unknown.

MicroRNAs are a class of small non-coding regulatory RNAs that have been gaining functional importance in the nervous system. These regulatory RNAs are known to negatively regulate gene expression at the post-transcriptional level by binding to specific sequences in the 3'UTRs of their target mRNAs and repress translation. Several studies have recently reported temporal changes in miRNA expression following spinal cord injury as well as in sciatic nerve following axotomy (Zhou et al., 2011; Yu et al., 2011). These studies suggest direct roles of miRNAs in neural repair through translational regulation of protein expression. Recent miRNA profile analysis in injured sciatic nerves reported by Yu et al. (2011) utilized RNA samples isolated from whole sciatic nerve lysate. Although their analysis provides insight into overall changes in miRNA expression that occur in the sciatic nerve during regeneration, examining changes in axon-specific miRNAs becomes problematic since RNA samples isolated from whole sciatic nerve lysate also contain RNA contribution from Schwann cells and other cells in the nerve tissue.

To examine changes in axon-specific miRNAs in response to peripheral nerve injury, I induced crush injury in rat sciatic nerve and carried out deep sequencing studies on the axoplasmic RNA extracted from the proximal nerve stump at five different time points following injury [Uninjured sham, 1-, 4-, 7-, and 14-days post injury (DPI)]. I found that 63 of 141 annotated miRNAs exhibit differential alterations in their levels across all time points after injury, compared to sham operated uninjured control. Further assessments of the relationship between the axoplasmic levels of those 63 miRNAs in uninjured nerves and in those of regenerating sciatic nerves revealed a

similarity between the miRNA profiles of uninjured nerve, 1 and 7 DPI, while 4 and 14 DPI miRNA profiles were separated into distinct clusters. These results indicate that temporal changes in axoplasmic miRNA levels following sciatic nerve injury do not correlate with the regenerative response that occurs in PNS axon regeneration. To gain a deeper understanding of how axoplasmic miRNAs respond to peripheral nerve injury, I grouped miRNAs that showed similar responses using clustering analysis. My analysis revealed three distinct clusters of axoplasmic miRNAs. Since miRNAs have the potential of regulating hundreds of mRNA targets and a single transcript can contain multiple binding sites for different miRNAs, a similarity in the responses of these axoplasmic miRNAs to nerve injury could suggest cooperative regulatory mechanisms of miRNAs in precisely regulating intra-axonal protein expression during nerve regeneration. Together, my findings suggest that the regulatory response of axon-specific miRNAs following nerve injury is more complex than it was originally thought.

To my surprise, my small-RNA sequencing study revealed another distinct class of small noncoding regulatory RNAs, piRNA, in the axoplasm of regenerating nerves. Initially, piRNA expression was thought to be restricted in the germ cells, where it plays a role in preserving genomic integrity by silencing mobile genetic elements (transposon) via interaction with P-element induced wimpy testis (Piwi) protein. With advances in high throughput sequencing technology, studies over the past years have uncovered the presence of piRNAs in various somatic cells. In particular, piRNAs were found to be highly abundant in neurons. Previous studies

have implicated the role of piRNAs in long-term memory formation and dendritic spine morphogenesis (Rajasethupathy et al., 2012; Lee et al., 2011). However, the study presented here is the first to report the presence of piRNA in regenerating mammalian axons. Subsequent studies in our lab demonstrated that sequences annotated to piRNA bank from small-RNA sequencing indeed showed characteristic features of mammalian piRNAs and immunoprecipitated with Miwi, a mouse homologue protein of Piwi (Phay et al., 2016). I further performed bioinformatics analysis and found that levels of axoplasmic piRNAs also exhibited temporal changes in response to nerve injury. To examine the effect of loss of function of the piRNA pathways in neurons, RNAi knockdown of Miwi was carried out in cultured sensory neurons preconditioned with nerve injury. Interestingly, knockdown of Miwi resulted in an increase in axon growth (Phay et al., 2016). This result is consistent with a recent study reported by Kim et al. (2018) using the *C. elegans* model. Altogether my dissertation work presented in chapter 2 provides new insight into the regulatory role of small noncoding RNAs in nerve repair. Future studies will not only need to address the mRNA targets of differentially regulated miRNAs in response to axon injury but also the regulatory targets of differentially regulated piRNAs.

Selective transport of specific miRNAs into distal axons of sensory neurons

While we now know that specific miRNAs are enriched in distal processes of PNS neurons, little is known about how these miRNAs are selectively transported to axons. Currently, there are three working hypotheses for the selective localization of

miRNAs to neuronal processes; 1) transport of individual mature miRNA, 2) co-transport of miRNA bound to its mRNA target, and 3) transport of precursor miRNA (pre-miRNA) followed by subsequent processing of pre-miRNA into the corresponding mature miRNA (Kosik et al., 2006). Previous studies in our lab and others showed that both pre-mRNAs and protein components of their processing machinery are localized to distal axons of sensory neurons (Kim et al., 2015). These findings provide evidence to support the third hypothesis. In chapter 3, I have shown that pre-miR-433 is selectively localized to axons and identified the terminal loop region of pre-miR-433 structure as a *cis*-element that strongly governs the localization of RNA into distal axons. Although miRNA precursors and the core protein component of pre-miRNA processing complex, Dicer, are known to be localized in distal axons, no studies have demonstrated that axonally localized endogenous pre-miRNAs are processed into their corresponding mature miRNAs. Taking advantage of a compartmentalized culture system and the fact that axons can be metabolically sustained up to 6 hours after being severed from their neuronal cell bodies before undergoing degeneration, I demonstrated that pre-miR-433 is locally processed into mature miR-433-3p in severed axons. Altogether, my findings further support the hypothesis that some of selectively enriched miRNAs in distal axons are derived from local processing of their corresponding miRNA precursors.

Although my research identified the terminal loop structure of pre-miR-433 as a *cis*-element that determines the localization of RNA into axon, the identity of the *trans* acting RNA binding protein(s) that mediate the localization of pre-miRNA into

distal axons has yet to be identified. Future study will need to identify not only RNA binding protein that localizes pre-miRNAs into axon but also signals that trigger local axonal maturation of miRNA precursors as well as the protein components that regulate their processing.

Biological function of mature miR-433-3p in regenerating axons.

Peripheral nerve injury has been shown to induce rapid intra-axonal translation of mRNA encoding RanBP1, a GTPase effector protein that plays an essential role in facilitating the incorporation of injury signal cargo into the retrograde trafficking complex (Yudin et al., 2008). Although we now know that intra-axonal translation of *RanBP1* mRNA is triggered by influx of calcium ions caused by axonal damage, the mechanism that silences axonal expression of RanBP1 protein when it is no longer needed is unknown. In chapter 3, I showed that mature miR-433-3p binds to the extended 3'UTR of *RanBP1* mRNA and negatively regulated the expression of RanBP1 protein in distal axons of culture DRG neurons, leading to attenuation in axon growth. The decreased in axon growth caused by the reduction of RanBP1 expression is consistent with previous reports by the Fanzilber lab indicating that DRG neurons of RanBP1 knockout mice cultured after conditional lesion exhibit a decrease in neurite outgrowth and a reduction in axonal length. Interestingly, I have shown that removal of the cell body fraction from cultured DRG neurons, which emulates axonal injury, triggers processing of localized pre-miR-433 into mature miR-433-3p in severed anucleate axons by 2 hours after removing the neuronal cell body. These findings

suggest that intra-axonal processing of pre-miR-433 induced by nerve injury could provide local source of mature miR-433-3p that function to silence intra-axonal translation of *RanBP1* mRNA when it is no longer needed.

Although my study provide an example of the functional role of axonally processed mature miRNA in response to axon injury, it will be interesting to see the functional role of other axonal miRNAs that are derived from miRNA precursors. Since we now know that axonal miRNA activity can be regulated by controlling the processing of its precursor, this pathway can be manipulated to introduce and regulate the activity of small RNAs in axons to enhance the regeneration as well as a therapeutic approach to treat neurodegenerative diseases.

REFERENCES

- Huebner EA, Strittmatter SM (2009) Axon Regeneration in the Peripheral and Central Nervous Systems. *Results Probl Cell Differ* 48:339-351.
- Jung H, Yoon BC, Holt CE Axonal mRNA localization and local protein synthesis in nervous system assembly, maintenance and repair. *Nat Rev Neurosci* 13:308-324.
- Kim HH, Kim P, Phay M, Yoo S (2015) Identification of precursor microRNAs within distal axons of sensory neuron. *J Neurochem* 134:193-199.
- Kim KW, Tang NH, Andrusiak MG, Wu Z, Chisholm AD, Jin Y (2018) A Neuronal piRNA Pathway Inhibits Axon Regeneration in *C. elegans*. *Neuron* 97:511-519.e516.
- Kosik KS (2006) The neuronal microRNA system. *Nat Rev Neurosci* 7:911-920.
- Lee EJ, Banerjee S, Zhou H, Jammalamadaka A, Arcila M, Manjunath B, Kosik KS (2011) Identification of piRNAs in the central nervous system. *RNA*, 1090-1099.
- Phay M, Kim HH, Yoo S (2018) Analysis of piRNA-Like Small Non-coding RNAs Present in Axons of Adult Sensory Neurons. *Mol Neurobiol* 55:483-494.
- Rajasethupathy P, Antonov I, Sheridan R, Frey S, Sander C, Tuschl T, Kandel ER (2012) A role for neuronal piRNAs in the epigenetic control of memory-related synaptic plasticity. *Cell* 149:693-707.
- Verma P, Chierzi S, Codd AM, Campbell DS, Meyer RL, Holt CE, Fawcett JW (2005) Axonal protein synthesis and degradation are necessary for efficient growth cone regeneration. *J Neurosci* 25:331-342.
- Yoo S, van Niekerk EA, Merianda TT, Twiss JL (2010) Dynamics of axonal mRNA transport and implications for peripheral nerve regeneration. *Exp Neurol* 223:19-27.

- Yu B, Zhou S, Wang Y, Ding G, Ding F, Gu X (2011) Profile of MicroRNAs following Rat Sciatic Nerve Injury by Deep Sequencing: Implication for Mechanisms of Nerve Regeneration. In: PLoS One
doi.org/10.1371/journal.pone.0024612.
- Yudin D, Hanz S, Yoo S, Iavnilovitch E, Willis D, Gradus T, Vuppalanchi D, Segal-Ruder Y, Ben-Yaakov K, Hieda M, Yoneda Y, Twiss JL, Fainzilber M (2008) Localized regulation of axonal RanGTPase controls retrograde injury signaling in peripheral nerve. *Neuron* 59:241-252.
- Zheng JQ, Kelly TK, Chang B, Ryazantsev S, Rajasekaran AK, Martin KC, Twiss JL (2001) A functional role for intra-axonal protein synthesis during axonal regeneration from adult sensory neurons. *J Neurosci* 21:9291-9303.
- Zhou S, Yu B, Qian T, Yao D, Wang Y, Ding F, Gu X (2011) Early changes of microRNAs expression in the dorsal root ganglia following rat sciatic nerve transection. *Neurosci Lett* 494:89-93.

Appendix A

IACUC APPROVAL



Institutional Animal Care and Use Committee
1600 Rockland Road
Wilmington, DE 19803
p (302) 651-6826 f (302)-651-6881
IACUC@nemours.org

MEMORANDUM

DATE: February 16, 2017
TO: Soonmoon Yoo, Ph.D.
FROM: Paul T. Fawcett, PhD
SUBJECT: Axonal non-coding regulatory small miRNA's in regenerating nerve.

The Institutional Animal Care and Use Committee (IACUC) have reviewed the full protocol submission on the above referenced project and the following decision has been made:

Action: **Approved**

Date of Action: **February 16, 2017**

Approval Period: February 16, 2017 through February 15, 2018 for annual renewal. February 16, 2017 through February 15, 2020 for three year renewal.

Protocol Approval Number: NBR-2014-001

Approved Number of Animals:		Yearly Number	Project Total
135	Adult Rat, Sprague- Dawley	120	

Please submit your Biosafety Classification form electronically to the Alfred I. duPont Hospital for Children Institutional Biosafety Committee via the link:

<http://www.nemours.org/research/committee/ibc.html>

Please note that the study cannot begin until the Office of Regulatory Compliance in Research Administration has received all approvals.

Please maintain this approval with your project records. A tally of the number of animals approved and the number ordered for the project will be maintained in the Life Science Center. If changes occur in your protocol or if you require more animals than approved, an amendment to your protocol will need to be submitted for consideration



Institutional Animal Care and Use Committee
1600 Rockland Road
Wilmington, DE 19803
p (302) 651-6826 f (302)-651-6881
IACUC@nemours.org

MEMORANDUM

DATE: March 22, 2017
TO: Soonmoon Yoo, Ph.D.
FROM: Paul T. Fawcett, PhD
SUBJECT: NBR-2017-001 MiRNA-controlled Na⁺ channel level in nociceptors to SCI-induced neuropathy.

The Institutional Animal Care and Use Committee (IACUC) have reviewed the submitted annual review on the above referenced project and the following decision has been made:

Action: **Approved**

Date of Action: **March 22, 2017**

Approval Period: March 22, 2017 through March 21, 2018 for annual renewal.
March 22, 2017 through March 21, 2020 for three year renewal.

Approved Number of Animals: **180 yearly of Sprague-Dawley rats.**

Please submit your Biosafety Classification form electronically to the Alfred I. duPont Hospital for Children Institutional Biosafety Committee via the link:

<http://www.nemours.org/pediatric-research/approval/biosafety-committee.html>

Please note that the study cannot begin until the Office of Regulatory Compliance in Research Administration has received all approvals.

Please maintain this approval with your project records. A tally of the number of animals approved and the number ordered for the project will be maintained in the Life Science Center. If changes occur in your protocol or if you require more animals than approved, and amendment to your protocol will need to be submitted for consideration

If you have any questions regarding this memorandum, please contact Paul T. Fawcett, Ph.D. at x 6776 or email: pfawcett@nemours.org.

Appendix B
PERMISSION LETTER



Thank you for your message. PLOS ONE publishes all of the content in the articles under an open access license called "CC-BY." This license allows you to download, reuse, reprint, modify, distribute, and/or copy articles or images in PLOS journals, so long as the original creators are credited (e.g., including the article's citation and/or the image credit). Additional permissions are not required. You can read about our open access license here: <http://journals.plos.org/plosone/s/licenses-and-copyright>

There are many ways to access our content, including HTML, XML, and PDF versions of each article. Higher resolution versions of figures can be downloaded directly from the article.

Thank you for your interest in PLOS ONE and for your continued support of the Open Access model. Please do not hesitate to be in touch with any additional questions.

Kind regards,

Emma Darkin
Staff EO
PLOS ONE

Case Number: 05859362